ornl

ORNL/TM-13061

OAK RIDGE NATIONAL LABORATORY

MARTIN MARIETTA

Postirradiation Evaluations of Capsules HANS-1 and HANS-2 Irradiated in the HFIR Target Region in Support of Fuel Development for the Advanced Neutron Source

G. L. Hofman
G. L. Copeland
J. L. Snelgrove

August 1995

Advanced Neutron Source

MANAGED BY
MARTIN MARIETTA ENERGY SYSTEMS, INC.
FOR THE UNITED STATES
DEPARTMENT OF ENERGY

ORNL/TM-13061

POSTIRRADIATION EVALUATIONS OF CAPSULES HANS-1 AND HANS-2 IRRADIATED IN THE HFIR TARGET REGION IN SUPPORT OF FUEL DEVELOPMENT FOR THE ADVANCED NEUTRON SOURCE

G. L. Hofman*
G. L. Copeland
J. L. Snelgrove*

*Argonne National Laboratory
9700 Cass Avenue
Argonne, Illinois 60439

August 1995

Prepared by
OAK RIDGE NATIONAL LABORATORY
Oak Ridge, Tennessee 37831-6285
managed by
LOCKHEED MARTIN ENERGY SYSTEMS, INC.
for the
U.S. DEPARTMENT OF ENERGY
under contract DE-AC05-84OR21400

CONTENTS

LIST OF FIGURES

LIST OF FIGURES (continued)

LIST OF FIGURES (continued)

Figure *Page*

LIST OF TABLES

ACRONYMS

ANL	Argonne National Laboratory
ANS	Advanced Neutron Source
B&W	Babcock and Wilcox Company
CERCA	Compagnie pour l'Etude et la Realization de Combustibles Atomiques, Romans-sur-Isere, France
dph	diamond-pyramid hardness
EDX	energy-dispersive X-ray analysis
EMP	electron microprobe
HEU	highly enriched uranium
HFIR	High Flux Isotope Reactor
LEU	low-enriched uranium
NUKEM	NUKEM GmbH, Federal Republic of Germany
ORNL	Oak Ridge National Laboratory
ORR	Oak Ridge Research Reactor
RERTR	Reduced Enrichment Research and Test Reactor
SEM	scanning electron microscope

ABSTRACT

This report describes the design, fabrication, irradiation, and evaluation of two capsule tests containing U_3Si_2 fuel particles in contact with aluminum. The tests were in support of fuel qualification for the Advanced Neutron Source (ANS) reactor, a high-powered research reactor that was planned for the Oak Ridge National Laboratory. At the time of these tests, the fuel consisted of U_3Si_2 containing highly enriched uranium dispersed in aluminum at a volume fraction of ~0.15. The extremely high thermal flux in the target region of the High Flux Isotope Reactor provided up to 90% burnup in one 23-d cycle. Temperatures up to 450°C were maintained by gamma heating. Passive SiC temperature monitors were employed. The very small specimen size allowed only microstructural examination of the fuel particles but also allowed many specimens to be tested at a range of temperatures. The determination of fission gas bubble morphology by microstructural examination has been beneficial in developing a fuel performance model that allows prediction of fuel performance under these extreme conditions. The results indicate that performance of the reference fuel would be satisfactory under the ANS conditions. In addition to U_3Si_2, particles of U_3Si, UAl_2, UAl_x, and U_3O_8 were tested.

1. INTRODUCTION

The Advanced Neutron Source (ANS) is being designed as a user-oriented neutron research laboratory around the most intense continuous beams of thermal and subthermal neutrons in the world. The ANS is based on a new research reactor of about 330-MW fission power with an unprecedented peak thermal flux of 7×10^{19} $m^{-2} \cdot s^{-1}$. There also will be extensive facilities for materials irradiation, isotope production, and analytical chemistry.

The reactor core for the ANS consists of cylindrical shell fuel elements. The entire core is replaced for refueling after each cycle (~17 d). Each element consists of involute fuel plates welded into nonfueled cylindrical side plates. The fuel plates and the coolant channels are 1.27 mm thick. The fuel plates consist of a "meat" of U_3Si_2 particles dispersed in aluminum, a "filler" section of aluminum, and a burnable poison insert on both ends consisting of B_4C particles dispersed in aluminum. The fuel meat varies in thickness in both the radial and axial directions. The plates are clad completely with 6061 aluminum alloy, and the sideplates are 6061 alloy.

An early core design for the ANS was an extremely compact core with very high specific uranium density.[1] The core volume was 35 L with a highly enriched uranium loading of ~19 kg, necessitating a uranium loading in the meat of ~3.5 Mg/m^3. The only promising fuel for this high density is U_3Si_2, which was developed by the Reduced Enrichment Research and Test Reactor (RERTR) program at Argonne National Laboratory (ANL). The data upon which the U. S. Nuclear Regulatory Commission based its approval of the use of the U_3Si_2 fuel for conversion (to low-enriched uranium) of licensed nonpower reactors are in the report *Safety Evaluation Report Related to the Evaluation of Low-Enriched Uranium Silicide-Aluminum Dispersion Fuel for Use in Non-Power Reactors*, NUREG-1313.[2] The fuel has been shown to perform well at loadings and fission densities beyond those required for the ANS core, although at conditions of fission rate and temperature well below those anticipated for the ANS. Therefore, an irradiation testing program was put into place to verify the performance at conditions as near as possible to those of the ANS. A fuel performance model was developed to consolidate the data from the various types of tests and to predict the performance of the fuel under various conditions.

The ANS conceptual design core[3] of 1993 was both larger and lower-loaded than the original compact core. This change lowered the uranium density to the level where both U_3O_8 and UAl_x* can be fabricated as dispersions in aluminum. The loading of this core design was originally 1.05 Mg U/m^3, but it gradually increased to about 1.7 Mg U/m^3, which is expected to provide sufficient excess reactivity to account for the losses resulting from experimental facilities in the reflector.† Much irradiation data and experience exist for these fuels in research and test reactors. However, this irradiation experience is also at much lower temperatures and fission rates than those planned for the ANS.

U_3Si_2 is retained as the reference fuel for the ANS because the higher particle density yields a lower volume fraction of fuel and thus facilitates fabrication and improves the thermal conductivity and stability of the dispersion. Both U_3O_8 and UAl_x are considered to be viable backup fuels for the conceptual design core and are being included in the early irradiation tests in order to obtain performance data at high temperatures and fission rates. In addition, UAl_2 has been included in the tests. As discussed in Sect. 4.5.4, UAl_2 converts to UAl_x during fabrication and irradiation, but may offer some advantage over UAl_x during fabrication because of its higher density. Based on existing data, UAl_x appears to be the most stable of all

*A mixture of the intermetallic compounds UAl_2, UAl_3, and UAl_4, with $x \approx 3$. Typical compositions are 7–9 wt % UAl_2, 79–84 wt % UAl_3, and 9–13 wt % UAl_4.

†An even larger core consisting of three elements was baselined in December 1994. This core uses uranium enriched to only 50% ^{235}U and would require a uranium density of 3.5 Mg U/m^3, which eliminates the U_3O_8 and UAl_x from consideration as alternative fuels. This new core design will not be specifically addressed in this report.

the prospective fuels in its retention of fission gas. Based on experience at B&W,* it appears that U_3O_8 may be the fuel most easily fabricated to the exacting tolerances of the ANS. It retains fission gas well and behaves stably up to a level of burnup (perhaps beyond the ANS requirements), which decreases as the fuel loading increases. Fabrication of U_3Si_2 is roughly equivalent to fabrication of UAl_x. The existing irradiation behavior data for U_3Si_2 show behavior similar to the aluminide in that no limits need to be set on burnup; however, the silicide shows some small fission gas bubbles and the aluminide does not. A few samples of the highest-density uranium silicide, U_3Si, were also included in the HANS tests in order to provide data for a general understanding of silicide irradiation behavior. Although U_3Si was not considered to be a viable fuel for the ANS because earlier tests had shown it susceptible to breakaway swelling,† the results of the HANS irradiations indicate that it might be usable in the ANS (see Sect. 4.5.4).

The irradiation performance data for $_3Si_2$ have been generated by the United States' RERTR program, which was established in 1978 to provide the technical means to convert research and test reactors from the use of highly enriched uranium (HEU) fuel to low-enriched (LEU) fuel,[4] a change requiring greatly increased uranium content to maintain the excess reactivity required for the continued operation of the reactors. To this end, the RERTR program pursued both increasing the volume fraction of existing fuel compounds and developing new, higher-density fuel compounds. In 1978, the highest density fuels in common use in plate-type research reactor fuel elements were dispersions of uranium aluminide (UAl_x) and uranium oxide (U_3O_8) in aluminum, with fuel meat densities of 1.7 and 1.3 Mg U/m^3, respectively. These two types of fuels were developed and tested for LEU applications up to their practical fabrication limits of 2.4 Mg U/m^3 for UAl_x and 3.2 Mg U/m^3 for U_3O_8. Still higher fuel densities were required for some applications, and higher-density compounds were investigated for these. The compound U_3Si_2 was found to perform extremely well during irradiation and could be fabricated successfully at densities up to at least 4.8 Mg U/m^3.

The development and testing of U_3Si_2 in the United States progressed from miniature fuel plates (miniplates),[5] to experimental elements,[6] and to a full demonstration core for the Oak Ridge Research Reactor (ORR).[7] The demonstration core operated for about 15 months and was fueled by elements from three commercial fabricators: NUKEM,‡ CERCA,** and B&W. This test program ultimately led to approval by the U.S. Nuclear Regulatory Commission of the use of U_3Si_2 for the HEU-to-LEU conversion of licensed nonpower reactors.[2] The RERTR program involved international cooperation. Miniplates, full-sized plates, and/or test elements were fabricated in France, Germany, Argentina, and Indonesia and tested in reactors in France, Germany, Sweden, the Netherlands, Japan, and Indonesia. Some fabrication and testing has also been done in China and the U.S.S.R.

Summaries of the irradiation experience base for U_3Si_2 when the ANS project began are depicted in Figs. 1.1 and 1.2. This base represents 58 miniplates and 85 elements (1,587 full-sized plates), which were carefully evaluated and represent completely satisfactory performance. No plate failures have yet been attributed to the U_3Si_2-Al fuel dispersion. Figure 1.1 shows fission density in the fuel particles vs uranium density in the meat. Figure 1.2 shows fission density in the meat (combined fuel particles and aluminum matrix) vs uranium density in the meat. Both factors are important in the performance of the fuel during irradiation. The bulk of the data are for high-uranium-density loadings of LEU fuel. Thus, the data extend beyond the range expected for

---

*Babcock and Wilcox Company, Lynchburg, Virginia.

†In this report, the term "breakaway swelling" is used to describe a condition characterized by an unstable fission gas bubble morphology in which bubble coarsening and interlinkage can lead to rapid increase in bubble volume. Unless the fuel particles are well-separated by the matrix aluminum (i.e., unless the fuel volume fraction is sufficiently low so that fuel particles cannot grow together over extended areas) or unless sufficient external restraint is applied to the fuel particles, breakaway swelling of the fuel particles can lead to failure of the fuel plate.

‡NUKEM GmbH, Hanau, Fed. Rep. of Germany.

**Compagnie pour l'Etude et la Realization de Combustibles Atomiques, Romans-sur-Isere, France.

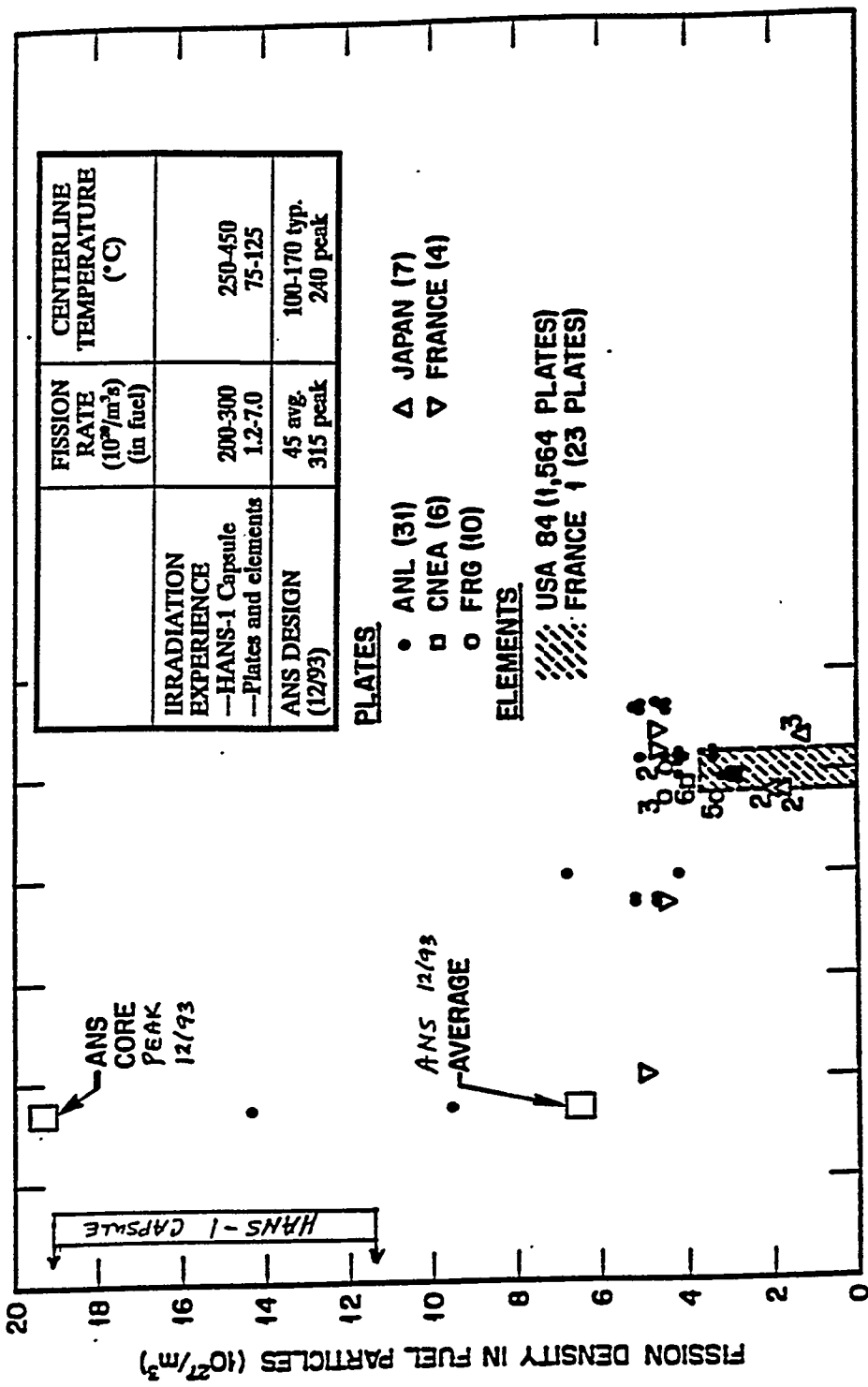

Fig. 1.1. Fuel irradiation conditions for the ANS preconceptual core compared to U_3Si_2 irradiation experience at the beginning of the ANS Project—fuel particle basis.

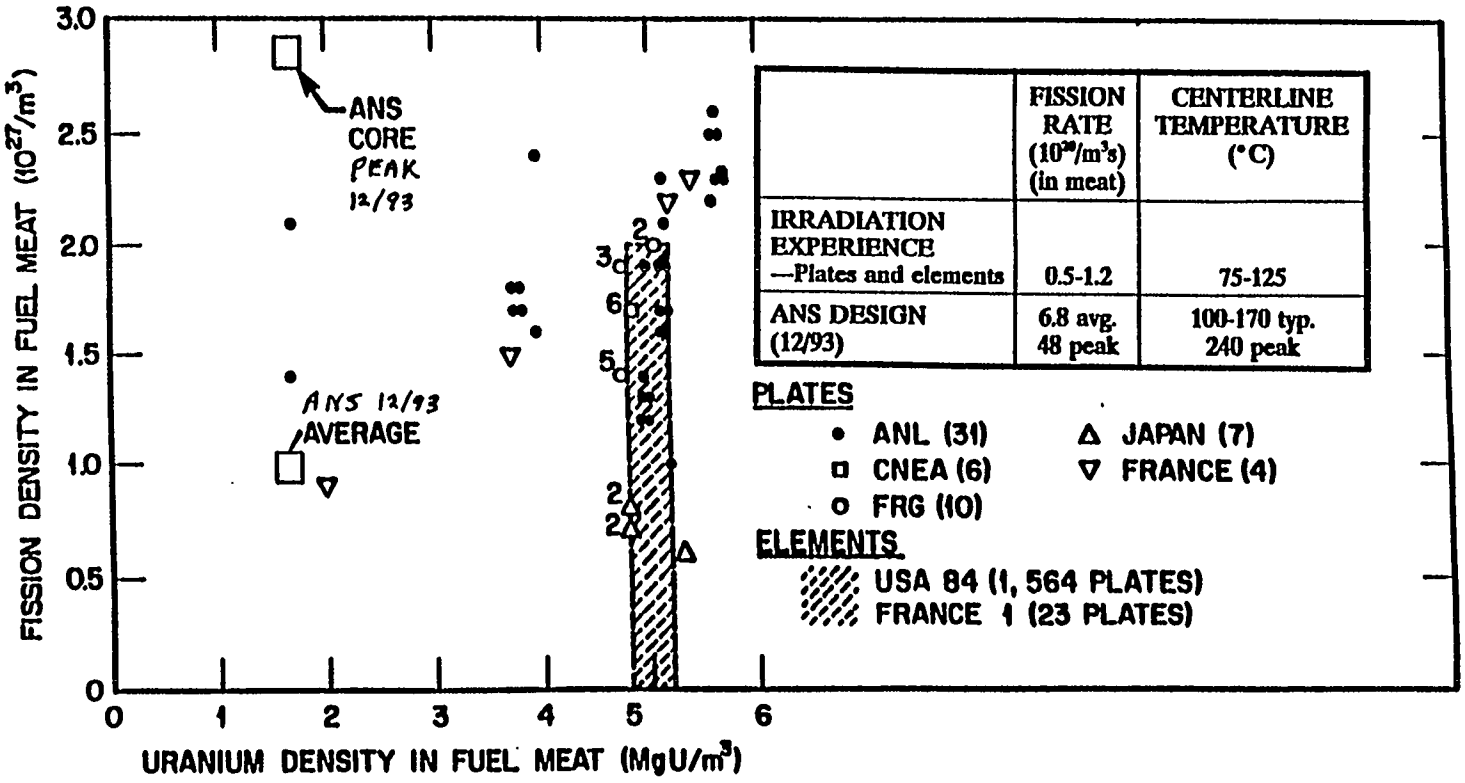

Fig. 1.2. Fuel irradiation conditions for the ANS preconceptual core compared to U_3Si_2 irradiation experience at the beginning of the ANS Project—fuel meat basis.

the ANS in terms of fission density in the meat. (The ANS has a low-uranium-density of HEU fuel). Up to ~20×10^{27} fissions/m^3 in the particle (~90% burnup) are expected in the ANS in small regions at the edges and ends of the plates, where the meat is very thin. The average for the core is ~9×10^{27} fissions/m^3. Since the fuel volume fraction is ~0.15, the corresponding values are ~3.0 and 1.4×10^{27} fissions/m^3, respectively, in the meat.

Only two miniplates of HEU U_3Si_2 have been irradiated to date. These were irradiated by the RERTR program to give some experience well beyond any burnup possible with LEU.[5] These plates with a meat density of 1.66 Mg U/m^3 (0.147 volume fraction) were irradiated in the ORR to burnups of about 42 and 63%, corresponding to 1.4 and 2.1×10^{27} fissions/m^3, respectively, in the meat and 9.5 and 14.3×10^{27} fissions/m^3, respectively, in the particles. The plates retained good mechanical integrity, and the swelling was somewhat lower than that projected from LEU data. The fuel-meat-swelling values were 4.9 and 11.6%, respectively, and the particle-swelling values were 38 and 84%, respectively. Microstructural examination showed the stable structure typical of U_3Si_2. Optical metallography revealed virtually no fission gas bubbles in the fuel particles irradiated to 42% burnup and a regular distribution of small bubbles in the fuel particles irradiated to 63% burnup (see Fig. 4.7). Higher magnification examination with the scanning electron microscope (SEM) revealed a stable morphology of very small fission gas bubbles (see, for example, Fig. 4.19).

The swelling of U_3Si_2 particles of various enrichments as obtained from miniplate data is shown in Fig. 1.3. The swelling is lower for higher enrichment fuel, as a result of its higher fission rate. It is hypothesized that this is the result of a delay in transition from the lower swelling rate to the higher swelling rate that corresponds to the formation of fission gas bubbles that can be resolved with the SEM (~30 nm). That is, before the knee of the curve, gas bubbles are not observed. Above the knee of the curve (in the higher swelling rate region), gas bubbles are observed with the SEM. It is hypothesized that this transition is the result of a recrystallization into extremely fine subgrains ~1 μm in diameter with the gas bubbles precipitating on the subgrain boundaries.[8]

The performance requirements for the ANS fuel represent a realistic advancement of existing technology. The projected temperatures and fission rates for the ANS are beyond the experience base for any of the research reactor fuels. The primary goal of the irradiation testing program is to validate the performance of the fuel at conditions as close as can be obtained to the temperatures and fission rates of the ANS. The goal of these first two capsule tests is to obtain high-temperature, high-fission-rate irradiation performance data for the three fuel materials being considered. The fuel content in the specimens is kept low to allow placement in the target region of the High Flux Isotope Reactor (HFIR), which has a higher thermal flux than most of the fueled region of ANS. The low fuel content also allows most of the heat to be generated by gamma heating rather than by fission so that the temperature remains nearly constant during the test. The primary evaluation criterion is fission gas bubble morphology as determined by microstructural examination.

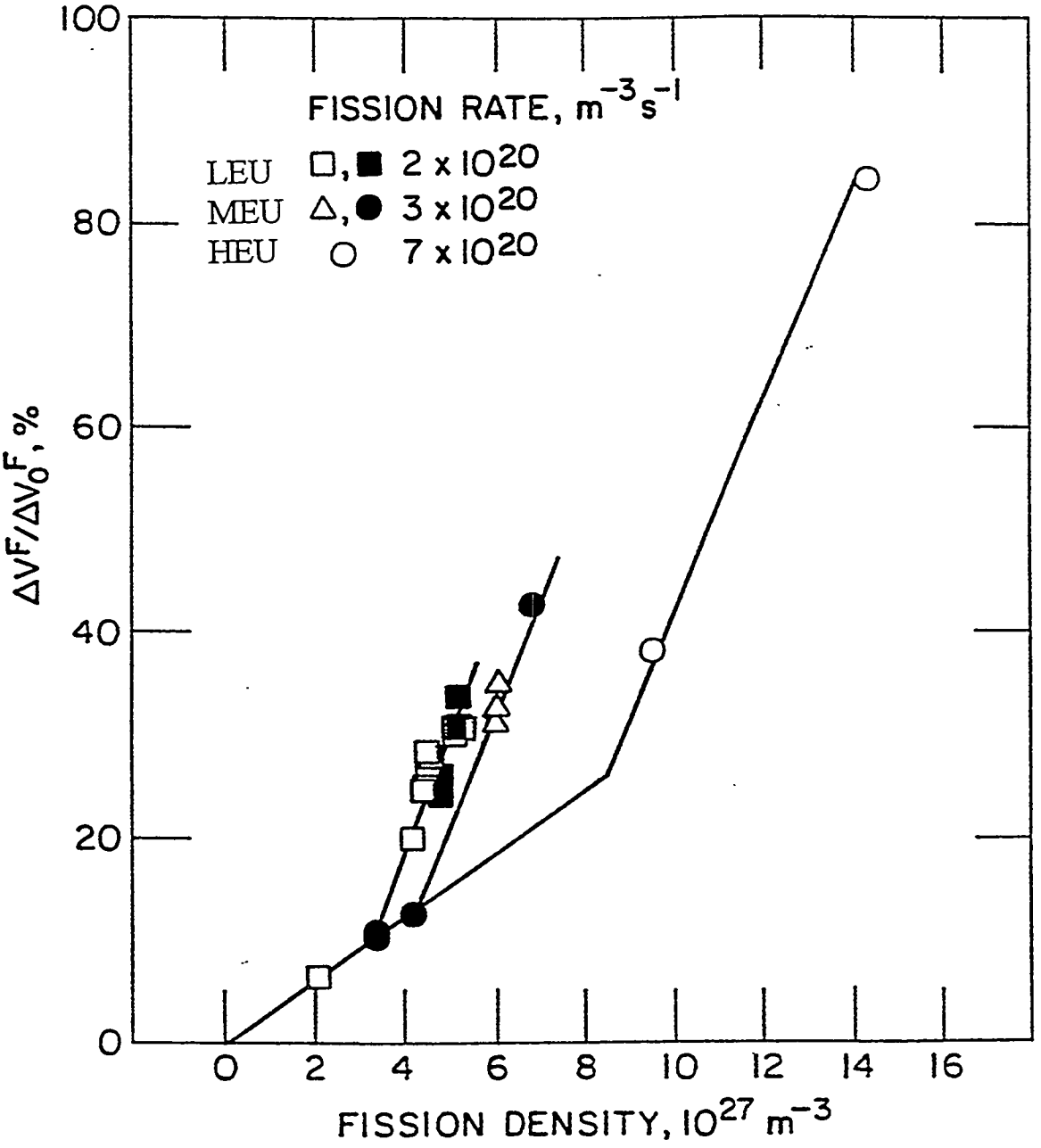

Fig. 1.3. Swelling of U_3Si_2 of various enrichments and fuel dispersion loadings as a function of fission density, including USi data.

2. DESCRIPTION AND DESIGN OF FUEL HOLDERS AND CAPSULES

2.1 OVERALL TEST DESIGN

As discussed in Sect. 1, a dispersion of U_3Si_2 in aluminum was chosen for the ANS because of its high density and because irradiation experience from the RERTR program indicated that the fuel would behave stably in the ANS. However, as shown in Fig. 1.1, even though fission densities approaching the maximum ANS values had been achieved in limited tests, anticipated fission rates and fuel meat temperatures for the ANS design are much higher than had been tested. Therefore, it was imperative that early tests be performed to demonstrate acceptable fuel behavior under ANS conditions.

The problem, of course, was that the neutron flux and power density in portions of the ANS core are significantly higher than those in the fuel testing regions of any existing reactor. From a number of preliminary neutronics investigations, it was clear that only in the target region of the HFIR could ANS fission rates be approached. The 2.4×10^{19} $m^{-2} \cdot s^{-1}$ thermal flux in the HFIR target actually approaches the peak in the fuel region of the ANS. However, heat removal capabilities are quite limited there. Fortunately, the RERTR program's investigations had shown that one could straightforwardly infer the behavior of the fuel meat from the behavior of the fuel particles. Therefore, it was concluded that irradiation tests of a small number of fuel particles embedded in aluminum would provide the needed information, while producing manageable amounts of heat. It was also decided to maintain a nearly constant temperature during the experiment in order to simplify determination of any effect of temperature on the irradiation behavior.

These considerations led to the fuel holder and capsule designs discussed below. In order to maintain a nearly constant temperature as the ^{235}U depletes during the irradiation, most of the heat would have to be produced by the nearly constant gamma field in the HFIR target region. The temperatures of the various fuel holders were adjusted by varying the thickness of the gas gap between the holder and the capsule wall. Calculations of fission and gamma heating performed by B. W. Patton of the ORNL Engineering Technology Division indicated that a fuel loading of 0.46 mg of ^{235}U in each fuel holder would result in 90% of the heat being generated by γ rays at the beginning of the irradiation cycle. The approximately 90% ^{235}U depletion expected during the irradiation cycle was calculated to result in an average temperature decrease of 18°C (range 9 to 36°C) for the 18 fuel holders of the HANS-1 experiment. Similar temperature decreases would be expected in the HANS-2 fuel holders during irradiation.

2.2 FUEL HOLDER DESIGN

The fuel holder, shown in Fig. 2.1, was machined from Al–6061 alloy. The overall length of each holder is 25.4 mm, and the diameters were such as to give the desired gas gap for temperature control in the capsule (see Sect. 2.3). Each holder contained two 1-mm-high fuel zones located near the axial midplane of the holder in the two 1-mm-diam holes located 180° apart on a 5.59-mm-diam circle. The fuel zone consisted of a mixture of fuel particles and aluminum powder, compacted under a pressure of 199 MPa. It should be noted that dispersion fuel plates are fabricated using a hot roll-bonding process, so there is much more intimate contact and a small amount of reaction between the fuel particles and the aluminum matrix. Hot-rolled samples have been irradiated in the HANS-3 capsule to determine if differences in sample fabrication method are important. Aluminum powder (without fuel) was compacted above and below the fuel zone, using the same compacting pressure. The remainder of each fuel hole was filled with Al (>99.5%) wire, and the holes were sealed by electron beam welding. A silicon carbide temperature monitor occupied the central cavity of each holder, held in place by a stainless steel set screw (average mass = 87 mg) and an alumina spacer (see Sect. 2.4). As also discussed in

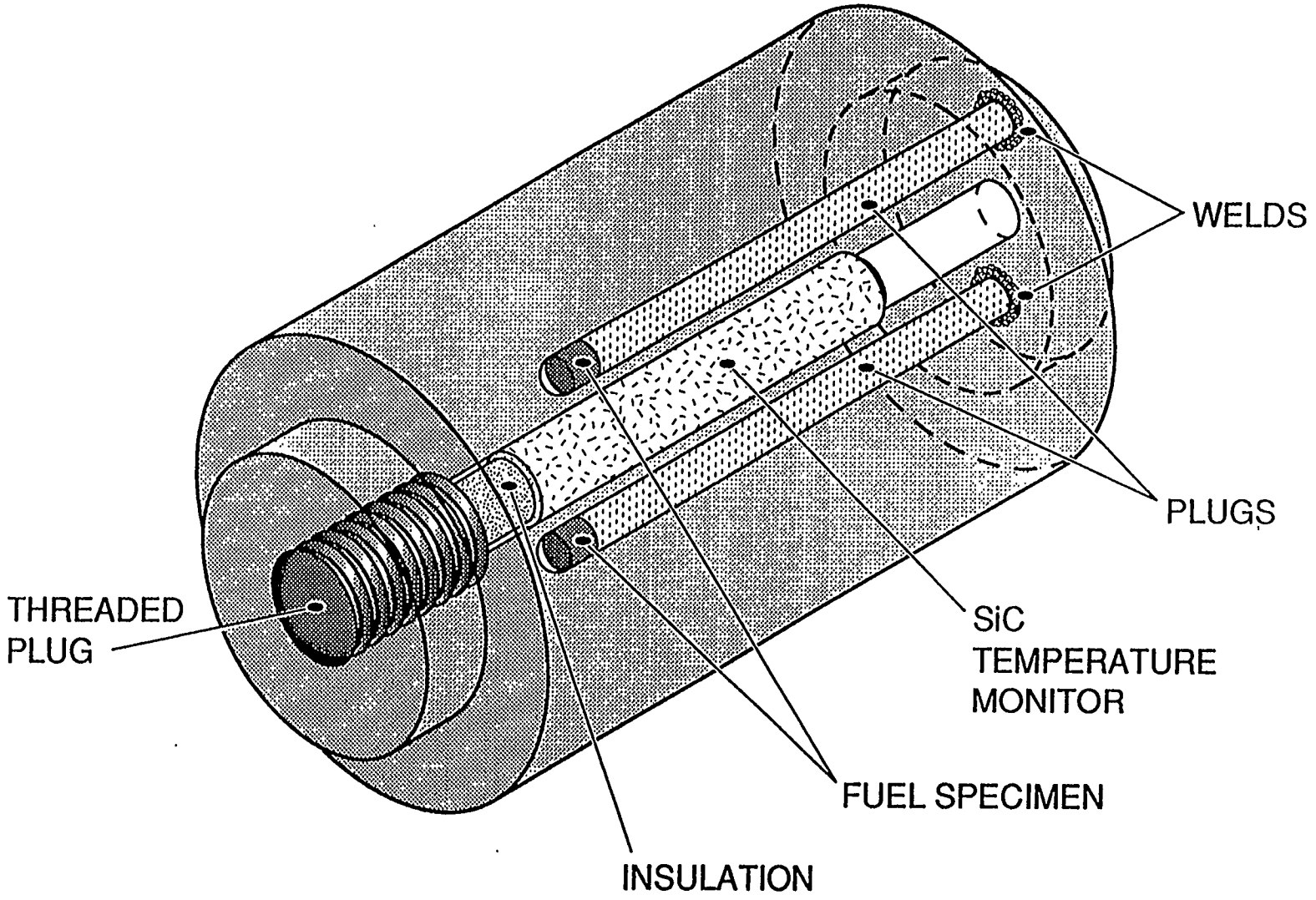

Fig. 2.1. Drawing of HANS specimen subassembly.

Sect. 2.4, melt monitors were used in five of the HANS-2 fuel holders. The melt monitors were placed in 1.73-mm-diam, 23.83-mm-deep holes located midway between the two fuel holes on the same circle. The fuel holder diameters and calculated temperatures during irradiation are listed in Table 2.1. Information about the HANS-1 and -2 fuel loadings is given in Tables 2.2 through 2.4. The chemical analysis data for the fuel holder materials and the fuels are given in Appendix A.

2.3 CAPSULE DESIGN

The capsule used for the HANS-1 and HANS-2 experiments is a standard design that replaces a target rod in the target basket in the central flux trap in the HFIR. It is basically a cylindrical tube of 6061 aluminum whose end fittings are compatible with the HFIR target basket. The tube length is 616 mm, which allows space for 18 fuel holders per capsule. The internal diameter is nominally 13.49 mm. The temperature of the fuel holders is maintained by a gas gap between the holders and the tube wall. This requirement necessitates centering the fuel holders and minimizing axial heat flow, which are accomplished by hexagonal spacers on the ends of the fuel holders contacting the tube at six points and by disk-shaped insulators between the holders. The layout of the capsule and its contents prior to loading is shown in Fig. 2.2. A closer view of the holder with an end spacer, spacer, axial insulator (and SiC temperature monitor with its insulator) is shown in Fig. 2.3. After assembly the capsule was baked out under vacuum, backfilled with pure helium to ~1.3 atm pressure, and sealed.

The material for the spacers and axial insulators needed a low thermal conductivity and high resistance to irradiation damage to withstand the HFIR target environment. The ceramic materials known to have good irradiation performance (such as Al_2O_3) have relatively high thermal conductivity. The "machinable ceramics" (glass-bonded mica products) seemed appropriate both for their low thermal conductivities and for their ability to be machined relatively easily into the spacer shapes. However, few data could be found on their irradiation stability. Two products in particular were of interest: Mykroy/Mycalex* grade 1100 amorphous glass-bonded mica with synthetic mica, and Macor,† which is a crystallized glass-bonded mica. No information was found on the irradiation stability of Macor. It contains some boron, which would react to form gaseous products during the test and was thus thought to be unsuitable. The Mycalex product was referred to as being usable in an irradiation environment at a fast neutron fluence up to 5.2×10^{20} m^{-2}. However, an exact source could not be found for these data.[9] We decided to use the Mycalex for the spacers and Macor for the axial insulators to determine if the products held up. The original assembly procedure for the capsule called for both products to be baked out at 500°C after a cleaning process. However, both products swelled to the point that they could not be assembled into the capsule, so the bakeout temperature was lowered to 150°C, which produced no measurable swelling.

2.4 TEMPERATURE MONITORS

Passive temperature monitors were used to simplify the test and to minimize the cost. A silicon carbide cylinder (2.3 mm diam × 12.7 mm long) was inserted into the center of each fuel holder in both tests. The SiC was held captive by a stainless steel set screw separated by an insulator. The set screw was inserted only loosely to ease removal and not to restrain the SiC. The irradiation temperature was determined by postirradiation annealing and measurement of the lengths. The length increases during irradiation. Upon sequential postirradiation annealing, the length should not change until the irradiation temperature is reached and then should decrease linearly until the damage is annealed.[10]

*Mykroy/Mycalex, Clifton, N.J.

†Corning Glass Works, Corning, N.Y.

Table 2.1. Fuel holder diameters and calculated irradiation temperatures

Position	HANS-1 capsule				HANS-2 cpsule		
	Fuel type	Holder diameter (mm)	Calculated initial temperature (°C)	Calculated final temperature (°C)	Fuel type	Holder diameter (mm)	Calculated initial temperature (°C)
1	U_3Si_2	12.238	424	388	U_3O_8	12.273	425
2	U_3Si_2	12.794	374	350	UAl_2	12.624	425
3	U_3Si_2	13.063	324	306	U_3O_8	13.233	250
4	U_3Si_2	13.269	250	238	UAl_2	13.259	250
5	U_3Si	13.335	227	218	U_3O_8	13.167	325
6	U_3Si_2	13.315	251	239	UAl_2	13.117	375
7	U_3Si_2	13.218	324	310	U_3O_8	13.142	375
8	U_3Si_2	13.150	374	357	UAl_2	13.061	425
9	U_3Si_2	13.076	425	406	U_3O_8	13.076	425
10	U_3Si_2	13.073	425	406	UAl_x	13.086	425
11	U_3Si_2	13.152	374	357	U_3Si_2	13.061	425
12	U_3Si_2	13.218	324	310	UAl_x	13.142	375
13	U_3Si_2	13.310	251	239	U_3Si_2	13.117	375
14	U_3Si	13.078	375	356	U_3Si_2	13.175	325
15	U_3Si_2	12.918	426	403	UAl_x	13.264	250
16	U_3Si_2	12.941	376	356	U_3Si_2	13.223	250
17	U_3Si_2	12.951	323	303	UAl_x	12.619	425
18	U_3Si_2	13.010	249	230	U_3Si_2	12.263	425

Table 2.2. Density and composition of fuel particles irradiated in HANS-1 and HANS-2

Fuel type	Fuel density (Mg/m^3)	Uranium content (wt %)	Uranium isotopic abundances (wt %)			
			^{234}U	^{235}U	^{236}U	^{238}U
UAl_x	6.35	70.57	1.019	93.057	0.402	5.522
UAl_2	8.06	80.87	0.556	93.048	0.426	5.971
U_3O_8	8.20	84.67	1.010	93.164	0.389	5.437
U_3Si_2	12.07	92.32	1.059	92.951	0.242	5.748
U_3Si	15.13	95.41	1.054	92.625	0.242	6.079

In addition to the SiC monitors, melt monitors were placed in five of the fuel holders in the HANS-2 capsule. These melt monitors consisted of powders of pure metals or eutectics seal-welded into small stainless steel canisters and placed in the fuel holders in a hole concentric with the fuel specimens. Three monitors were placed in the hole in each of the five holders, as shown in Table 2.5. The evaluation of these melt monitors was to be simply to determine by either radiography or metallography which of the powders had melted during the test operation.

Table 2.3. Fuel loading data for the HANS-1 capsule

Position	Fuel type	Weight of fuel in hole A (mg)	Weight of fuel in hole B (mg)	Number of particles in hole A	Number of particles in hole B	Average diameter of particles in hole A[a] (μm)	Average diameter of particles in hole B[a] (μm)
1	U_3Si_2	0.23	0.21	28	33	88	81
2	U_3Si_2	0.36	0.31	41	40	90	86
3	U_3Si_2	0.28	0.33	40	38	83	90
4	U_3Si_2	0.29	0.29	36	37	87	87
5	U_3Si	0.26	0.26	22	35	92	79
6	U_3Si_2	0.31	0.3	38	35	88	89
7	U_3Si_2	0.26	0.27	33	37	87	85
8	U_3Si_2	0.32	0.28	33	31	93	91
9	U_3Si_2	0.26	0.33	43	28	79	99
10	U_3Si_2	0.3	0.3	29	29	95	95
11	U_3Si_2	0.29	0.3	30	24	93	101
12	U_3Si_2	0.32	0.27	27	33	99	88
13	U_3Si_2	0.28	0.28	43	26	81	96
14	U_3Si	0.26	0.27	35	28	79	86
15	U_3Si_2	0.25	0.28	32	33	87	89
16	U_3Si_2	0.3	0.28	30	33	94	89
17	U_3Si_2	0.29	0.28	33	34	90	88
18	U_3Si_2	0.26	0.32	25	35	95	91

[a]Particles are assumed to be spherical.

Table 2.4. Fuel loading data for the HANS-2 capsule

Position	Fuel type	Weight of fuel in hole A (mg)	Weight of fuel in hole B (mg)	Number of particles in hole A	Number of particles in hole B	Average diameter of particles in hole A[a] (μm)	Average diameter of particles in hole B[a] (μm)
1	U_3O_8	0.26	0.29	>60	>60	<81	<84
2	UAl_2	0.34	0.27	46	29	97	105
3	U_3O_8	0.3	0.3	>60	>60	<85	<85
4	UAl_2	0.32	0.33	52	46	91	96
5	U_3O_8	0.31	0.29	>60	>60	<86	<84
6	UAl_2	0.35	0.29	45	43	99	94
7	U_3O_8	0.31	0.31	>60	>60	<86	<86
8	UAl_2	0.32	0.3	45	46	96	93
9	U_3O_8	0.3	0.27	>60	>60	<85	<82
10	UAl_x	0.34	0.38	>60	>60	<96	<100
11	U_3Si_2	0.28	0.29	30	29	92	94
12	UAl_x	0.34	0.34	>60	>60	<96	<96
13	U_3Si_2	0.26	0.32	33	32	87	94
14	U_3Si_2	0.31	0.28	30	27	95	95
15	UAl_x	0.37	0.38	>60	>60	<99	<100
16	U_3Si_2	0.26	0.26	27	30	93	90
17	UAl_x	0.37	0.38	>60	>60	<99	<100
18	U_3Si_2	0.25	0.28	29	28	89	94

[a]Particles are assumed to be spherical.

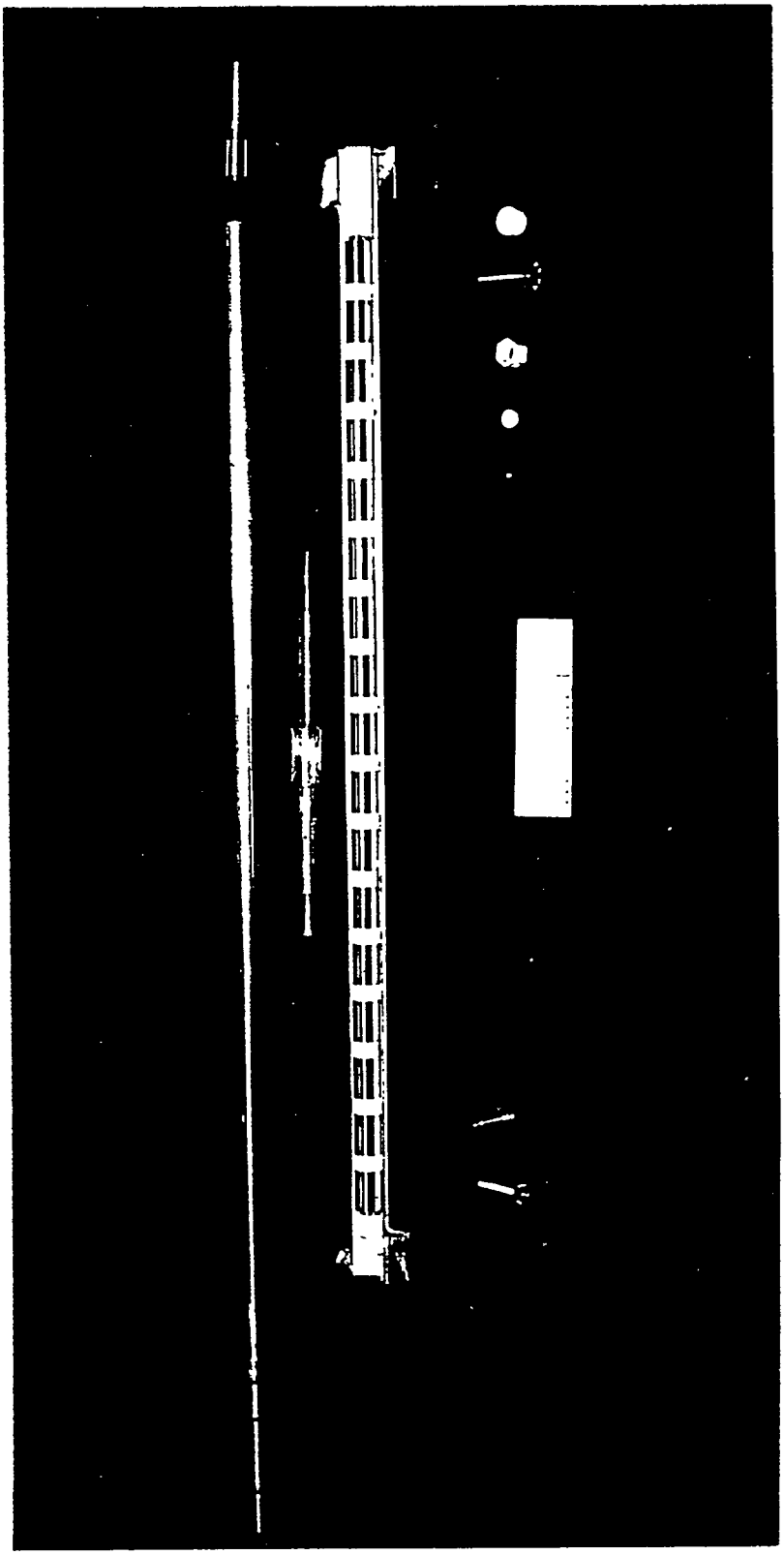

Fig. 2.2. Layout of a HANS capsule and its contents prior to loading.

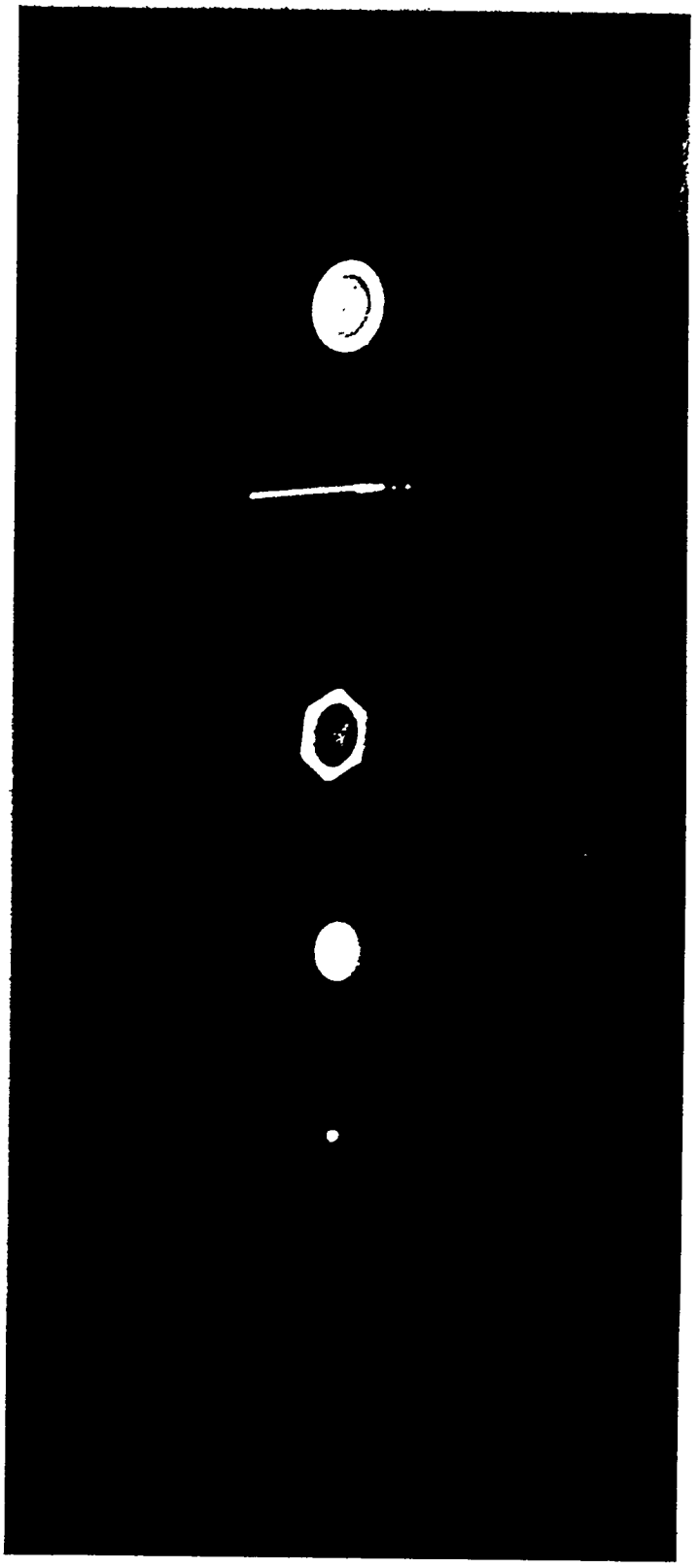

Fig. 2.3. A closer view of the HANS fuel holder with an end spacer, spacer, axial insulator, and SiC temperature monitor with its insulator.

Table 2.5. Melt monitors used in the HANS-2 experiment

Monitor material	Melting temperature (°C)	Monitors in holder at position number				
		2	4	5	7	9
Sn	232		X			
Pb-Sn	247		X	X		
Bi	271	X	X	X	X	X
Pb	327	X		X	X	X
Zn	420	X			X	X

3. IRRADIATION

The HANS-1 capsule was irradiated in position F7 of the HFIR target region during cycle 289, which began on June 26, 1990, and ended on September 7, 1990, with an integrated reactor power of 1881 MWd. This was the first cycle following a several-year shutdown of HFIR, and only 17% of the integrated power was accumulated before August 20. The nominal reactor power was 85 MW; however, the first 1.6 h of operation was at 8.5 MW.

The HANS-2 capsule was irradiated in position F7 of the HFIR target region during cycle 315, which began on January 19, 1993, and ended on February 10, 1993, with an integrated reactor power of 1861 MWd. The nominal reactor power was 85 MW.

Depletion of ^{235}U and fission densities in the fuel particles at the end of the irradiations were calculated using one-group[11] and two-group fluxes and cross sections for the target region. The calculated initial fission rates, final ^{235}U burnups, and final fission densities in the fuel particles of the various fuel holders are given in Table 3.1. These values are based on the average reaction rates derived from the one-group and two-group fluxes, assuming that the flux in the target region remained constant during the irradiation. As a point of reference, based on a conversion factor of 3.1×10^{10} fissions $W^{-1} \cdot s^{-1}$, the initial fission rate in the fuel particles in holders 9 and 10 of the HANS-1 capsule is 916 MW/L.

Table 3.1. Initial fission rate and final burnup and fission density in the fuel particles

Position number	HANS-1 Capsule			HANS-2 Capsule		
	Initial fission rate (10^{22} m^{-3} · s^{-1})	Final ^{235}U burnup (%)	Final fission density in particle (10^{27} m^{-3})	Initial fission rate (10^{22} m^{-3} · s^{-1})	Final ^{235}U burnup (%)	Final fission density in particle (10^{27} m^{-3})
1	1.56	72.6	16.4	0.97	72.2	10.2
2	1.80	77.4	17.5	1.05	77.1	10.2
3	2.03	81.3	18.4	1.27	81.0	11.4
4	2.25	84.4	19.1	1.32	84.1	11.1
5	3.14	86.7	25.3	1.52	86.4	12.2
6	2.59	88.4	20.0	1.52	88.2	11.7
7	2.72	89.6	20.3	1.70	89.3	12.6
8	2.80	90.3	20.4	1.64	90.1	11.9
9	2.84	90.6	20.5	1.77	90.4	12.8
10	2.84	90.6	20.5	1.14	90.4	8.2
11	2.80	90.3	20.4	2.80	90.1	20.4
12	2.72	89.6	20.3	1.09	89.3	8.1
13	2.59	88.4	20.0	2.59	88.1	19.9
14	3.14	86.7	25.3	2.44	86.4	19.5
15	2.25	84.4	19.1	0.90	84.1	7.7
16	2.03	81.3	18.4	2.03	81.0	18.3
17	1.80	77.4	17.5	0.72	77.0	7.0
18	1.56	72.6	16.4	1.56	72.2	16.3

4. POSTIRRADIATION EXAMINATIONS

4.1 DISASSEMBLY

The capsules were disassembled in the Irradiated Fuels Examination Laboratory at Oak Ridge National Laboratory (ORNL). The capsules were examined visually for evidence of damage. No evidence of bowing, swelling, or cracking was observed for either capsule. For the HANS-1 capsule, the first attempt to remove the fuel holders (by cutting the end fittings from the tube and pushing the holders and spacers out) was unsuccessful because of swelling of the spacers. The individual fuel holders were eventually removed by placing the tube in a lathe and cutting through the tube at about the midpoint of each fuel holder. The fuel holders could then be separated from the spacers. In the attempt to disassemble the HANS-2 capsule by cutting off the end caps and slitting through the outer capsule on two sides, the milling machine failed after about half of one cut. Again, each holder was cut out with the lathe in the same manner as for HANS-1.

The spacers and insulators were examined during the disassembly of HANS-1. The spacers and insulators performed satisfactorily although they underwent some swelling and cracking during the test. They did not deform the outer capsule tube and held everything in place (even during attempts at disassembly). After removing the Mycalex spacers from near the ends of the capsule (fuel holders 16 and 17), dimensional measurements could be made on some of the parts. The Macor insulator from holder 17 grew in thickness from 2.56 to 2.90 mm and in diameter from 8.64–8.66 to 8.97–8.99 mm. The Mycalex spacer from this region grew in thickness from 7.87 to 7.90 mm to 8.18 mm. The diameters of the spacers could not be measured because of breakage upon removal. The capsule tubing apparently restrained the radial growth of the spacers at the hexagonal points of contact, and the points rounded somewhat, as shown in Fig. 4.1. This photograph also shows the apparent extrusion of Mycalex material in between the Macor insulator and the fuel holder. The spacers showed some cracking before removal from the tubing, as shown in Fig. 4.2. Most broke into fragments upon removal, as shown in Fig. 4.3. The disk-shaped Macor insulators (also shown in Fig. 4.3) tended to remain intact near the ends of the capsule. However, near the center of the capsule where the fluence was higher, there were some indications that the Macor insulators had extruded into the hexagonal wrench socket of the stainless steel set screws in the bottoms of the fuel holders. It was decided to continue the use of these materials in future HANS capsules because they did serve their purpose of maintaining the fuel holders centered in the capsule, they did not harm the capsule or holders, and they have low thermal conductivity. The alumina insulators separating the SiC temperature monitors from the steel set screw remained in one piece, but they were not measured.

The SiC temperature monitors were quite difficult to remove from some of the fuel holders because of difficulty in removing the stainless steel set screws from the aluminum holders. The steel screws appeared to be tight or galled even though they were very loose when assembled. About half of the set screws in HANS-1 had to be removed by machining away the aluminum in the lathe. Some of the screws near the center also had the wrench sockets filled with material apparently from the Macor insulators. In HANS-2, the monitors that could not be removed simply by backing out the set screw were not removed.

4.2 EVALUATION OF TEMPERATURE MONITORS

The SiC temperature monitors were evaluated for each capsule by sequential annealing, followed by precision length measurements at room temperature. The results were mixed. Some of the monitors showed classic behavior with very little scatter in the data and a distinct point, identifiable within a few

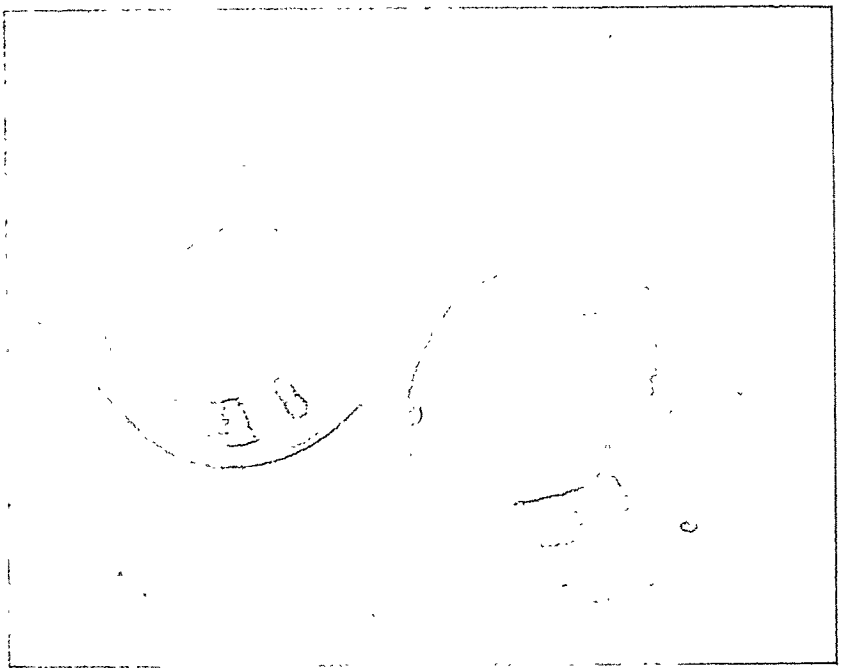

Fig. 4.1. A section of the HANS-1 capsule tube from holder 18 and a section from holder 16 containing a Mycalex spacer and a Macor insulator.

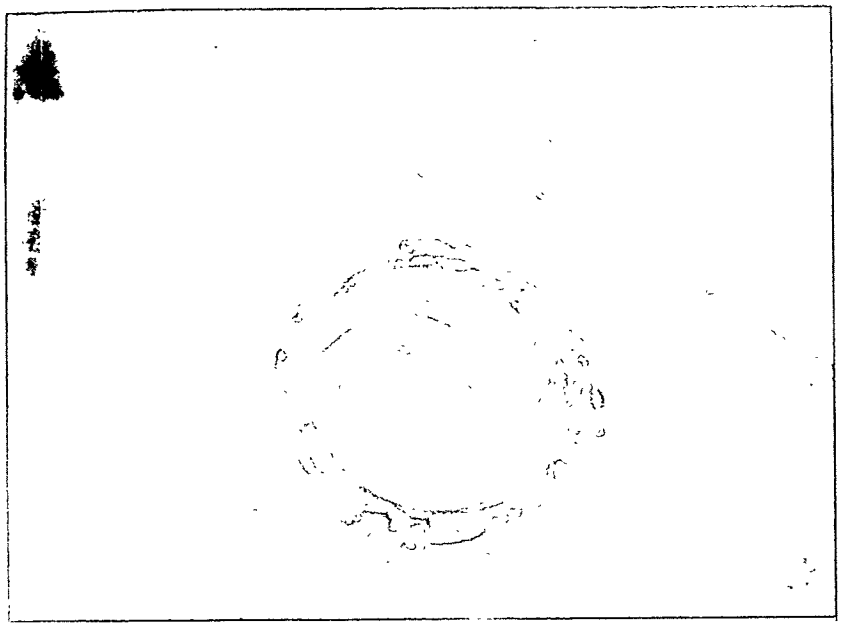

Fig. 4.2. Spacer and insulator from holder 18 showing cracks in Mycalex spacer before attempt to remove from tubing of the HANS-1 experiment.

Fig. 4.3. Crumbled Mycalex spacer and Macor insulator (disk) from holder 17 of the HANS-1 experiment.

degrees, that could be judged to be the irradiation temperature. Other monitors showed erratic behavior with either a lot of scatter in the data or no sharply defined slope change. Some examples of length vs annealing temperature curves are shown in Figs. 4.4 through 4.6.

For the HANS-2 capsule, the melt monitors were evaluated by examining the monitors metallographically to determine if the powders had melted during the irradiation. When allowance is made for about 50°C additional temperature in the melt wire capsules because of γ heating in them combined with the poor thermal conductivity of the powders, the melt monitor results are consistent with the design temperatures.

Table 4.1 presents the design temperatures of the fuel holders, along with an interpretation of data from the annealing of the SiC monitors and the results of the melt monitor evaluation. The conclusion from these data is that the best examples of the SiC evaluations tend to agree reasonably well with the design temperatures. Considering the apparent inaccuracy of many of the monitors, the design temperatures are thought to represent as good a measure of the actual temperature during irradiation as is available. During subsequent discussions, the design temperatures will be quoted as the irradiation temperature. For all practical purposes, the specimens may be considered to have been irradiated at high (300 to 450°C) or low (< 300°C) temperatures.

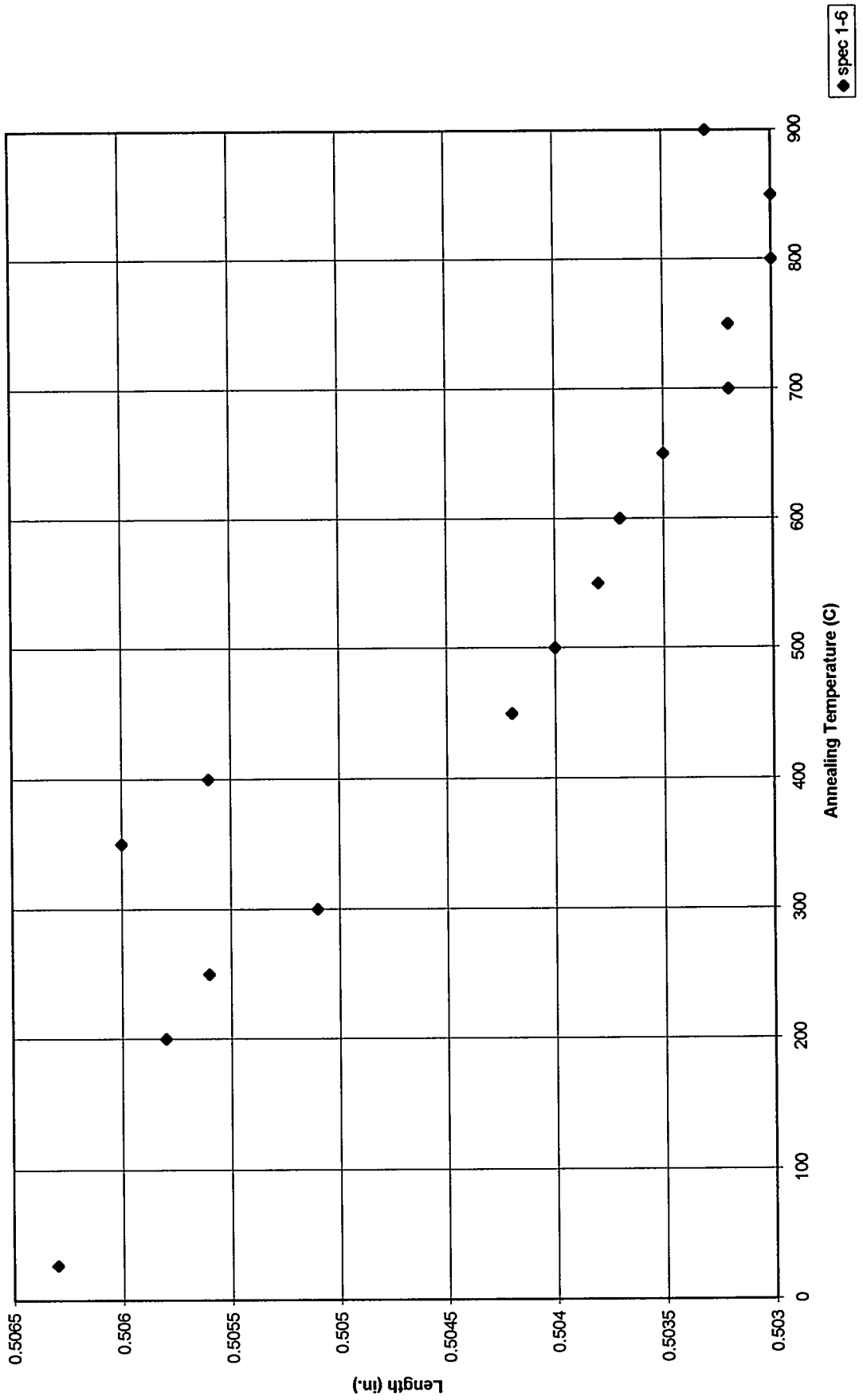

Fig. 4.4. Erratic data obtained during the postirradiation annealing of the SiC monitor from HANS-1 holder 6.

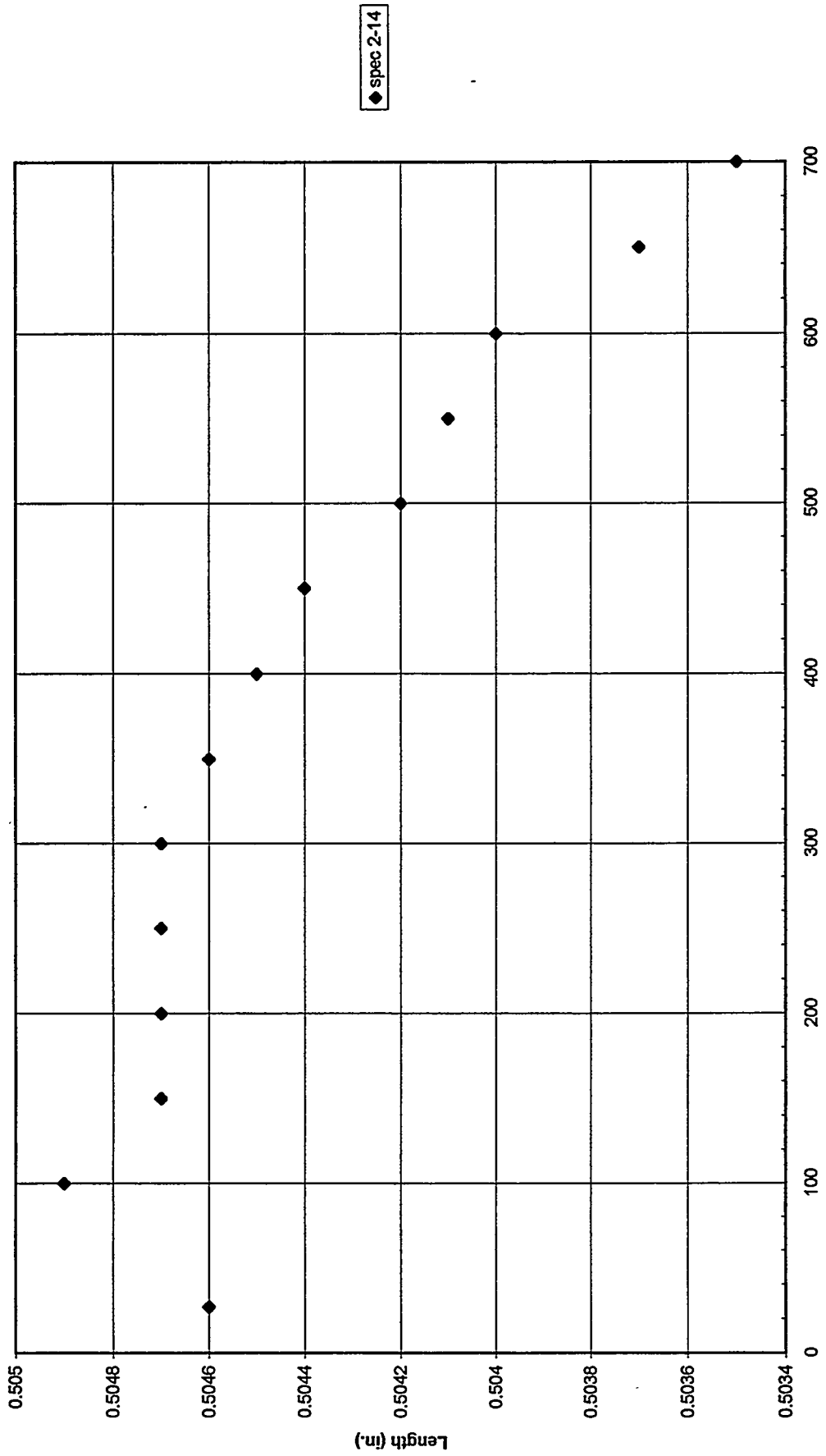

Fig. 4.5. Good data obtained during the postirradiation annealing of the SiC monitor from HANS-1 holder 14.

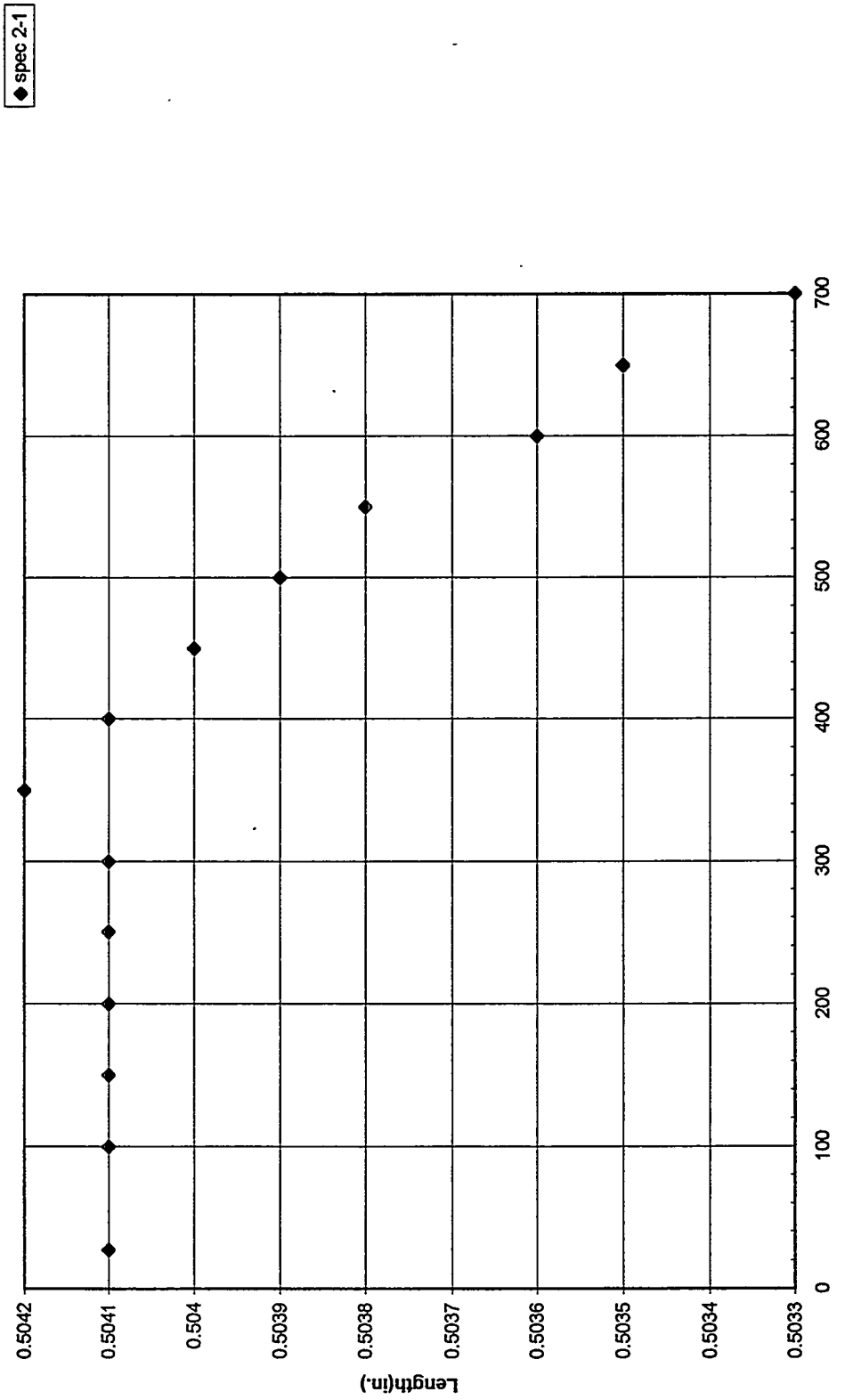

Fig. 4.6. Good data obtained during the postirradiation annealing of the SiC monitor from HANS-2 holder 1.

Table 4.1. Temperature monitor evaluation for HANS-1 and HANS-2

Fuel holder number	HANS-1		HANS-2		
	Design temperature (°C)	SiC monitor temperature (°C)	Design temperature (°C)	SiC monitor temperature (°C)	Melt monitor evaluation (°C)
1	425		425	400[a]	
2	375	300	425	370	327–420
3	325	310	250	200	
4	250	350	250	200[a]	≥271
5	<250	170	325	300[a]	≥327
6	250	200	375	280[a]	
7	325	290	375		327–420
8	375	325	425		
9	425	280[a]	425		
10	425	200	425		
11	375	225[a]	425		
12	325	275	375	200	
13	250	240	375		
14	375	450[a]	325	300[a]	
15	425	435[a]	250	285[a]	
16	375	300	250	250[a]	
17	325	315	425		
18	250	200[a]	425		

[a]Indicates better-looking curves.

4.3 BURNUP MEASUREMENTS

Mass spectrographic measurements of the uranium isotopic abundances in the burned fuel were performed on one of the fuel zones in HANS-1 samples 10 and 17 after dissolution of the fuel samples. The samples were submitted on July 1, 1992. Because of administrative restrictions in effect at ORNL at that time, there were long delays between processing steps. The actual mass spectrographic measurements were performed in late September or early October 1994. The results are shown in Table 4.2.

The ^{235}U burnup (depletion) of each sample was determined using the following relationship:

$$B = \frac{1 - A/A_0}{1 - (1 + C + D + E)A},$$

where

B = fractional ^{235}U depletion,
A_0 = fractional ^{235}U atomic abundance in fresh fuel,
A = fractional ^{235}U atomic abundance in burned fuel,
C = $^{238}U/^{235}U$ atomic depletion ratio during irradiation,

Table 4.2. Burnup Evaluation for HANS-1 holders 10 and 17

	Holder 10	Holder 17
Final ^{234}U abundance, at. %	2.01	2.23
Final ^{235}U abundance, at. %	48.6	44.30
Final ^{236}U abundance, at. %	29.72	36.21
Final ^{238}U abundance, at. %	19.67	17.26
$^{238}U/^{235}U$ atomic depletion ratio	0.00626	0.00415
$^{236}U/^{235}U$ atomic depletion ratio	–0.1442	–0.1475
$^{234}U/^{235}U$ atomic depletion ratio	0.00437	0.00344
"Measured" burnup, %	82.5	84.6
Calculated burnup, %	90.6	77.4

D = $^{236}U/^{235}U$ atomic depletion ratio during irradiation,
E = $^{234}U/^{235}U$ atomic depletion ratio during irradiation.

The parameters C, D, and E were derived from the reaction rate calculations discussed in Sect. 3. These parameters and the burnups derived from the reaction rate calculations are also tabulated in Table 4.2 along with the "measured" burnups. The burnups based on the mass spectrographic data are very similar to each other, differ from the calculated burnups by ~9%, and show an opposite burnup profile than would actually result from the axial flux profile of the reactor. Because there is no way that the actual burnup distribution could be reversed, either the samples were misidentified, or the measurements were inaccurate. Since it is highly unlikely that the samples were misidentified, perhaps the chemical dissolutions were not complete. Nevertheless, the high measured burnups do confirm that the samples reached burnups in the predicted range. Since no further data have been obtained, it has been assumed that the burnups based on calculated reaction rates are correct.

4.4 MICROSTRUCTURAL EXAMINATIONS

The microstructural examinations performed on the HANS-1 and HANS-2 samples are listed in Table 4.3. The results are discussed in the following section. In addition to the micrographs discussed and included in the text, more are in Appendix B. Negatives for most of these micrographs and others are on file at either ORNL or ANL.

4.5 DISCUSSION OF RESULTS

4.5.1 U_3Si_2-Al Interaction

Interaction between a fuel particle and the surrounding aluminum matrix during irradiation consists essentially of three items:

1. hardening of a thin shell of Al directly adjacent to the fuel particle surface, caused by fission fragment recoil damage,

Table 4.3. Microstructural examinations performed

Position	HANS-1 capsule				HANS-2 capsule		
	Fuel type	Optical metallography	Scanning electron microscopy	Electron microprobe microscopy	Fuel type	Optical metallography	Scanning electron microscopy
1	U_3Si_2				U_3O_8	X	X
2	U_3Si_2	X	X		UAl_2		
3	U_3Si_2	X	X		U_3O_8	X	
4	U_3Si_2	X	X		UAl_2	X	
5	U_3Si	X			U_3O_8		
6	U_3Si_2	X			UAl_2	X	
7	U_3Si_2	X			U_3O_8		
8	U_3Si_2	X			UAl_2	X	
9	U_3Si_2				U_3O_8		
10	U_3Si_2	X	X		UAl_x	X	X
11	U_3Si_2	X			U_3Si_2	X	
12	U_3Si_2	X			UAl_x	X	
13	U_3Si_2	X			U_3Si_2	X	
14	U_3Si	X			U_3Si_2	X	
15	U_3Si_2	X			UAl_x	X	X
16	U_3Si_2	Serial sections			U_3Si_2	X	
17	U_3Si_2	X	X	X	UAl_x	X	
18	U_3Si_2	X			U_3Si_2		

2. stress relaxation by plastic flow in the Al matrix in response to fuel particle swelling, and
3. interdiffusion of Al and U_3Si_2.

At the relatively low temperatures prevailing in existing research reactor fuels, these effects are all essentially athermal, i.e., their kinetics are determined primarily by the fission rate and the neutron flux.

Examples of these effects are shown in Fig. 4.7 for LEU and HEU dispersion fuel irradiated in the ORR, where the maximum temperature of the dispersion (meat) was approximately 100°C. The room-temperature microhardness of the matrix Al has changed from a preirradiation, fully annealed, value of 35 dph (diamond-pyramid hardness) to 75–80 dph at high burnup. This represents roughly a threefold increase in the yield strength and is in agreement with previous studies of irradiation hardening.[12] The recoil damage zone, with a width of about 12 μm, is clearly much harder yet, reaching dph values of 160 to 180.

Fuel plates are customarily finished with a cold-roll step, leaving the Al matrix with a preirradiation hardness of 50 to 60 dph. It has been shown, however, that at a relatively low neutron exposure (~10^{22} m^{-2}), this cold-worked Al recovers to the fully annealed state.[13] Thus, except for this brief initial irradiation period, both cold-worked and annealed Al have similar irradiation damage behavior.

This increase in the strength of the Al matrix does not necessarily imply a greater restraining force on the swelling fuel particle. Swelling data and modeling indicate that fuel-swelling-induced stress relaxation in the Al matrix occurs by creep. Below a temperature one-third the melting point of a material (311 K or 38°C for Al), in-reactor creep is athermal with a linear dependence on applied stress and neutron flux. With increasing temperature, irradiation-enhanced creep diminishes while classical thermally activated creep becomes more important, completely dominating the deformation above a temperature one-half the melting point (466 K or 193°C for Al). Thus, irradiation-enhanced creep primarily controls the mechanical interaction between swelling fuel particles and Al matrix in Materials Testing Reactor (MTR) type dispersion fuel. For the HANS samples, irradiated between 475 and 700 K (200 and 425°C), thermally activated creep is the controlling deformation mode.

An additional difference between hot-rolled dispersion fuel plates and the cold-compacted HANS samples is the relatively high porosity in the latter (see Fig. 4.8). The high creep rate and porosity of the Al matrix combine to lower the external force acting on the swelling fuel particles.

Interdiffusion of fuel and Al commonly occurs during irradiation at any temperature when intimate contact between fuel particle and matrix Al is established. Such contact is normally extensive in hot-rolled fuel plates, particularly after a certain amount of fuel swelling has eliminated the as-fabricated porosity that may have existed at the fuel-matrix interface. It is clear from Fig. 4.8 that in the cold-compacted HANS samples significant fractions of the fuel particle surface do not come in contact with the matrix Al during the entire irradiation and that, thus, no interdiffusion occurs at those locations.

Several annealing experiments with unirradiated U_3Si_2-Al dispersion fuel plates[14–16] have shown that the interdiffusion results in the formation of $U(Al,Si)_3$, a singular phase with the UAl_3 crystal structure wherein some of the Al atoms have been replaced by Si atoms. The two compounds UAl_3 and USi_3 are mutually soluble, as shown in the ternary phase diagram by Dwight[17] (Fig. 4.9). The composition of the interaction phase lies in the vicinity of $U_{25}Al_{60}Si_{15}$, i.e., where the tie-line between U_3Si_2 and Al crosses the singular USi_3-UAl_3 phase field. Estimates of the width of the interaction zone as a function of time and temperature are shown in Fig. 4.10. Based on this correlation, one would expect an interaction zone of <0.5 μm in the 250°C HANS irradiation after 30 d and a similar value in the ORR irradiations after ~300 d at 100 to 150°C. The actual interaction zones are much thicker, as shown in Figs. 4.7 and 4.11, and the thickness appears to correlate well with the fission density.

One may conclude that the interdiffusion at low temperatures (≤250°C) is fission enhanced. This conclusion is further supported by the results of an ORR irradiation of depleted U_3Si_2-Al. The interaction zone is barely visible (see Fig. 4.12) after an irradiation of ~250 d at the same neutron flux, but at a fission rate 1%

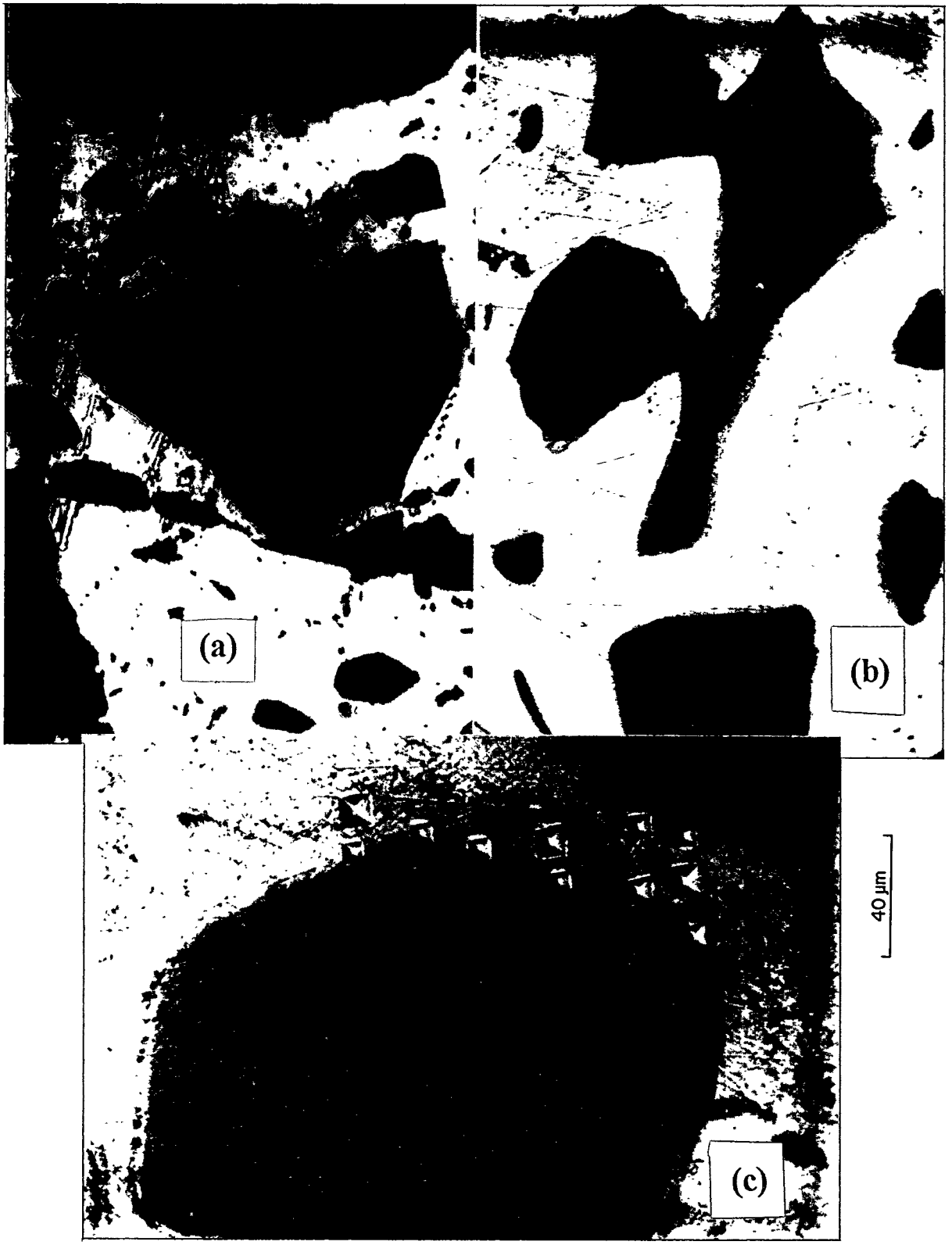

Fig. 4.7. Microstructure of LEU and HEU dispersion fuel irradiated in the ORR, showing Al-fuel interdiffusion zone surrounding fuel particles: (a) LEU, 95% burnup; (b) HEU, 42% burnup; (c) HEU, 63% burnup.

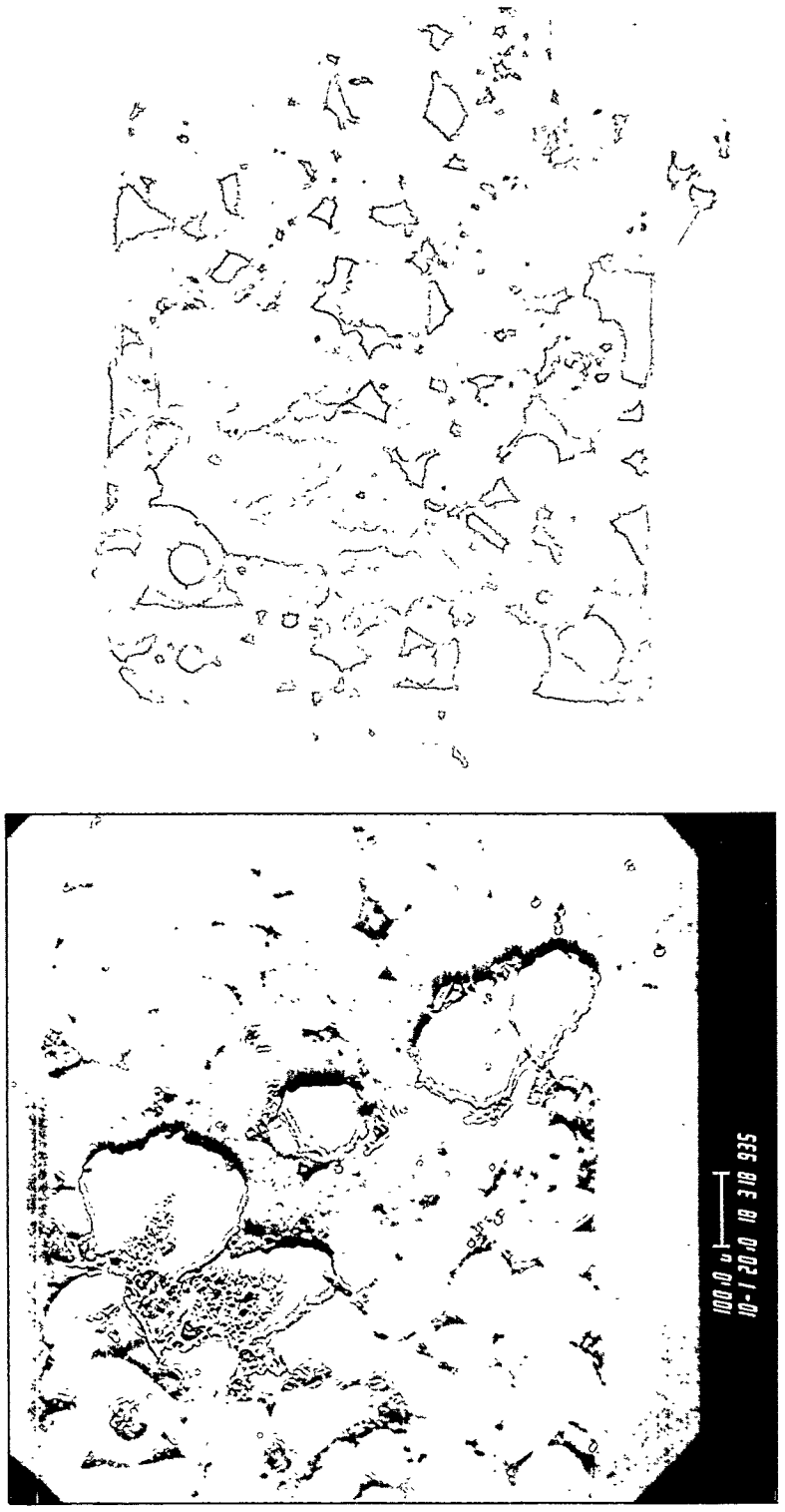

Fig. 4.8. Optical and SEM images of longitudinal section through HANS sample, showing areas with no Al-fuel contact.

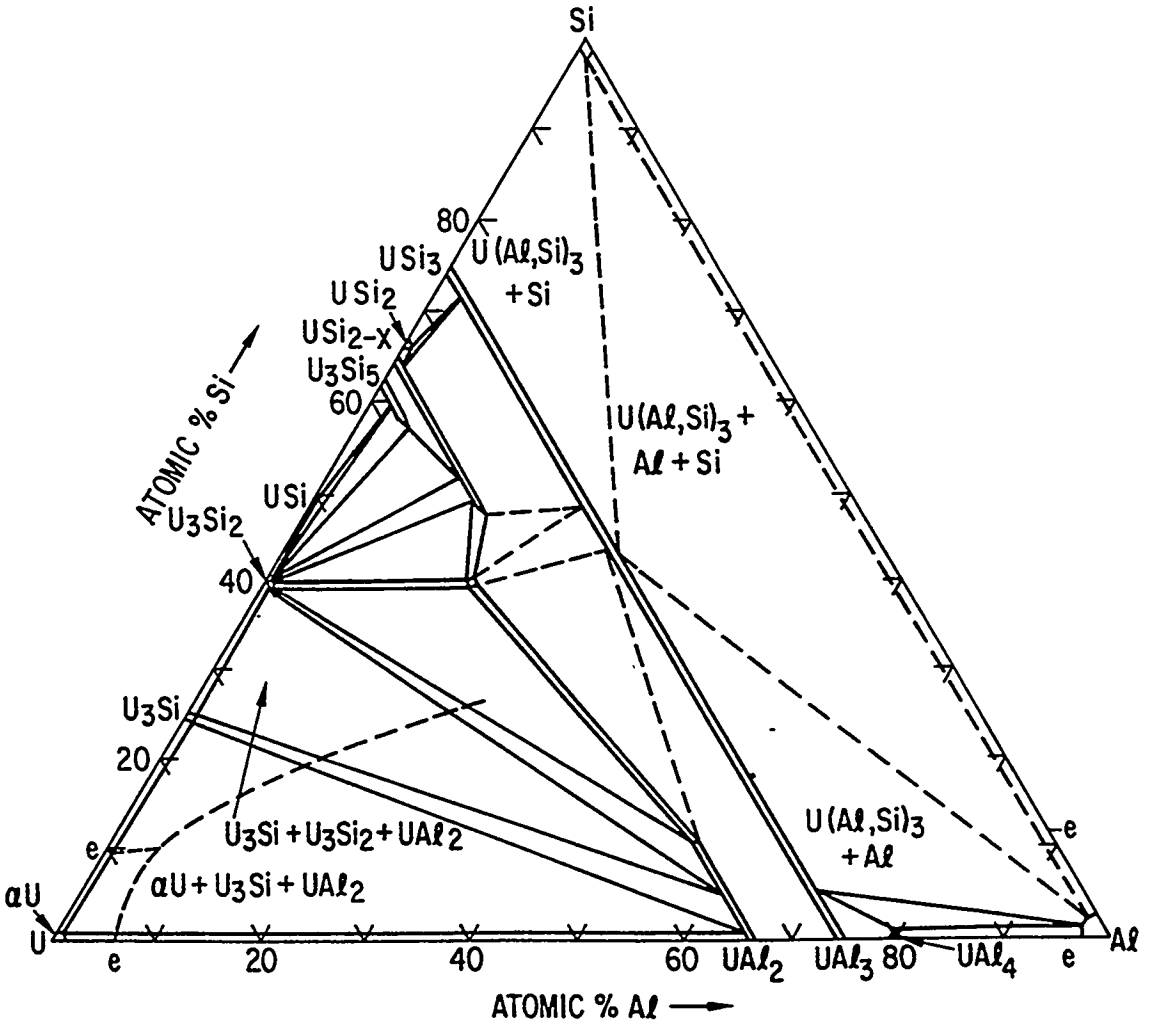

Fig. 4.9. Isothermal section of the U-Al-Si system at 400°C. *Source*: Ref. 17.

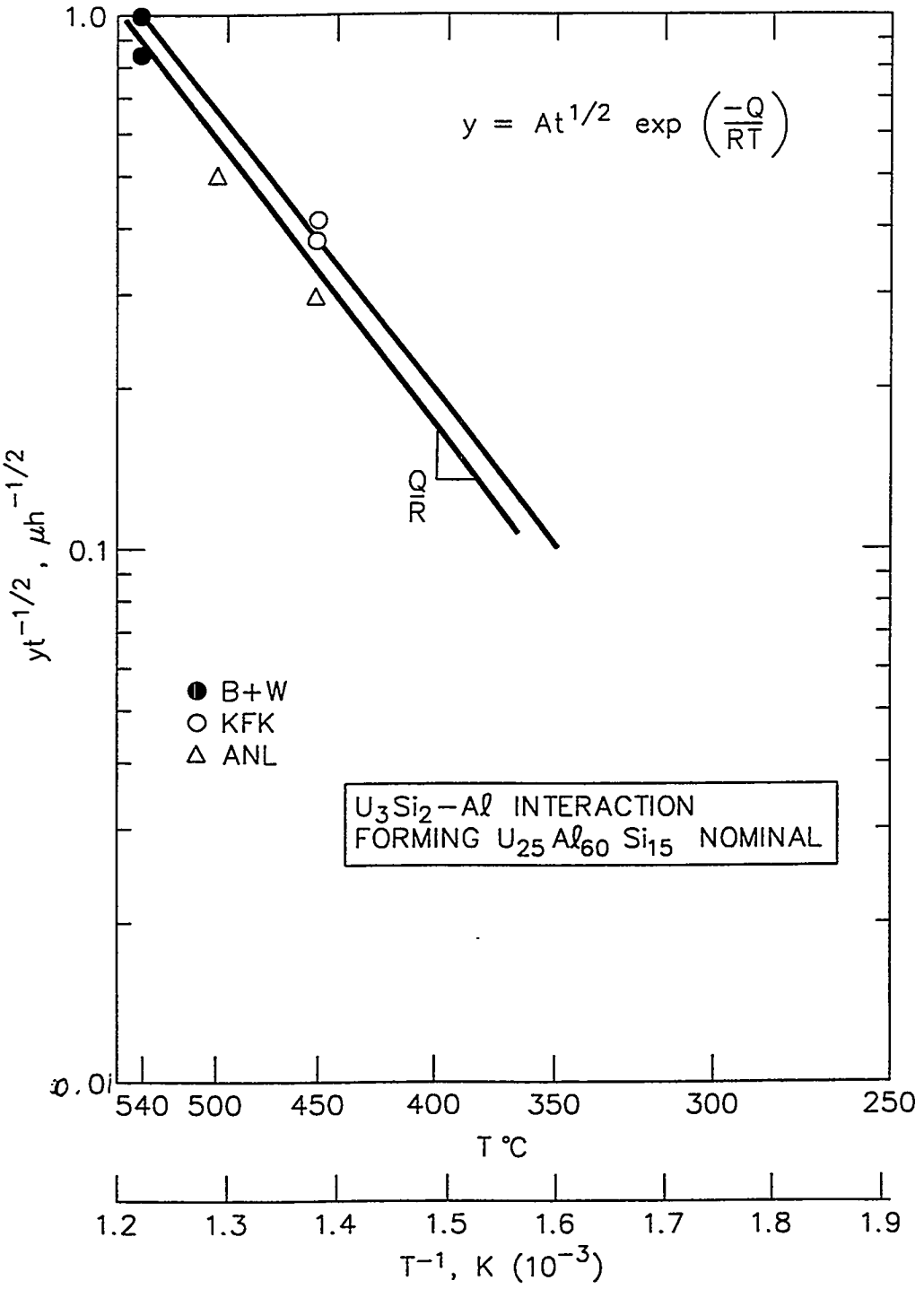

Fig. 4.10. Width of the Al-U_3Si_2 interaction zone as a function of temperature.

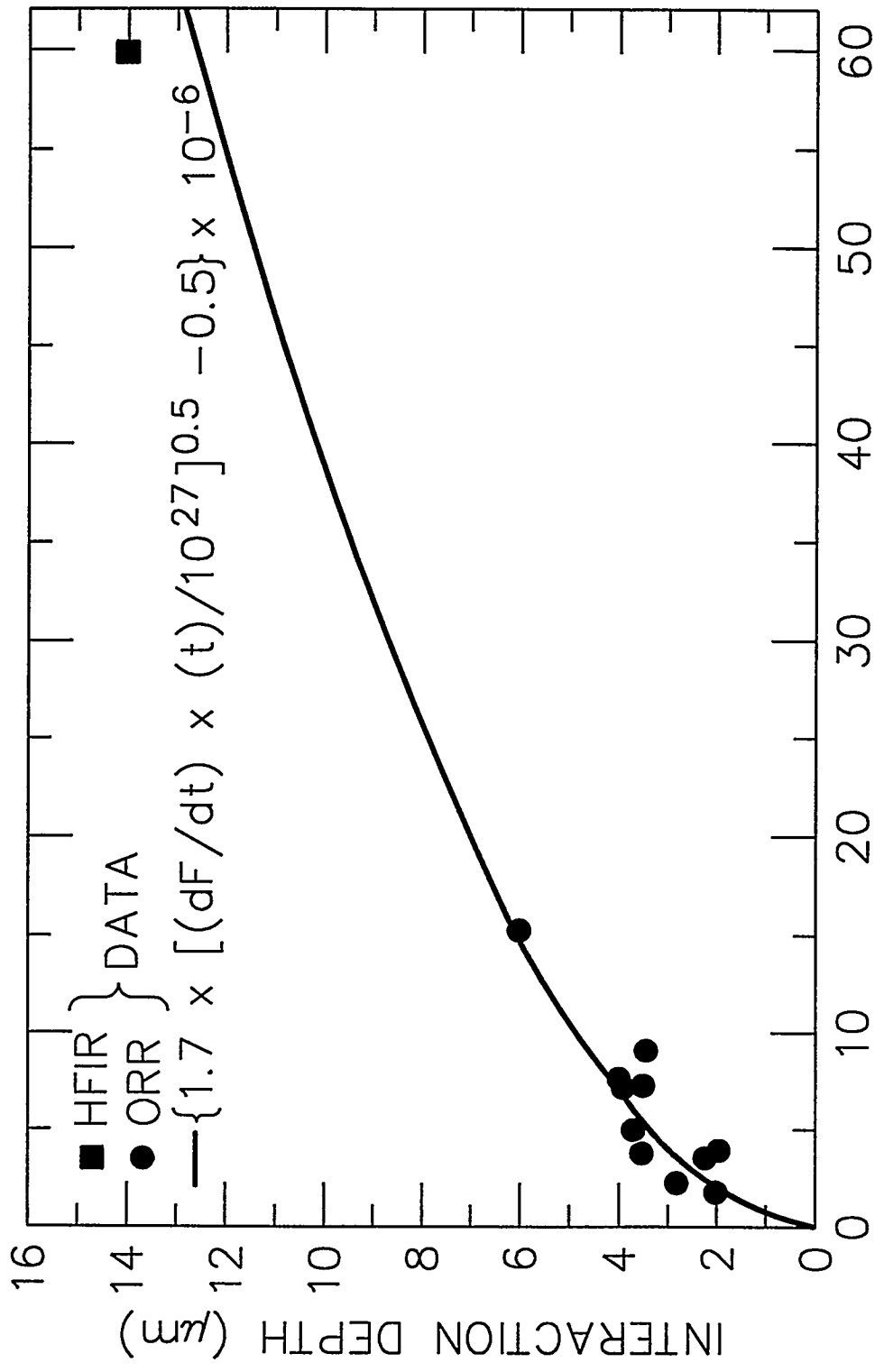

Fig. 4.11. Measured Al-U_3Si_2 interaction zone width as a function of fission density (T < 250°C).

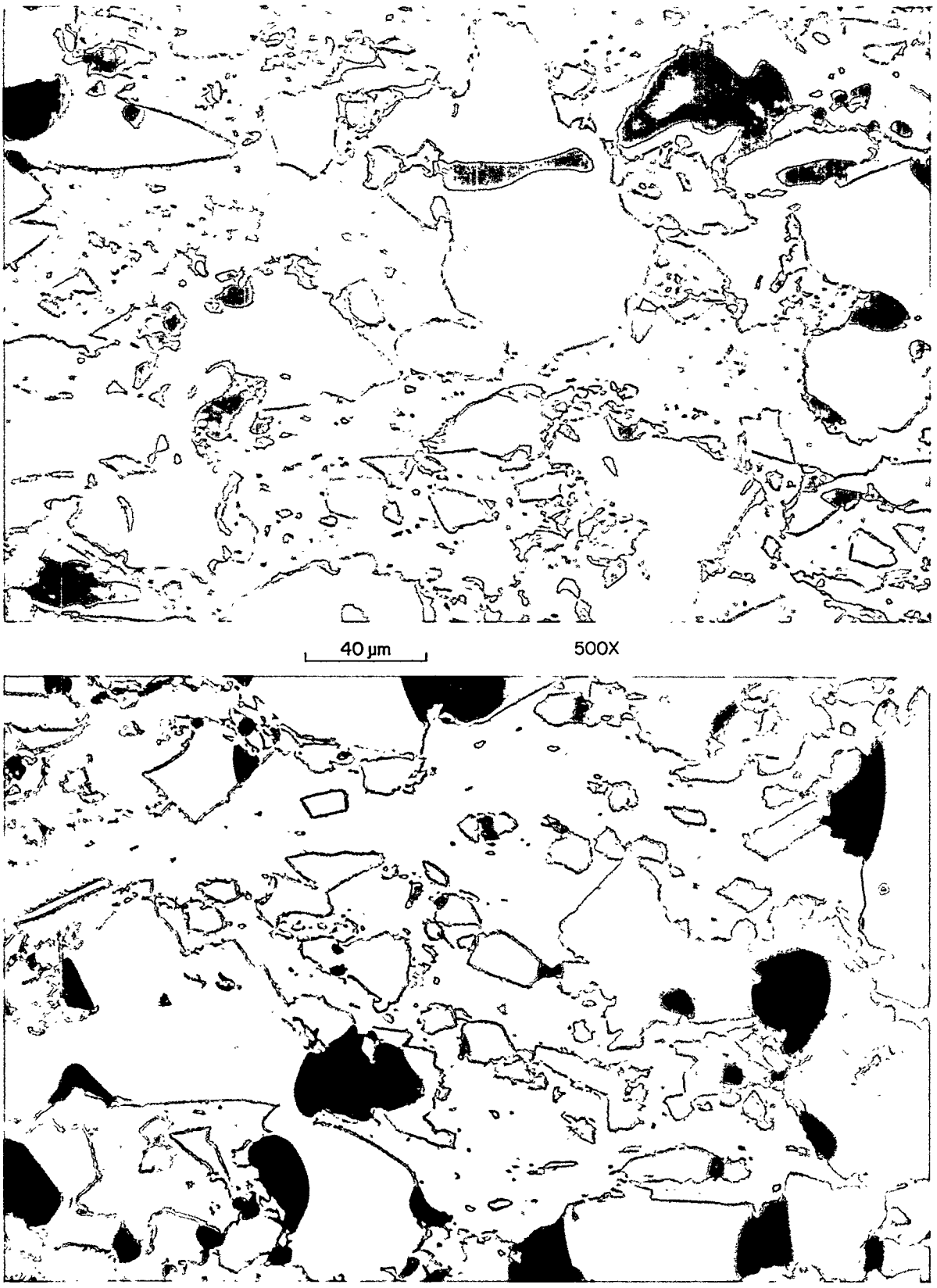

Fig. 4.12. Microstructure of depleted U_3Si_2-Al fuel plates irradiated for ~250 d in the ORR, showing absence of significant interaction.

that of LEU sibling fuel test plates. For the higher-temperature HANS samples, the correlation shown in Fig. 4.10 predicts considerable interdiffusion, e.g., 7 μm for an irradiation time of 30 d at 425°C.

Comparison of the interdiffusion behavior in annealing tests of unirradiated fuel with that during irradiation is complicated not only by direct fission enhancement but also by substantial changes in the fuel chemistry as a result of U burnup, particularly for the case of HEU in the HANS test where, at ~90% burnup, 84% of the original U has been transmuted to fission product elements. The resulting chemical changes likely affect the diffusivities in the interaction zone, and indeed the width of the zone in the high temperature HANS samples appears to be larger than the out-of-reactor correlation predicts. For modeling purposes, the correlation is adjusted to match the experimental observations. Despite these chemical changes, the irradiation behavior of the material in the interdiffusion zone remains very stable (see Fig. 4.13) and continues to resemble the fission-gas-bubble-free microstructure of UAl_3 up to high burnup.[18]

However, closer examination with the SEM suggests that the interaction phase at the particle periphery actually is composed of two different zones (see Fig. 4.14). Compositional analysis, using SEM energy-dispersive X-ray analysis (EDX) shows that the composition of these two zones is very similar and that their different appearance results from the differences in microstructure. This point will be elaborated in the discussion on fuel swelling.

The compositional analysis of the samples was difficult because of their high γ activity. Several samples were ground down to reduce the number of fuel particles and thereby the intensity of the γ radiation to the EDX detector. This was a delicate operation because of the small size of the dispersion samples and was only partially successful. Nevertheless, enough suitable samples were obtained to cover the temperature range in the HANS test. The results of the EDX analyses are listed in Table 4.4 both for the porous center and for the interaction zone at the periphery of representative fuel particles. Examination of the data reveals some inconsistencies. The U/Si ratio, which at 85 to 90% burnup should be around 0.4, (see Fig. 4.15) is significantly lower—except for sample 18. Also the fraction of fission product elements is much lower than their calculated yield at this burnup because of the X-ray peak broadening and background scattering owing to the high γ activity of most of the samples. Sample #18 had a substantially lower γ activity than the other samples, and the effect can be readily seen in the comparison of the X-ray energy spectra of sample #18 and the more-radioactive sample #17, shown in Fig. 4.16. In the more-radioactive sample, the peaks of Si as well as those of some fission products are poorly resolved, leading to inaccurate readings. The γ-ray background problem can be eliminated by using an electron microprobe (EMP), which utilizes X-ray wave length dispersion rather than energy dispersion to detect the elements in a sample. This type of examination is much more time consuming and costly, however, and was performed on only one sample. The results of the microprobe analysis on sample 17, a highly radioactive sample, are shown in Table 4.5. A comparison with the EDX data in Table 4.4 shows that the EMP data are quite different. The U/Si ratio is commensurate with the ^{235}U burnup experienced by the sample. Also, the fraction of high-yield fission product elements detected at the particle center (~35 at. % for Mo-Zr, Nd-Ce, Tc-Ru, and Cs) is not far from the calculated value at 85% ^{235}U burnup, namely, 30 at. %. It is therefore assumed that the EMP results most accurately reflect the postirradiation composition. The less accurate but more readily obtainable SEM-EDX data are used in a relative sense, primarily to delineate zones of high and low Al in the fuel particles.

4.5.2 U_3Si_2 Fuel Swelling

Swelling of U_3Si_2 has been well characterized during the RERTR program. As shown in Fig. 1.3, swelling appears to proceed with fission density in two distinct stages. At the lower fission density stage, fission gas bubbles are not observed with the SEM, which has a resolution limit of ~300 Å (30 nm) for features such as gas bubbles. This lack of observable bubbles is consistent with current fission gas behavior models, such as

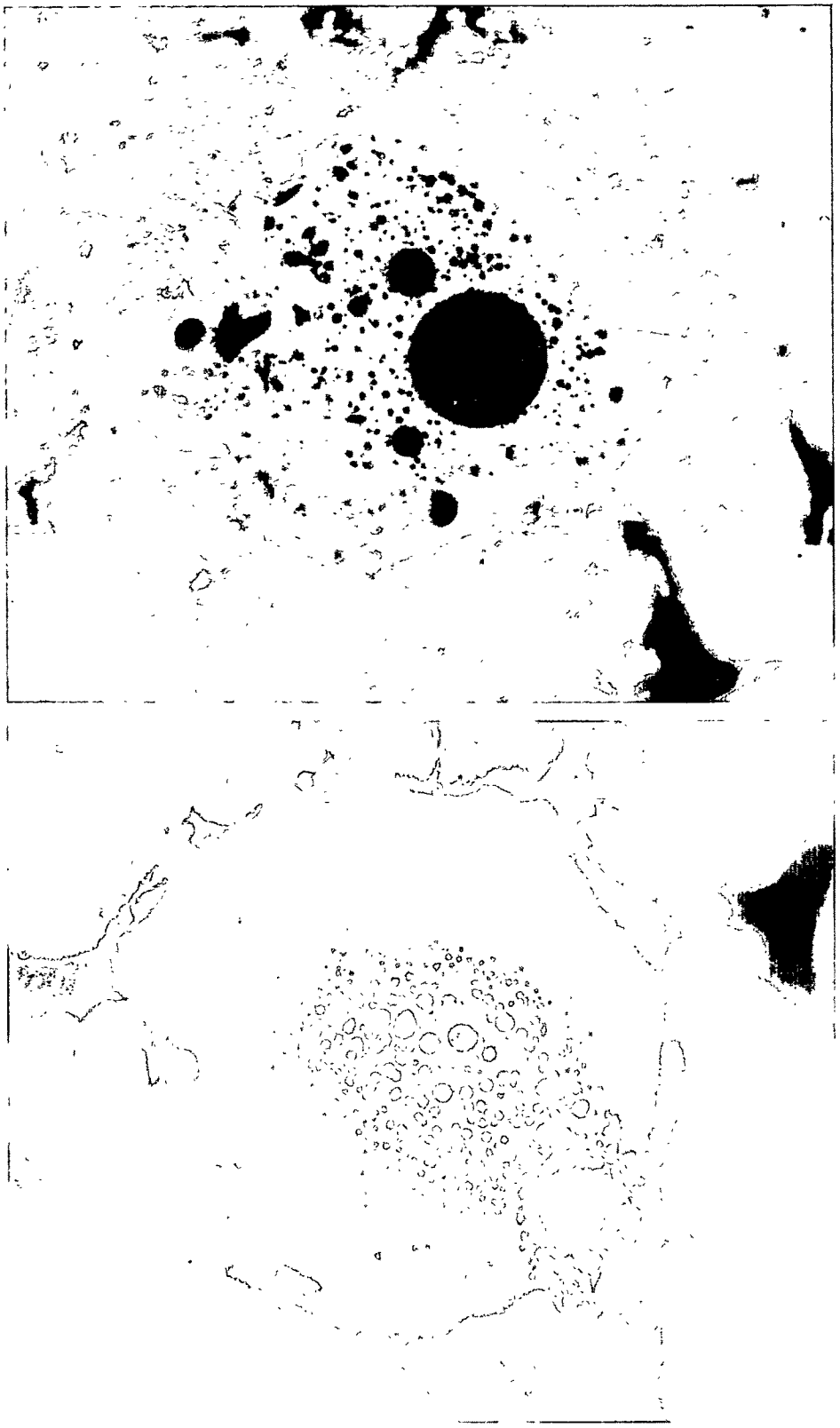

Fig. 4.13. Microscructure of U_3Si_2 fuel particles irradiated at 250 and 425°C the HANS-1 experiment, showing bubble-free interaction zone.

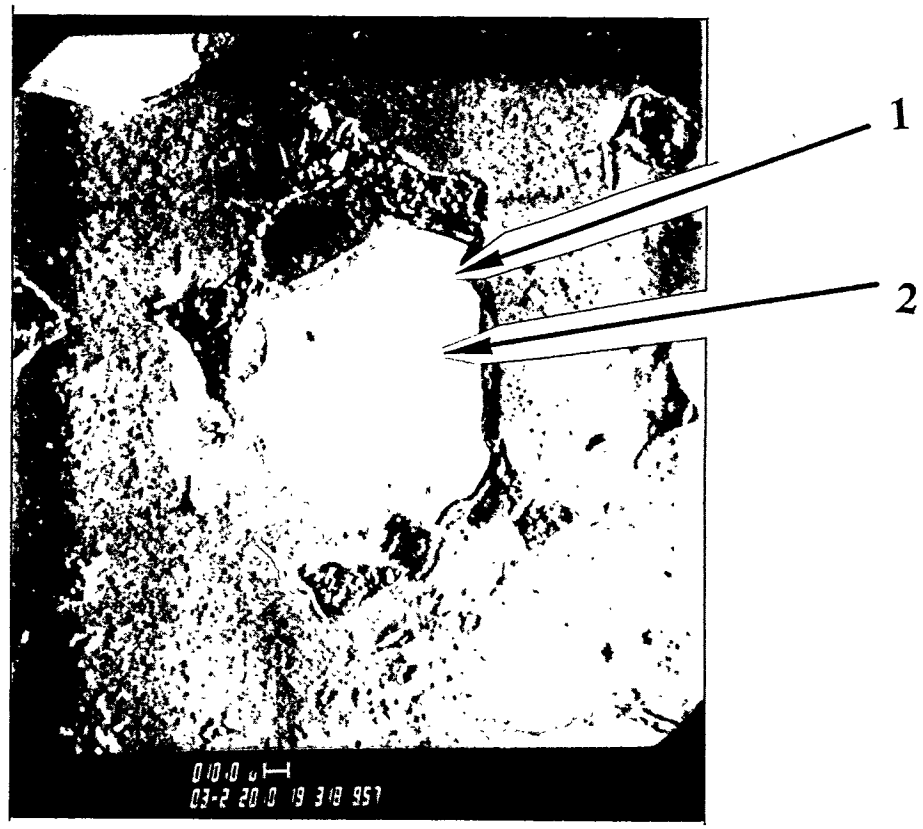

Fig. 4.14. SEM image of the interaction zone in U_3Si_2, showing presence of two zones.

Table 4.4. Compositional analysis by SEM-EDX of several U_3Si_2 samples from the HANS-1 experiment[a]

Sample	Temperature (°C)	Al (at. %)	Si (at. %)	U (at. %)	U/Si ratio	Fission products (at. %)
			Porous center of fuel particles			
2	375	29	55	5	0.09	11
16	375	30	51	6	0.12	13
17	325	21	61	8	0.13	10
18	250	18	50	18	0.36	14
			Periphery of fuel particles			
2	375	71	18	4	0.22	7
6	250	63	20	5	0.25	12
10	425	62	30	2	0.07	6
16	375	70	18	5	0.28	7
17	325	53	41	3	0.07	4
18	250	63	19	7	0.37	11

[a] Each entry represents an average of two or more data points.

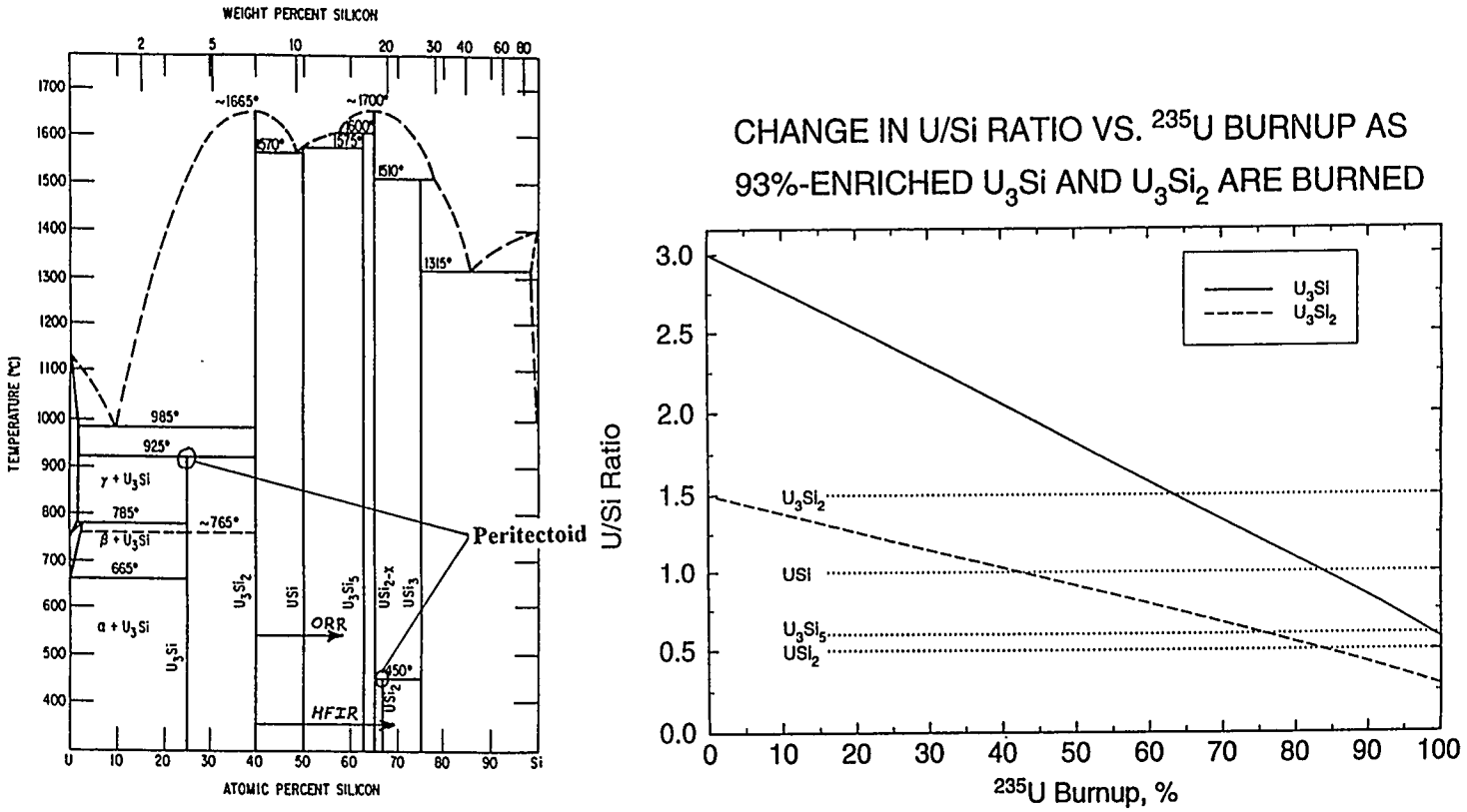

Fig. 4.15. U-Si phase diagram and change in U/Si ratio as HEU U_3Si and U_3Si_2 are burned.

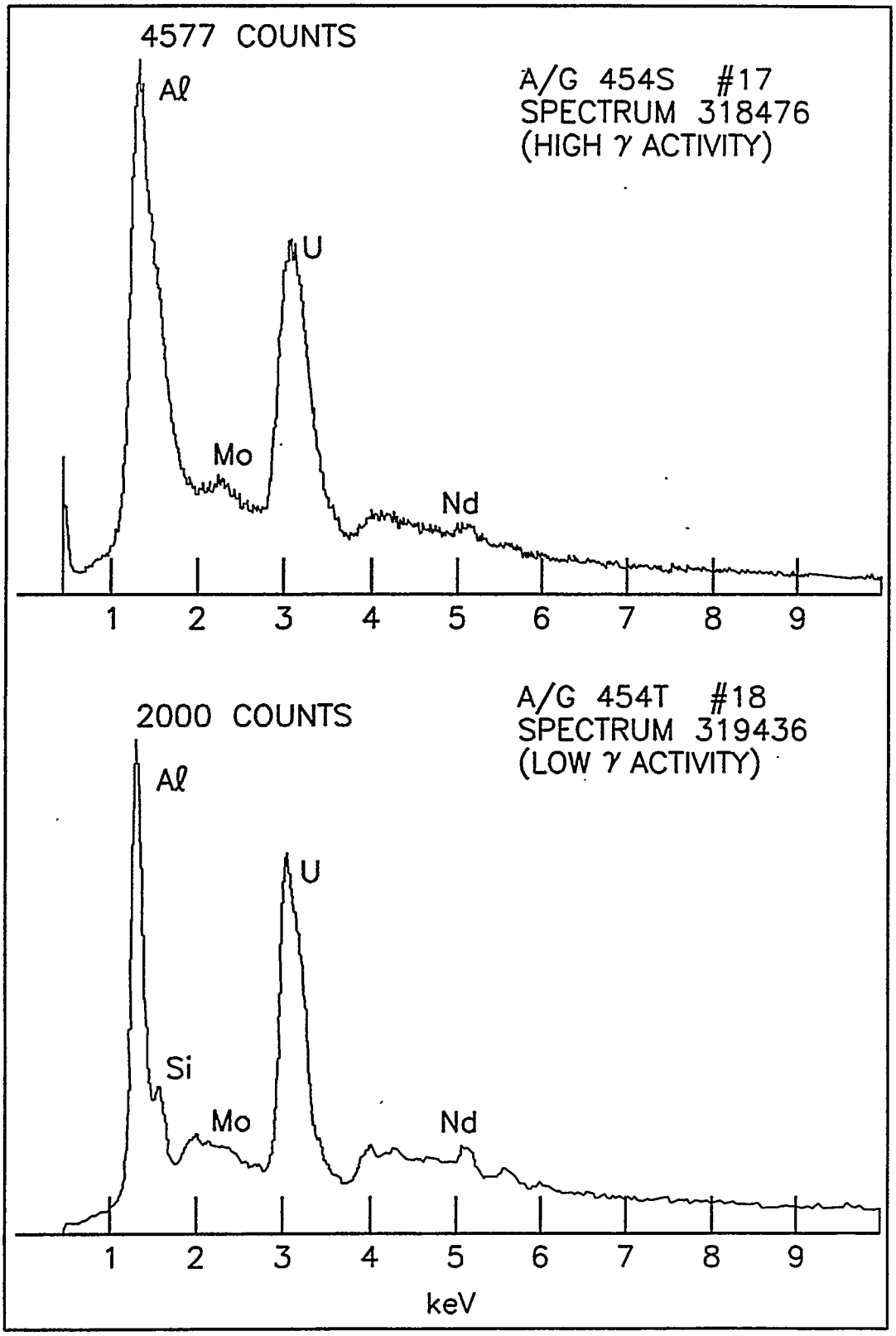

Fig. 4.16. X-ray energy spectra of HANS-1 samples 17 and 18.

Table 4.5. Electron microprobe measurements on U_3Si_2 sample 17 from the HANS-1 experiment, 325°C[a]

Location	Al (at. %)	Si (at. %)	U (at. %)	U/Si ratio	Fission products (at. %)
Porous center	28	32	10	0.31	30
Periphery	53	22	7	0.32	18

[a]Each entry represents the average of three data points.

GRASS-SST,[19] which predict the growth of bubbles of ~100 Å (10 nm) diam in a crystalline fuel at low temperature, even at high fission densities. Such models thus describe the low fission density swelling stage, which is characterized by the accumulation of solid fission products and very small fission gas bubbles in the U_3Si_2 matrix. At around the transition from the low fission density to the high fission density stage (the "knee" in the swelling plot) gas bubbles are beginning to appear, as shown in Fig. 4.17. The difference between the two curves "B" represents the additional swelling resulting from the volume of the gas bubbles.

From this point on, they rapidly multiply into a rather uniform population, as shown in Fig. 4.18. These gas bubbles grow in size with increasing fission density but do not interact, and, therefore, breakaway swelling does not occur in U_3Si_2 under these conditions. This fact is illustrated in Fig. 4.19, showing the gas bubble distribution in HEU irradiated in the ORR up to a ^{235}U burnup of ~63% (14×10^{27} fissions m^{-3}). In addition to the complete lack of bubble linkup, there appear to be two distinct bubble-size distributions. Another observation made in the postirradiation analysis of U_3Si_2 was an apparent effect of fission rate on gas bubble development. As shown in Fig. 4.20, the swelling and bubble distribution for HEU are equivalent to those for LEU but at nearly twice the fission density. Since LEU and HEU were irradiated under the same reactor conditions, the only distinguishing parameter is the rate of ^{235}U fissioning.

As mentioned before, existing fission gas behavior models did not allow the calculation of the observed bubble morphology and also did not provide an explanation for the apparent fission rate effect. The GRASS-SST code did, however, predict the correct bubble size on grain boundaries, if present. Indeed, as seen in Fig. 4.18(a), such bubbles are occasionally observed well before the second swelling stage at rare grain boundaries (the ground fuel particles are chiefly pieces of grain, i.e., single crystals). When the models in GRASS-SST were modified by the ad hoc introduction of small subgrains, at the "knee" in the swelling plot, with a size suggested by the bubble patterns in Figs. 4.19 and 4.20, the observed bubble morphology in the second swelling stage could be modeled. The fission rate effect was modeled by making the occurrence of the grain subdivision (or grain refinement) dependent on fission rate. Support for this phenomenon was found in earlier observations of fission-induced grain refinement in uranium oxides.[20] It will be shown in the following discussion of the HANS tests that grain refinement does in fact occur in U_3Si_2.

Although the stable and predictable swelling behavior of U_3Si_2 experienced in the RERTR program boded well for the ANS fuel, the much more severe projected operating conditions are well beyond the existing data base. Temperature, fission rate, and burnup are all substantially higher, and the HANS tests that covered the ANS parameter range did indeed show some new aspects in the irradiation behavior of U_3Si_2.

The most remarkable feature is the presence of an irregular distribution of relatively large fission gas bubbles at the centers of practically all fuel particles. Examples representing the range of irradiation temperatures in the HANS test are shown in Fig. 4.21. Apart from the peripheral zones that have been transformed to some aluminum compound, as described in the preceding section, the fuel appears to have reached a breakaway swelling stage in which bubbles interlink and grow to rather large size.

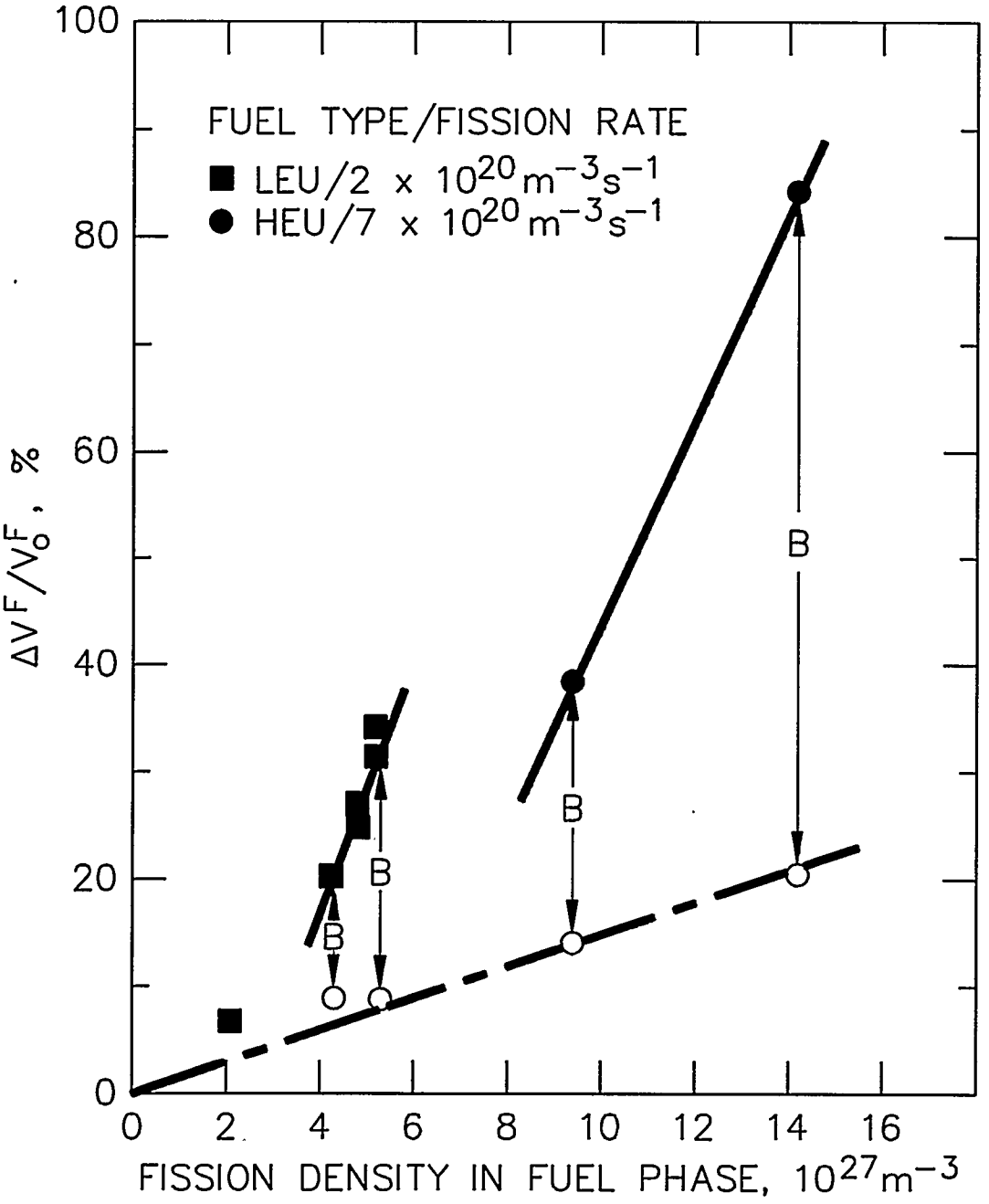

Fig. 4.17. Swelling behavior of U_3Si_2. The quantity "B" is the measured swelling owing to fission gas bubbles visible in the SEM. The open circles represent the difference between the measured gross swelling (from immersion density) and the measured swelling owing to gas bubbles.

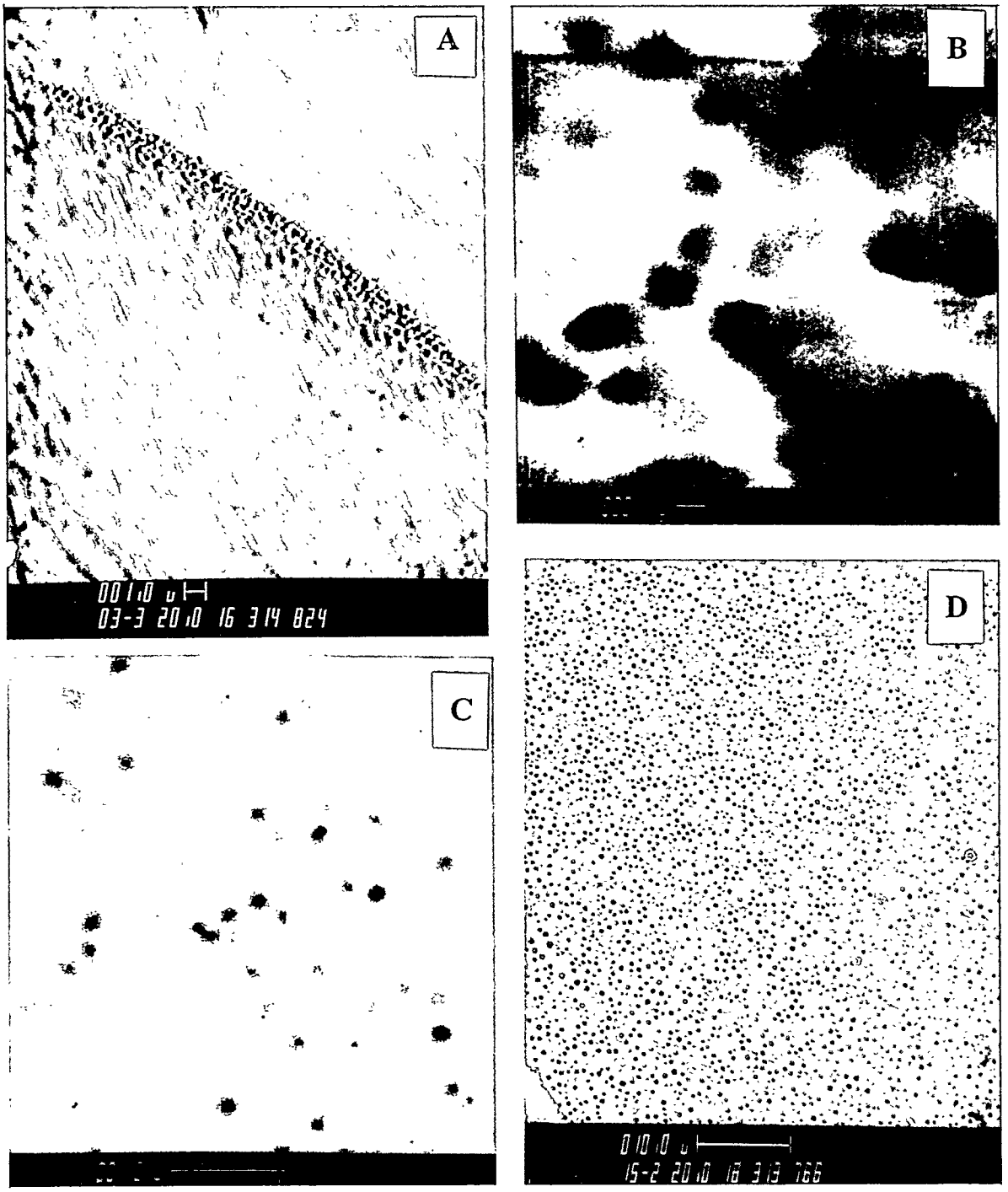

Fig. 4.18. SEM images of U_3Si_2, showing evolution of fission gas bubbles. (a) Bubbles formed before the "knee" of the swelling curve on an original grain boundary (sample is ion etched), (b) and (c) first evidence of fission gas bubbles in LEU U_3Si_2 forming just at the "knee" of the swelling curve, (d) uniform bubble population beyond the "knee" of the swelling curve.

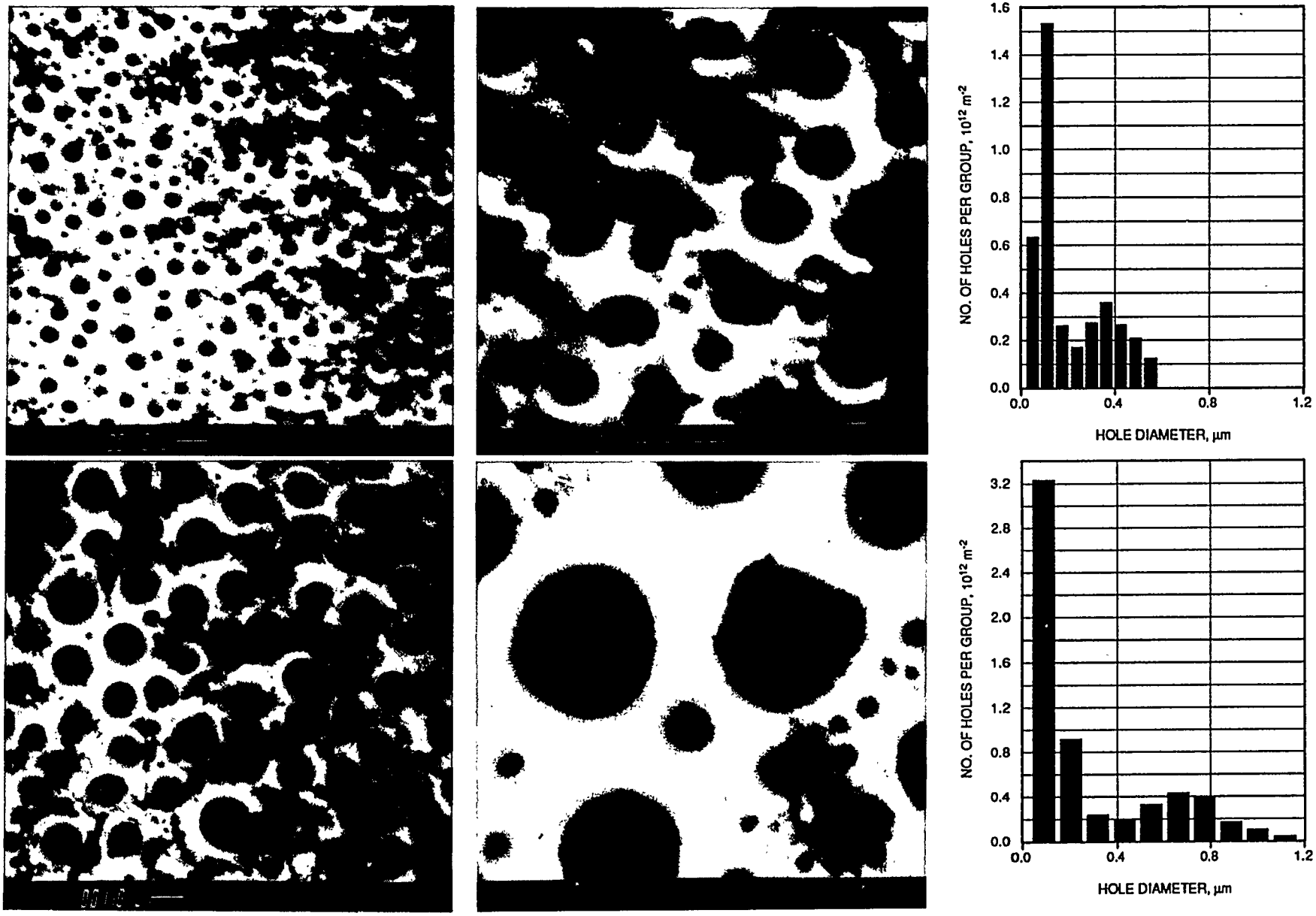

Fig. 4.19. Fission gas bubble distributions in HEU U_3Si_2 irradiated in the ORR to 9×10^{27} and 16×10^{27} fissions m^{-3} at 7×10^{20} fissions m$^{-3} \cdot$ s^{-1}.

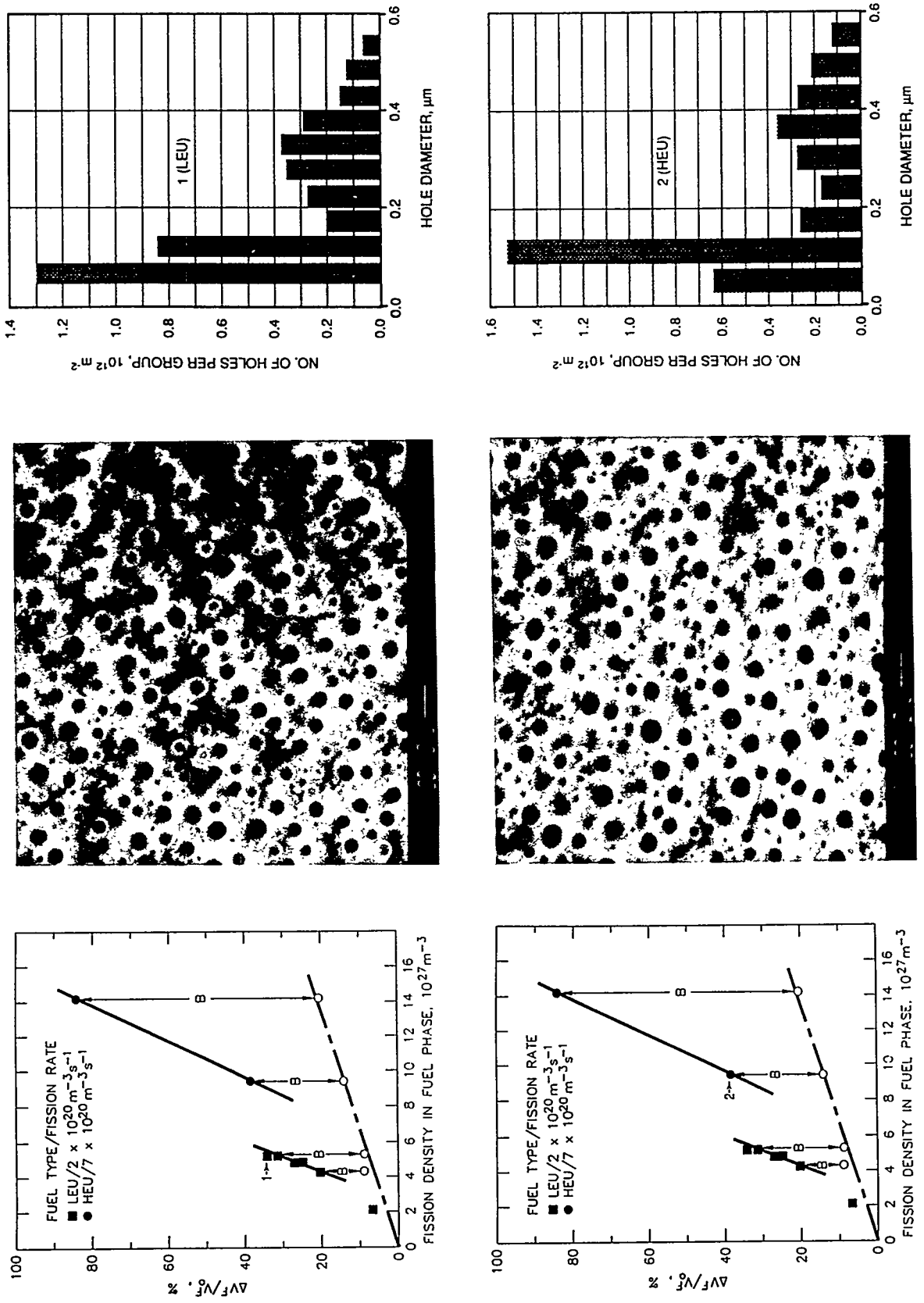

Fig. 4.20. Fission gas bubble distributions of LEU (upper) and HEU (lower) U_3Si_2 irradiated in the ORR.

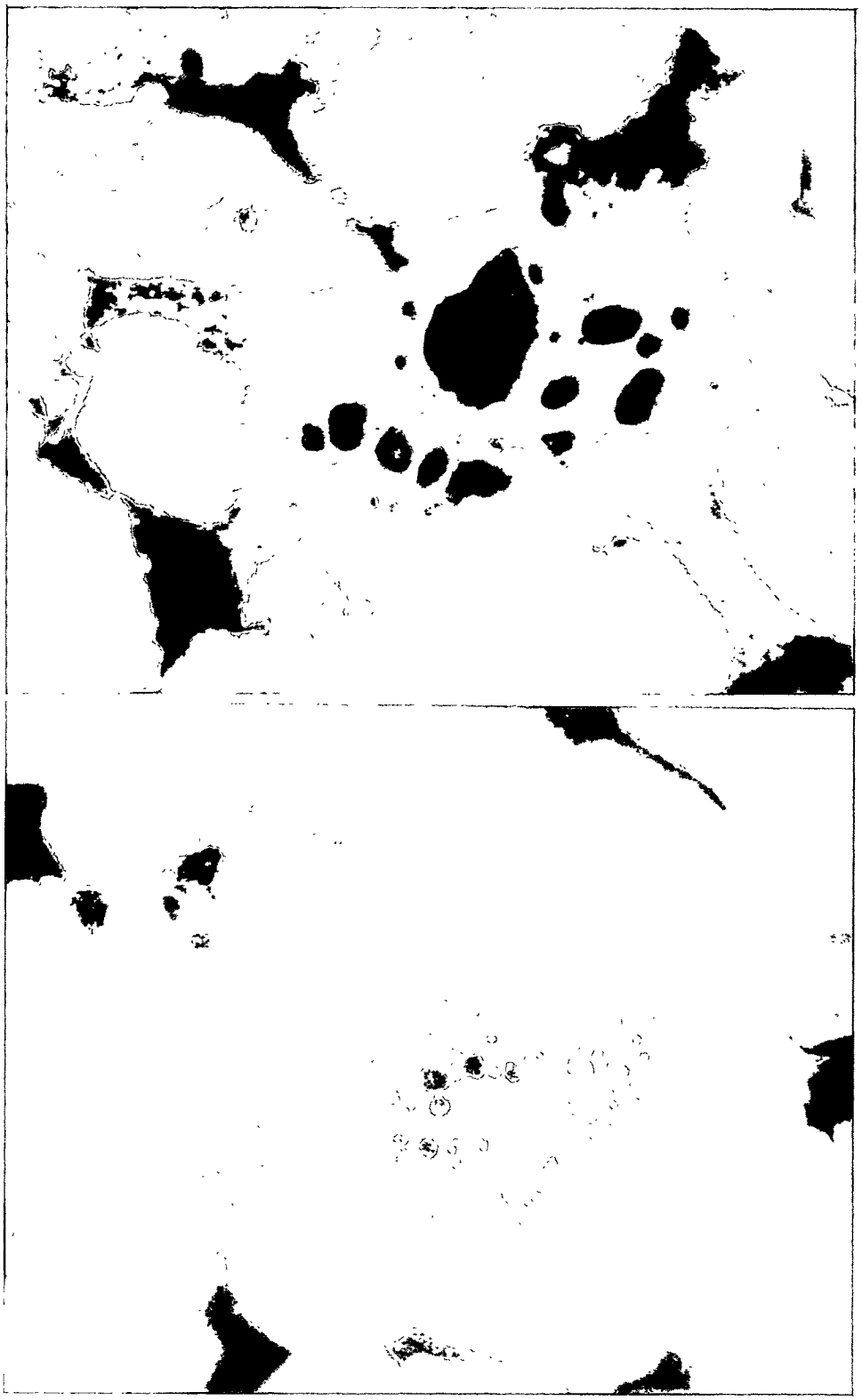

Fig. 4.21. Microstructures of U_3Si_2 fuel particles irradiated in the HANS-1 experiment at 250 and 425°C, showing the presence of large bubbles at the centers of the fuel particles.

Some particles appear bubble free, but this effect is simply the result of the random section through the sample, by which some particles are cut through their bubble-free peripheral zone rather than their centers. The often-observed asymmetric patterns are a result of the cold compaction of the sample, which left voids at the fuel particle-aluminum interface. These voids are also the site of oxide accumulation. If, as would be the case for a roll-bonded dispersion, the fuel particles were completely encased and in intimate contact with the aluminum matrix, the peripheral zone and central porous zone would be concentric. This expectation is clearly supported by the sequence of serial sections through two adjacent particles shown in Fig. 4.22.

One of the lowest burnup samples (sample 18) has some very interesting features in its porous center. This is a 250°C sample and therefore has a small aluminide zone and conversely a large porous center zone, as shown in Fig. 4.23. In most of this center zone, the gas bubbles are clearly coarsening, and the fuel is in breakaway swelling except for some areas (marked "A" in Fig. 4.23) that look very similar to the lower-burnup ORR HEU fuel shown in Fig. 4.7(c). It seems that this sample is in a transition from "typical" U_3Si_2 gas bubble behavior to a breakaway mode. The other higher-burnup samples have all made this transition at the end of the HANS irradiation period. It may be concluded that the centers of all particles up to a certain burnup, perhaps ~80%, had the uniform bubble patterns characteristic of U_3Si_2.

As was noted in the preceding section on fuel-Al interaction, the bubble-free (high-Al) zone at the particle periphery actually comprises two structurally different subzones that are revealed by SEM examinations (see Fig. 4.24). At high magnification, it appears that only the outer zone is truly gas bubble-free with the featureless appearance characteristic of UAl_x. The intermediate zone, while having an Al content similar to that of the outer zone, has a distinct substructure resembling small grains. The boundaries of these grains are visible in the SEM image shown in Fig. 4.25, most likely because fission gas has collected on them. More defined gas bubbles are present at several grain boundary junctions. This substructure is very similar to that observed previously in uranium oxides and forms the basis for the fission gas behavior model.

4.5.3 U_3Si_2 Irradiation Behavior Model

A detailed description of the irradiation behavior model of U_3Si_2-Al is presented in a report on the DART code by J. Rest[21] and in several publications written during the course of this project and referenced in the DART code report. The metallurgical understanding that has evolved from the RERTR tests through the HANS experiments, which forms the basis for the models used in the DART code, can be summarized as follows.

At a certain burnup or corresponding fission density, U_3Si_2 undergoes complete recrystallization into submicron-size grains, a process referred to as "grain refinement." Fission gas precipitates on the boundaries and boundary junctions between these small new grains, resulting in a rather uniform, bimodal distribution of noninteracting gas bubbles that grow in size with increasing fission density.

Prior to the recrystallization event, fission gas forms very small bubbles in the original U_3Si_2 matrix, so small that they cannot be seen with the SEM. This change in fission gas behavior results in two stages of swelling as a function of fission density, where the swelling rate in the second stage is approximately three times that of the first stage. The onset of the second stage shifts to a higher fission density with increasing fission rate. At very high fission density corresponding to ~80% HEU burnup, the regular fission gas bubble distribution breaks down and breakaway swelling occurs in that part of the fuel that is no longer uranium silicide but rather an unknown alloy of Si, fission product, and a minor fraction of U.

Aluminum diffusion into the fuel takes place during the entire irradiation. At 250°C and below, the diffusion rate is athermal and fission enhanced. At higher temperatures thermal activation determines the diffusivity. Diffusion of Al occurring prior to recrystallization results in an aluminide-type $U(Al,Si)_3$ interaction zone. Continued diffusion after recrystallization may transform a second zone into small-grained $U(Al,Si)_3$. Minor Al diffusion may extend into the center of the fuel particle without affecting the transformation to aluminide, but this Al may have an effect on the final breakaway swelling behavior at the fuel particle centers. These concentric zones thus formed each have their own characteristic irradiation behavior, as illustrated in Fig. 4.26.

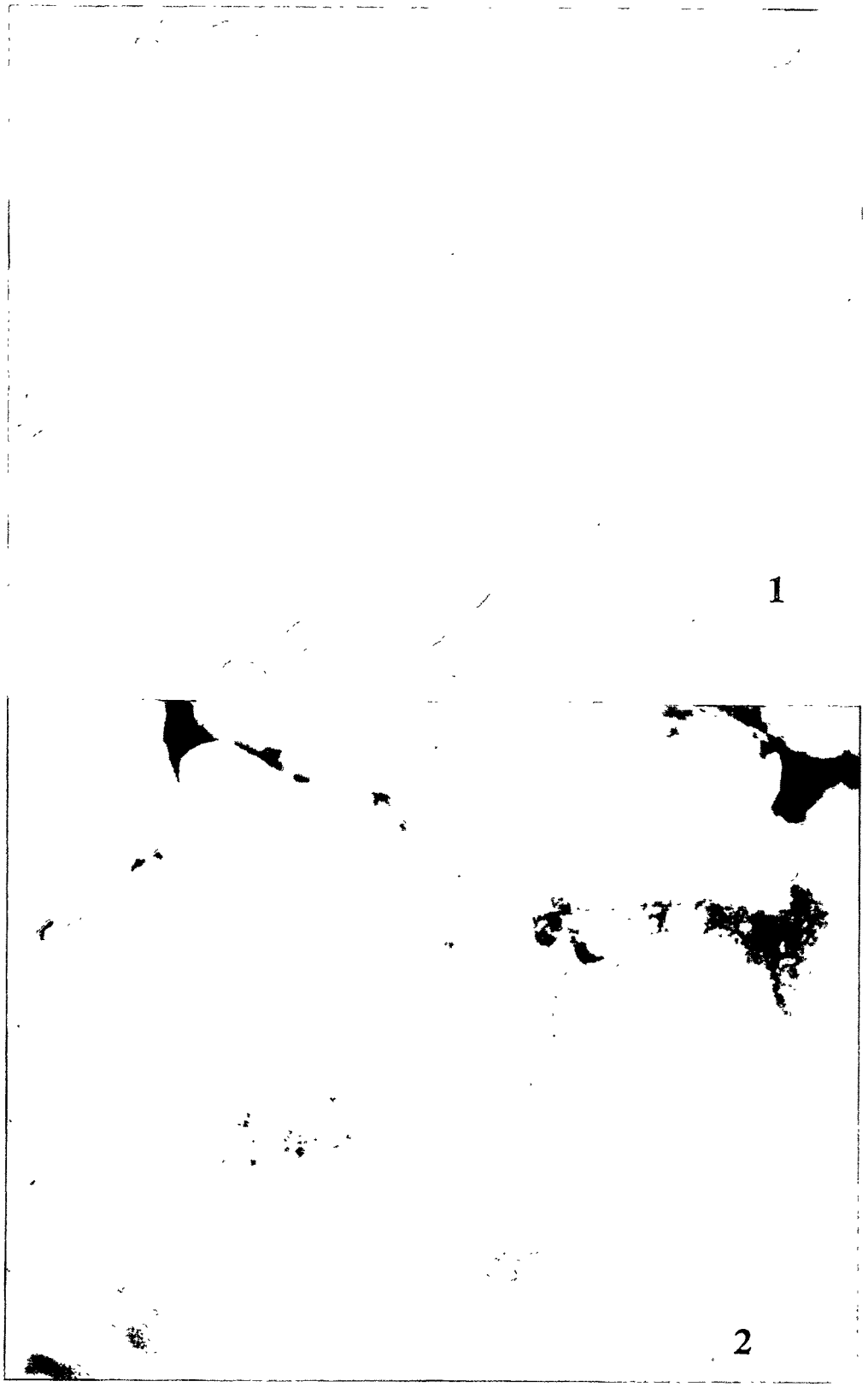

Fig. 4.22. Serial sections through a U_3Si_2 fuel particle irradiated in the HANS-1 experiment at 425°C to ~90% burnup.

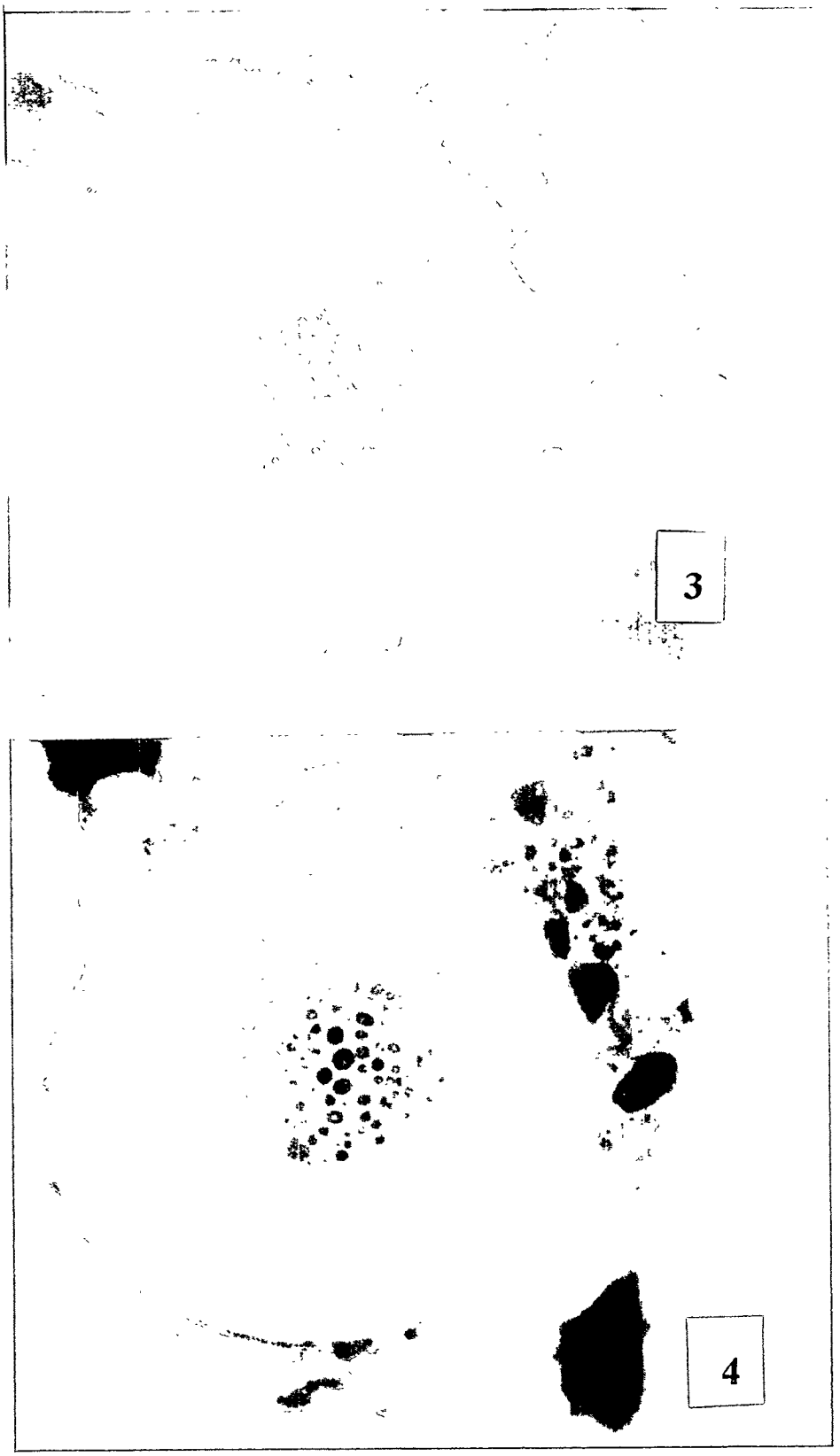

Fig. 4.22 (continued). Serial sections through a U_3Si_2 fuel particle irradiated in the HANS-1 experiment at 425°C to ~90% burnup.

Fig. 4.23. Bubble morphology in a U_3Si_2 fuel particle irradiated in the HANS-1 experiment at 250°C to ~85% burnup, showing region of small, uniform bubbles.

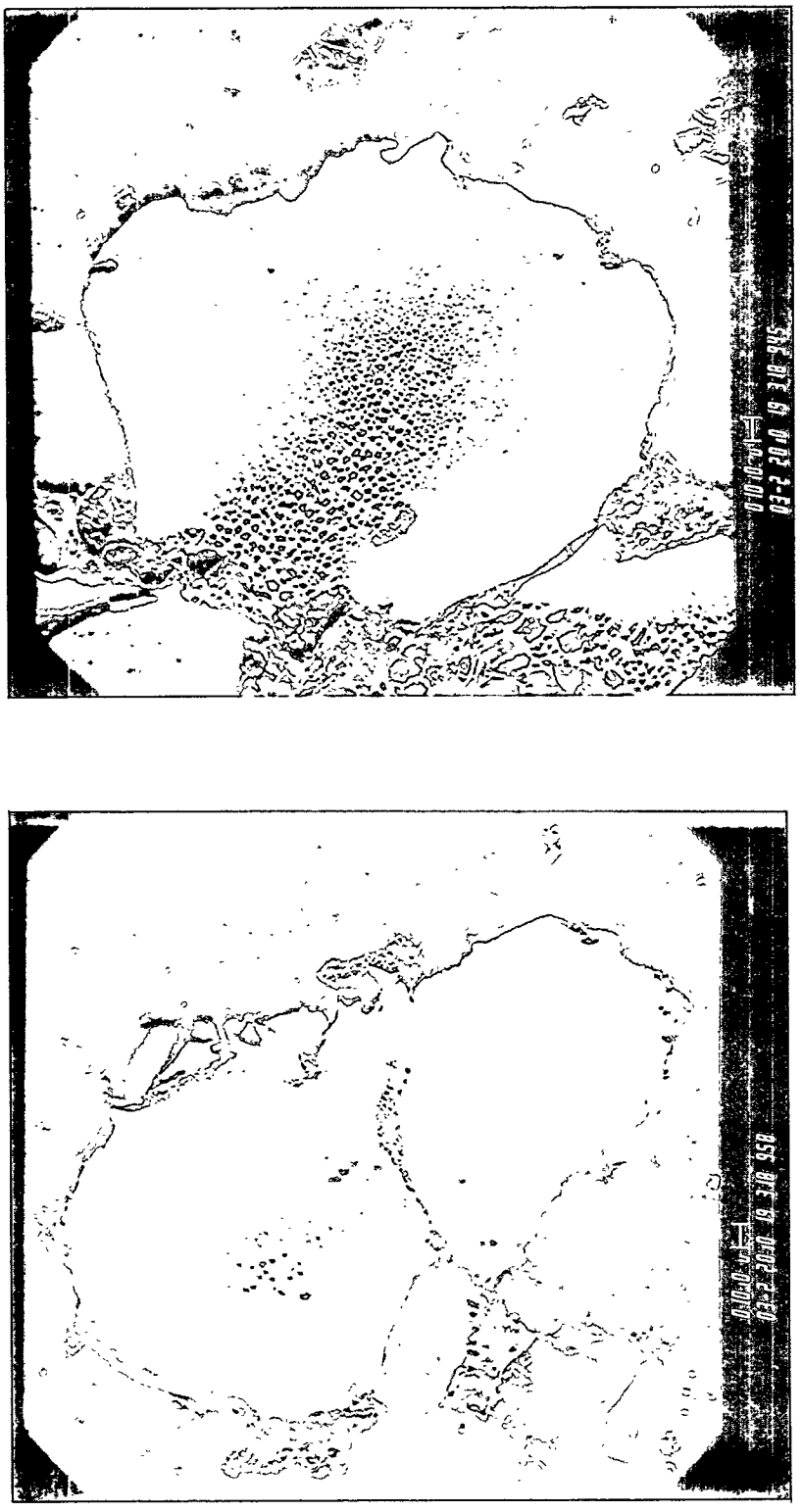

Fig. 4.24. Microstructural zones in U_3Si_2 irradiated in the HANS-1 experiment to ~90% burnup.

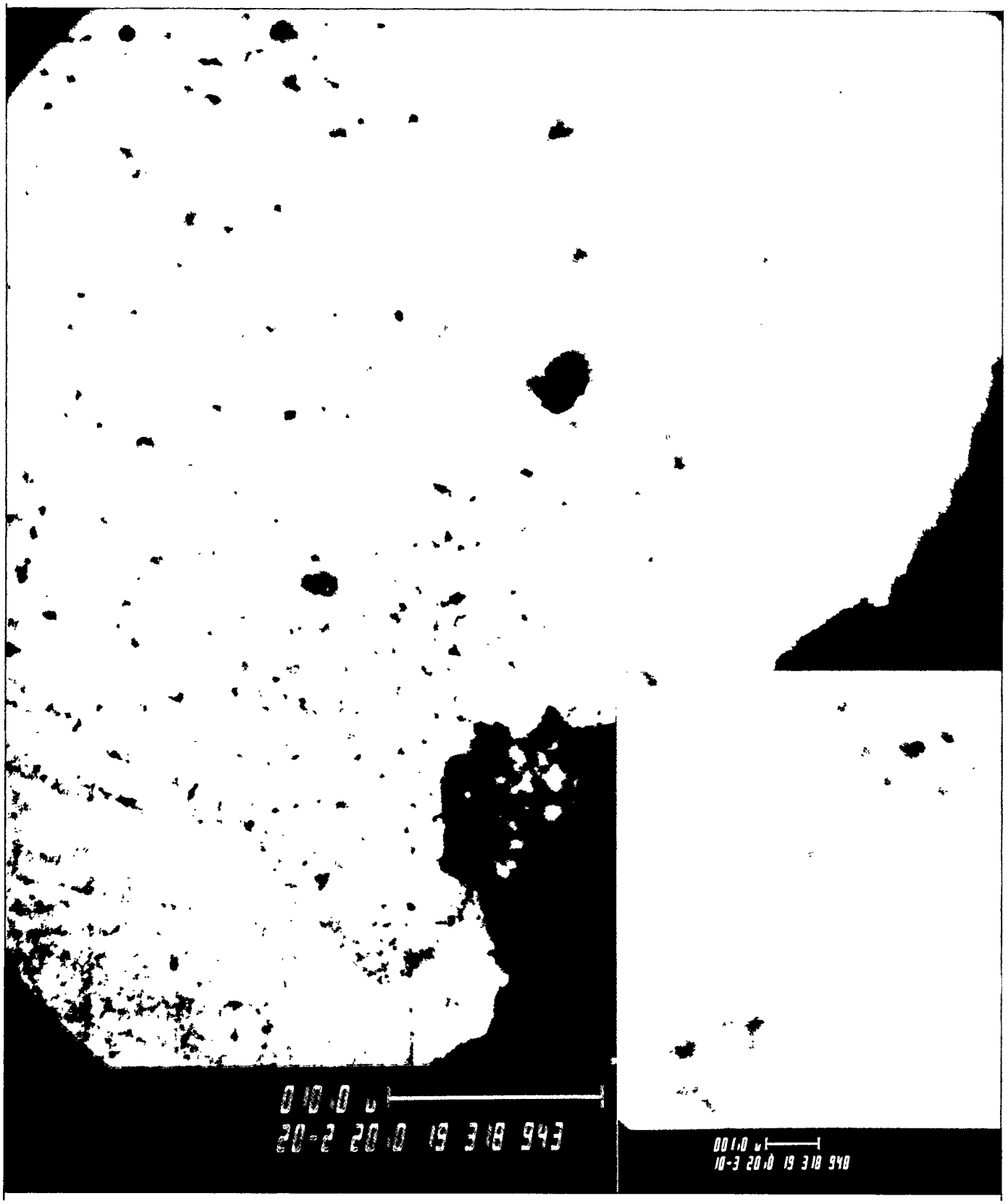

Fig. 4.25. Evidence of small grains in a U_3Si_2 fuel particle irradiated in the HANS-1 experiment.

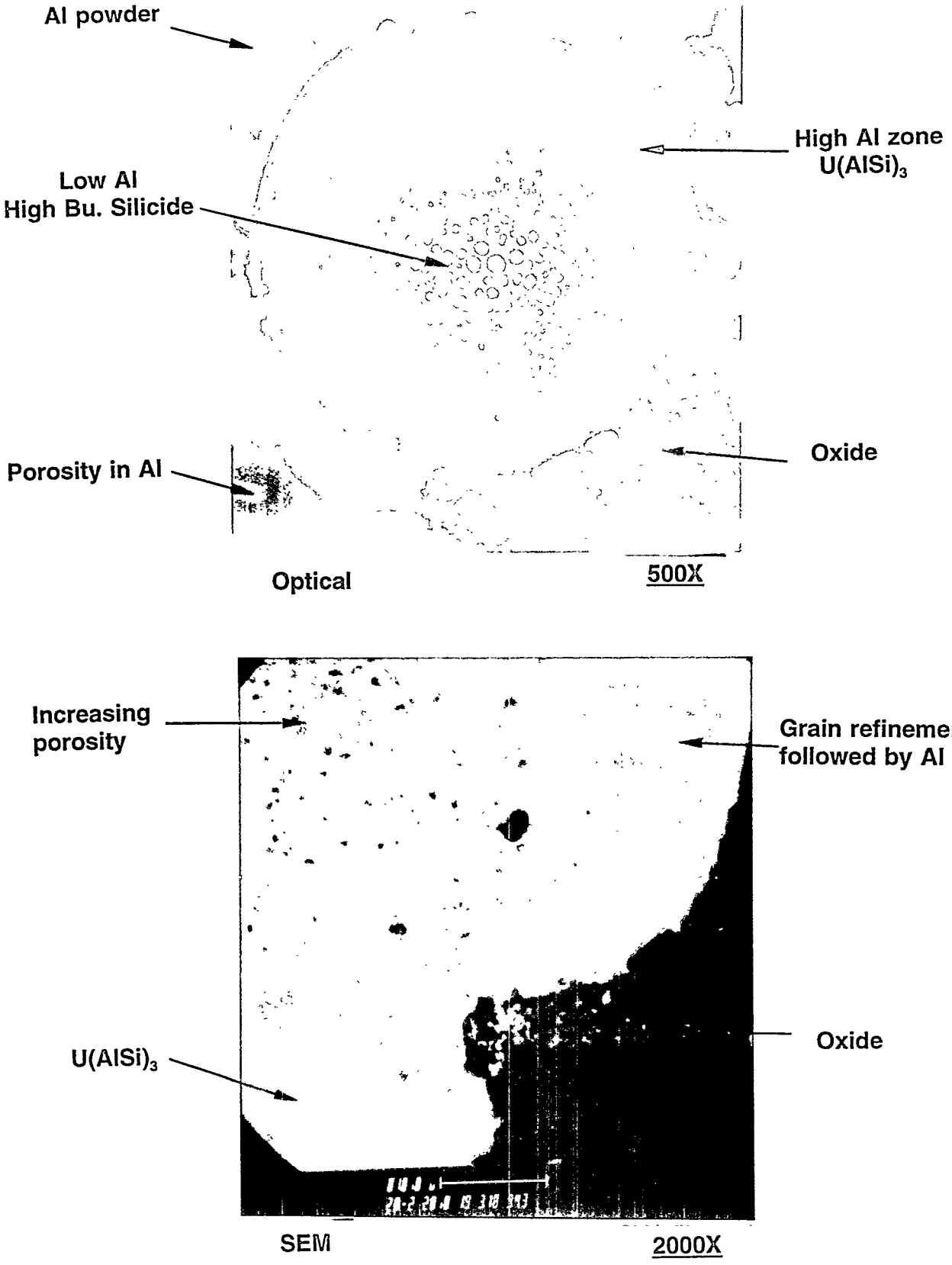

Fig. 4.26. Various zones described in the U_3Si_2 irradiation behavior model.

4.5.4 Backup Fuels

As mentioned in Sect. 1, several other fuel compounds in addition to U_3Si_2 were included in the HANS tests. HANS-1 contained only U_3Si samples, but HANS-2 contained UAl_x, UAl_2, and U_3O_8.

The highest-density silicide compound, U_3Si, was included to test our general interpretation of silicide irradiation behavior. It had been found in the RERTR program that U_3Si exhibited breakaway swelling at medium burnup. This behavior was ascribed to a crystalline-to-amorphous transformation induced by fission events.[22] Above a certain temperature (~350°C), such transformation does not occur, and U_3Si remains crystalline. It has been hypothesized that U_3Si in this crystalline state would not be susceptible to breakaway swelling. The HANS test appears to confirm this hypothesis, as the <250°C samples indeed showed the expected breakaway gas bubble growth, but in the 375°C sample, shown in Fig. 4.27, large interconnected gas bubbles are entirely absent, as expected in a crystalline compound at this temperature.

The effect of temperature on the irradiation behavior of U_3O_8 was just as profound as that in U_3Si. This compound has been thoroughly tested since the 1950s at temperatures up to ~300°C. It was found that U_3O_8 reacts with Al to form a multiphase reaction product consisting of UAl_4 and Al_2O_3. At high burnup, fission gas bubbles of rather large size develop in this reaction product.[23] In the HANS test, the low-temperature samples (250°C) did exhibit the familiar, large breakaway-type gas bubbles. However, even though it had completely reacted with the surrounding Al, the 425°C sample showed a total absence of such bubbles (see Fig. 4.28). One of the reaction phases, Al_2O_3, does become amorphous by fission damage, and it has been suggested that the large gas bubble growth occurs in this phase.[24] It is possible that at 425°C Al_2O_3 remains crystalline and, as is the case for U_3Si, is therefore more stable with respect to gas bubble formation.

The uranium aluminide compounds UAl_2 and UAl_3 are known to react with matrix aluminum to form, respectively, UAl_3 and UAl_4, during irradiation and at moderate temperatures of ~400 to 500°C even without the presence of fission events. The aluminide compounds have always exhibited exceedingly stable swelling behavior; in fact, fission gas bubbles such as those seen in silicides have never been observed in UAl_x. In the HANS test, however, a breakdown of this stable behavior was observed, as shown in Fig. 4.29. This is most likely the combined result of high U burnup, which has the result of moving the fully reacted fuel particles into the two-phase field beyond UAl_4 into the U-Al phase diagram, and high temperature. The high-burnup fuel thus consists of UAl_4 and some Al–fission product phase. This effect is particularly evident at temperatures above 250°C, where fuel-Al interaction has been most thorough. In this multiphase structure, breakaway fission gas bubble morphology has developed. The low-temperature (250°C) sample shown in Fig. 4.30 still largely retains the characteristic bubble-free microstructure of UAl_x.

As for the suitability of these alternative compounds as fuel candidates, U_3Si would behave satisfactorily if the fuel volume fraction in the meat could be kept low enough so that interconnection of fuel particles is prevented throughout the irradiation. Since U_3Si appears stable at high temperatures, this is a concern only below ~350°C, where U_3Si becomes amorphous.

Because U_3O_8 and UAl_x are of lower uranium density than are either U_3Si or U_3Si_2, their application would require substantially higher fuel volume fractions in the meat. The breakaway gas bubble behavior of U_3O_8 at low temperature and of UAl_x at high temperature would render this compound less suitable for high-burnup service.

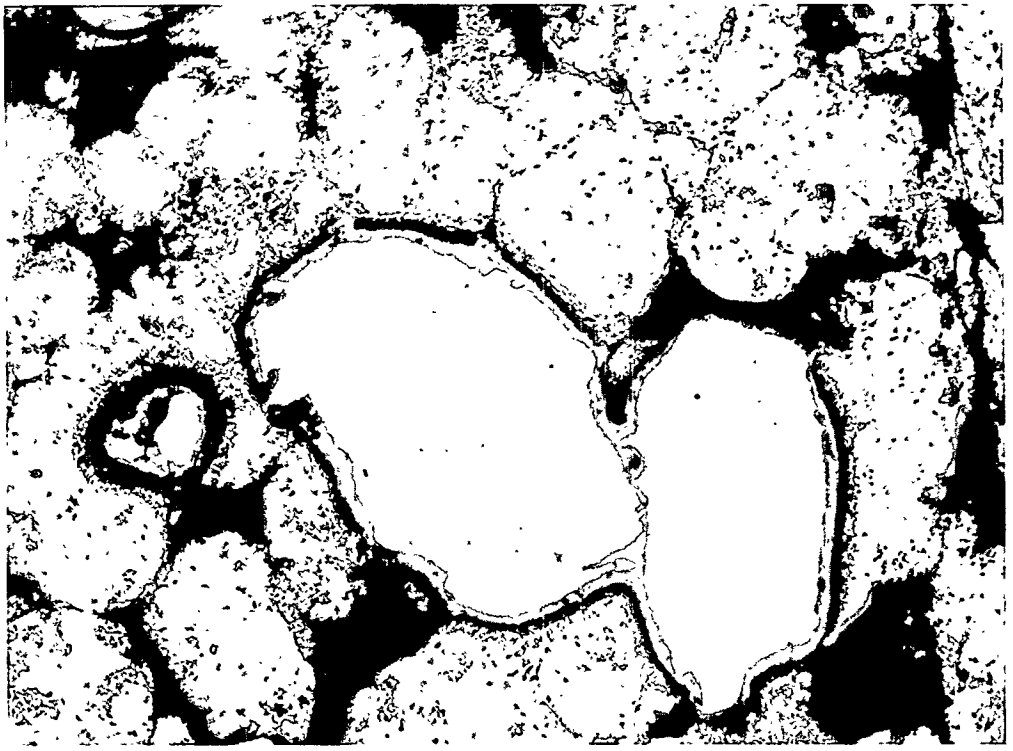

250X

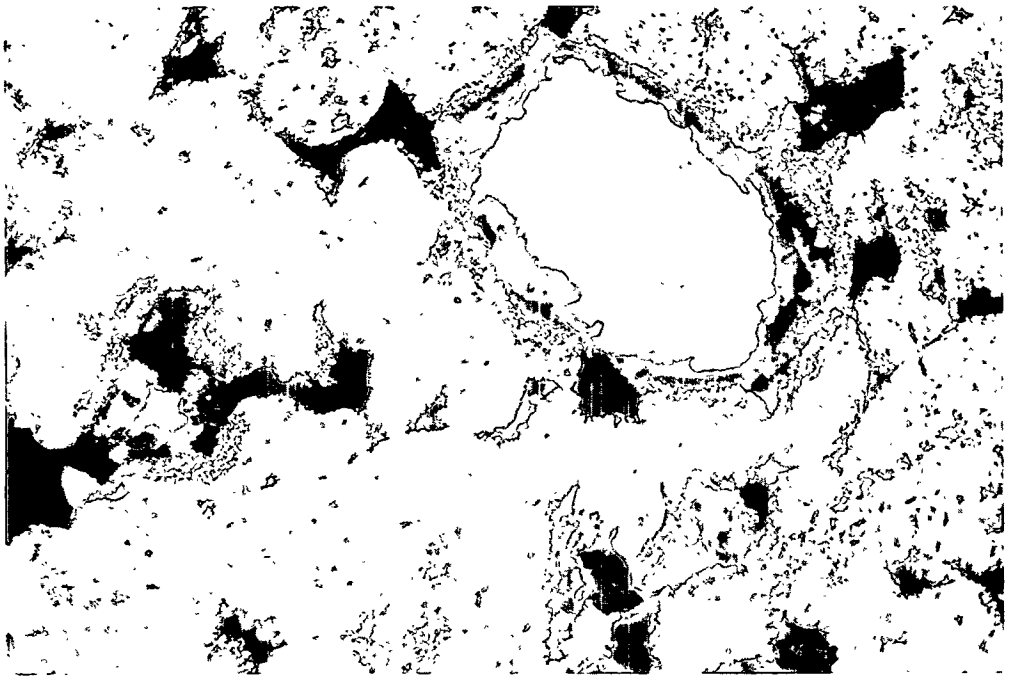

500X

Fig. 4.27. Microstructure of U_3Si irradiated in the HANS-1 experiment at 375°C to ~86% burnup, showing the absence of large fission gas bubbles.

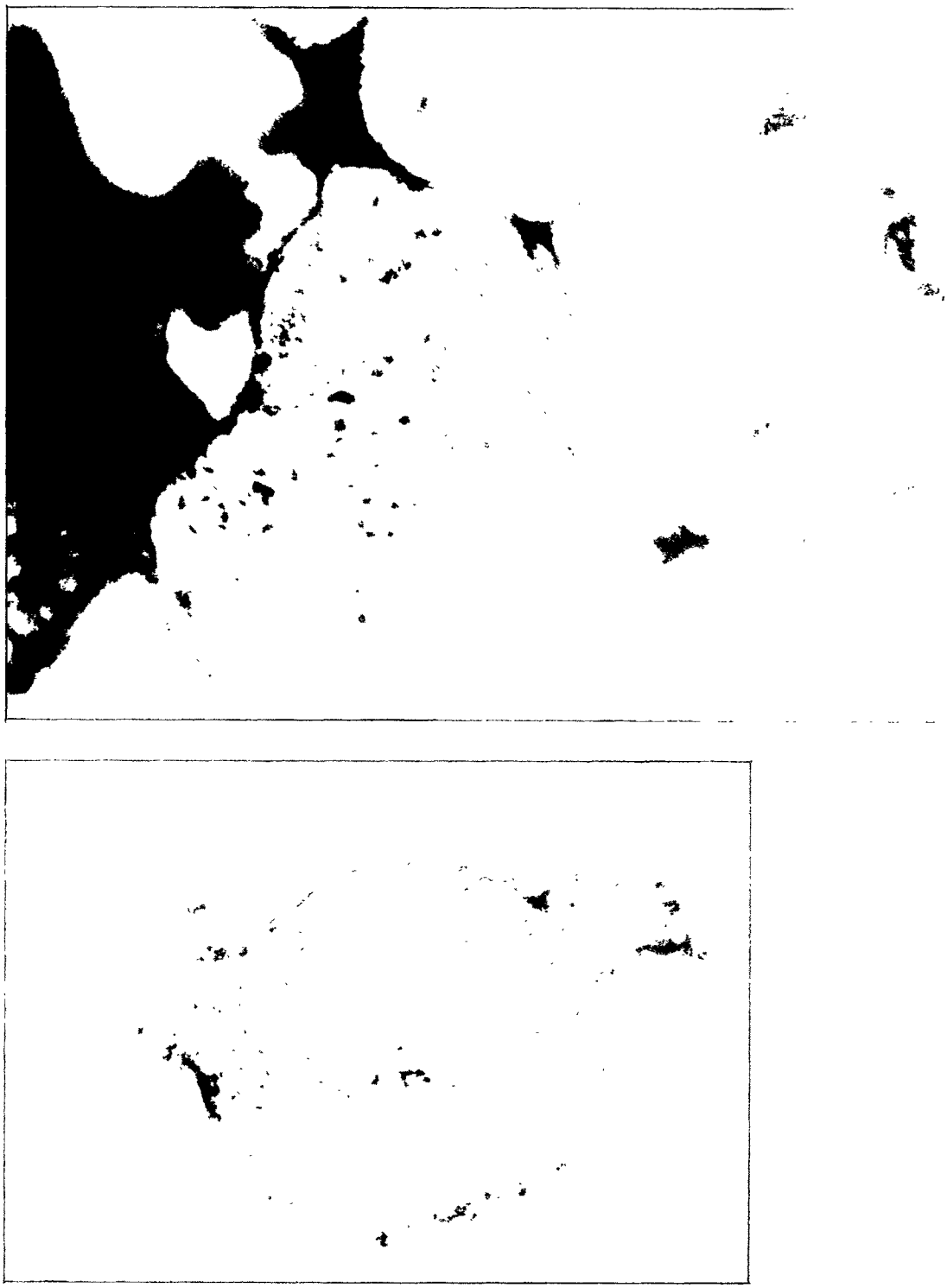

Fig. 4.28. Microstructure of U_3O_8 irradiated in the HANS-2 experiment at 425°C to ~72% burnup, showing the absence of large fission gas bubbles.

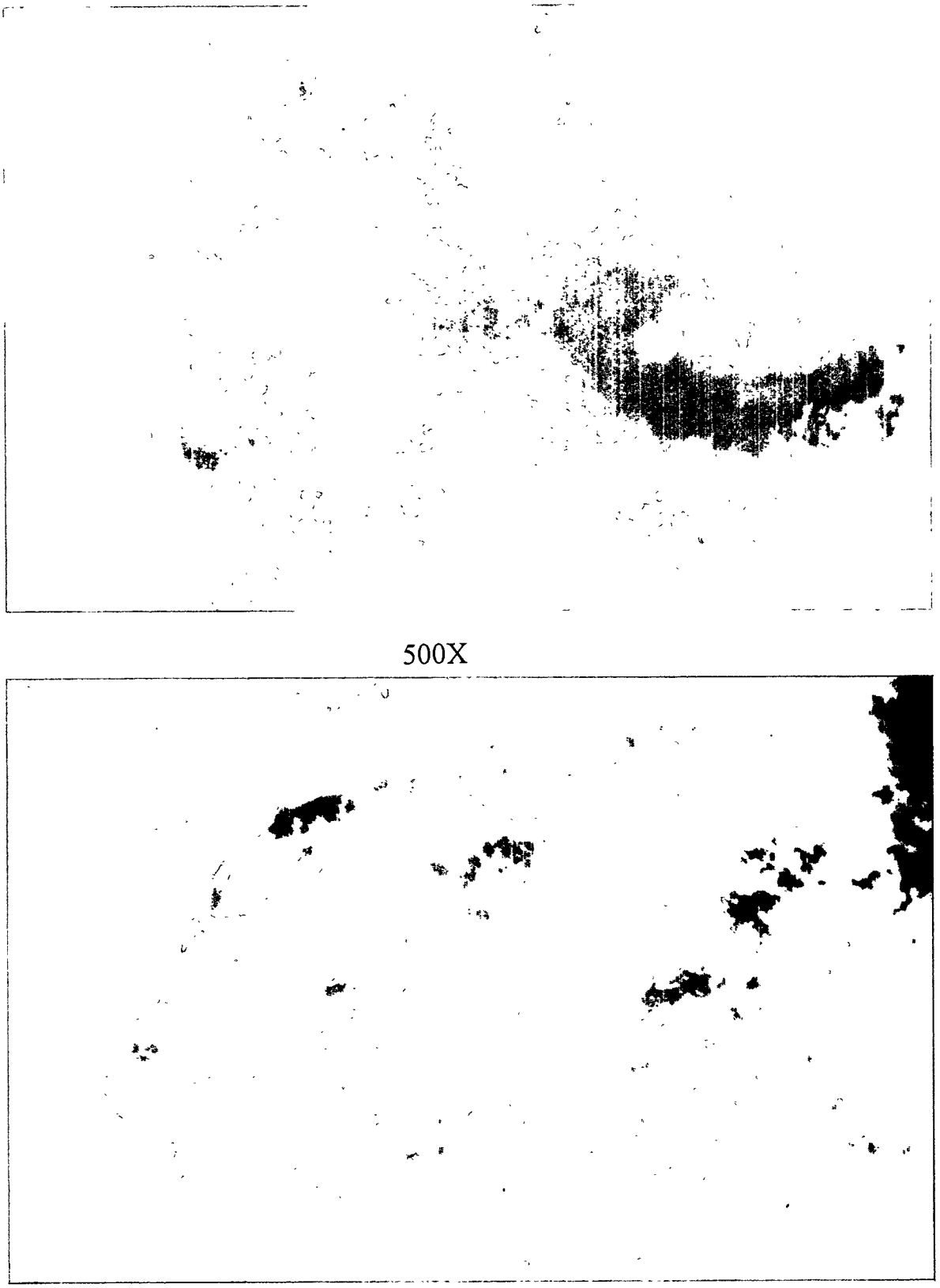

Fig. 4.29 Microstructure of UAl_x irradiated in the HANS-2 experiment at 425°C to ~90% burnup, showing the presence of large fission gas bubbles.

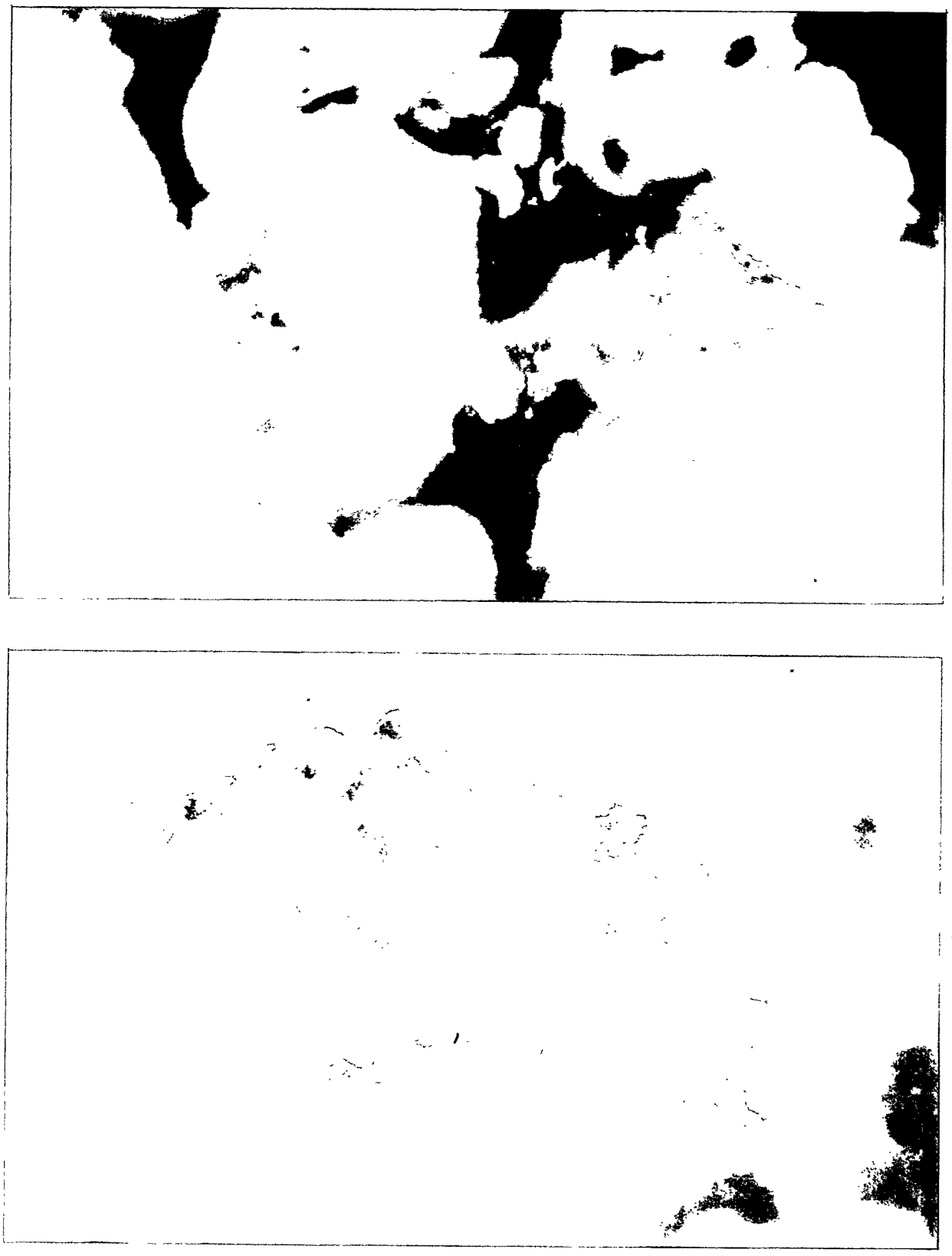

Fig. 4.30. Microstructure of UAl_x irradiated in the HANS-2 experiment at 250°C to ~84% burnup, showing the absence of large fission gas bubbles.

5. SUMMARY AND CONCLUSIONS

These capsule tests were highly successful in providing, at a very modest cost relative to plate tests, much information on the prospective performance of these fuels at unprecedented temperatures and fission rates. Of course, plate tests would eventually be needed (and were planned) to determine swelling rates, structural integrity, etc. under near prototypic conditions to qualify the fuel performance fully. However, these early results on fission gas bubble morphology and chemical interactions were extremely helpful in developing the fuel performance model. All indications are that temperature and burnup values were in the expected range.

Breakaway swelling has been mentioned throughout this report, and all fuel compounds tested appear to be afflicted by it at some combination of temperature and burnup. Breakaway swelling, a phenomenon characterized by rather rapid coarsening of an existing fission gas bubble distribution, is in itself not detrimental to fuel plate behavior. In order to result in excessive deformation (swelling) of a fuel plate, fuel particles in the fuel meat must interlink to allow the formation of large interparticle gas bubbles. Thus, even fuel compounds that exhibit breakaway swelling can be utilized if the individual fuel particles in the meat are prevented from interlinking by keeping the volume fraction of the fuel compound sufficiently low.

Depending on the required fissile loading, low fuel compound volume fractions may be practical only for high-density compounds such as U_3Si_2 and U_3Si. Although the HANS-1 and HANS-2 tests have shown that HEU U_3Si_2 at very high burnup exhibits breakaway swelling, the relatively low fuel volume fraction required for the ANS fuel plates ensures that virtually every fuel particle is surrounded by matrix aluminum during the entire irradiation cycle. This condition precludes the aforementioned interlinkage of fission gas bubbles, which is a prerequisite for excessive plate swelling. In addition, aluminum-U_3Si_2 interdiffusion forms, around each fuel particle, a shell consisting of an aluminum-type compound that is very stable in swelling behavior. This shell restrains to some extent the swelling of each fuel particle and also prevents interparticle linkage of gas bubbles, where particle contact should occur.

In conclusion, at the volume fraction of ~0.15 planned for the HEU ANS fuel plates, U_3Si_2 would perform well under the full range of operating parameters envisioned.

6. REFERENCES

1. G. L. Copeland et al., *Advanced Neutron Source Final Preconceptual Reference Core Design*, ORNL/TM-11234, Martin Marietta Energy Systems, Inc., Oak Ridge Natl. Lab., August 1989, p. 6.

2. *Safety Evaluation Report Related to the Evaluation of Low-Enriched-Uranium Silicide-Aluminum Dispersion Fuel in Non-Power Reactors*, NUREG-1313, U.S. Nuclear Regulatory Commission, July 1988.

3. *Conceptual Design Report—Summary*, ORNL/ANS/INT-34/S1, Martin Marietta Energy Systems, Inc., Oak Ridge Natl. Lab., June 1993.

4. J. L. Snelgrove et al., *The Use of U_3Si_2 Dispersed in Aluminum in Plate-Type Fuel Elements for Research and Test Reactors*, ANL/RERTR/TM-11 (October 1987) and, with minor revision, ANL/NPR-93/002, Appendix D1 (February 1993), Argonne National Laboratory, Chicago.

5. J. L. Snelgrove, *RERTR Program Fuel Testing and Demonstration—An Update*, ANL/RERTR/TM-6, Argonne National Laboratory, Chicago, July 1985, pp. 137–145.

6. G. L. Copeland et al., *Performance of Low-Enriched U_3Si_2-Aluminum Dispersion Fuel Elements in the Oak Ridge Research Reactor*, ANL/RERTR/TM-10, Argonne National Laboratory, Chicago, October 1987.

7. J. L. Snelgrove, G. L. Copeland, and G. L. Hofman, "Postirradiation Examination of ORR Demonstration Elements," pp. 151–160 in *Reduced Enrichment for Research and Test Reactors—Proceedings of the 12th International Meeting, Berlin, 10–14 September 1989*, Forschungszentrum Jülich GmbH, Berlin, 1991.

8. G. L. Hofman, J. Rest, and J. L. Snelgrove, *A New Swelling Model and Its Application to Uranium Silicide Research Reactor Fuel*, ANL/RERTR/TM-19 Argonne National Laboratory, Chicago, July 1993, pp. 186–96.

9. John S. Nordyke, ed., *Lead in the World of Ceramics*, American Ceramic Society, Columbus, Ohio, 1994, p. 9.

10. J. E. Palentine, "The Development of Silicon Carbide as a Routine Irradiation Temperature Monitor, and Its Calibration in a Thermal Reactor," *J. Nucl. Mater.* **61**, 243–53 (1976).

11. M. J. Kania and A. M. Howard, *HTCAP-1 – A Program for Calculating Operating Temperatures in HFIR Target Irradiation Experiments*, ORNL/TM-7336, Union Carbide Corp., Oak Ridge Natl. Lab., June 1980.

12. K. Farrell, "Response of Aluminum and Its Alloys to Exposure in the High Flux Isotope Reactor," pp. 73–76, in *Dimensional Stability and Mechanical Behaviour of Irradiated Metals and Alloys*, British Nuclear Energy Society, London, 1983.

13. Z. H. Ismail and H. G. Mohammed, "Effect of Prior History on the Response of Some Commercial Aluminium Alloys to Low Dose Neutron Irradiation," *Scr. Metal.* **23**, 2067–72 (1989).

14. S. Nazaré, *Investigations of Uraniumsilicide–based Dispersion Fuels for the Use of Low Enrichment Uranium (LEU) in Research and Test Reactors*, KfK 3372, Kernforschungszentrum Karlsruhe, July 1982.

15. T. C. Wiencek, R. F. Domagala, and H. R. Thresh, *Thermal Compatibility Studies of Unirradiated Uranium Silicide Dispersed in Aluminum*, ANL/RERTR/TM-6, Argonne National Laboratory, Chicago, July 1985, pp. 61–74.

16. G. L. Garner, K. E. Bogacik, and J. W. Oswood, *LEU Silicide Programs at Babcock and Wilcox*, ANL/RERTR/TM-9, Argonne National Laboratory, Chicago, May 1988, pp. 80–115.

17. A. E. Dwight, *A Study of the Uranium-Aluminum-Silicon System*, ANL-82-14,Argonne National Laboratory, Chicago, September 1982.

18. G. L. Hofman, "Fission Gas Bubbles in Uranium-Aluminide Fuels," *Nucl. Technol.* **77**, 110–15 (April 1977).

19. J. Rest, *GRASS-SST: A Comprehensive Mechanistic Model for the Prediction of Fission-Gas Behavior in UO_2-Base Fuels During Steady-State and Transient Conditions*, ANL-78-53, Argonne National Laboratory, Chicago, June 1978.

20. M. L. Bleiberg, R. M. Berman, and B. Lustman, "Effects of High Burn-up on Exide Ceramic Fuels," pp. 319–428 in *Radiation Damage in Reactor Materials*, International Atomic Energy Agency, Vienna, 1963.

21. J. Rest, "*The DART Dispersion Analysis Research Tool: A Mechanistic Model for the Prediction of Fission Product Induced Swelling of Aluminum Dispersion Fuels*," to be published at Argonne National Laboratory, Chicago.

22. G. L. Hofman, "Crystal Structure Stability and Fission Gas Swelling in Intermetallic Uranium Compounds," *J. Nucl. Mater.* **140**, 256–63 (1986).

23. G. L Hofman, G. L. Copeland, and J. E. Sanecki, "Microscopic Investigation into the Irradiation Behavior of U_3O_8-Al Dispersion Fuel, *Nucl. Technol.* **72**, 338–44 (March 1986).

24. M. L. Bleiberg, W. Yeniscavich, and R. G. Gray, *Effect of Burnup on Certain Ceramic Fuel Materials*, WAPT-T-1274, Westinghouse Bettis Atomic Power Laboratory, Pittsburgh, 1961.

Appendix A. CHEMICAL ANALYSIS DATA FOR FUEL HOLDER MATERIALS

38-030 6/76

8/78 RFO

DOW CORNING

Information about Polycrystalline Silicon

DAN CLOSS
Semiconductor Products Sales

FTS # 226-6000

DOW CORNING Dow Corning Corporation
Hemlock, MI 48626 (517) 642-5201

DOW CORNING POLYCRYSTALLINE SILICON

- One-piece crucible charge for Czochralski growth
- Rod for float zoning
- Nuggets for Czochralski growth

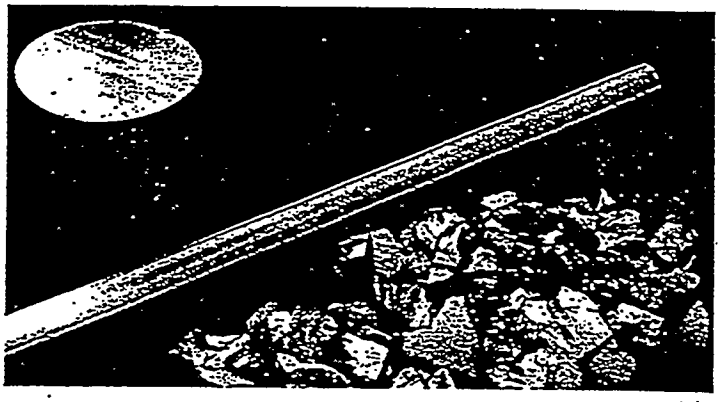

DESCRIPTION

Polycrystalline silicon is the basic raw material used throughout the world in manufacturing semiconductor devices such as transistors, rectifiers, and integrated circuits. Dow Corning manufactures polycrystalline silicon to the exacting quality requirements demanded by today's semiconductor industry.

High purity material is manufactured by Dow Corning in an automated, process controlled, computerized facility to assure uniformity, quality, and purity of polycrystalline silicon. This facility is the first and only fully integrated facility in the United States for the production of hyperpure polycrystalline silicon by the Siemens process of trichlorosilane decomposition. Dow Corning has more than a quarter century of experience in the production and purification of trichlorosilane—a chemical basic to the production of high purity silicon as well as silicones.

QUALITY CONTROL

Dow Corning's manufacturing process is continuously monitored to assure the highest purity silicon with uniformity from lot to lot. Quality evaluation techniques of the most advanced type are employed to assure exacting physical and electrical properties.

1. Each lot of trichlorosilane is evaluated before it is fed into the production process. The evaluation is determined by growing a sample rod, zone refining it, and then subjecting it to resistivity measurements.

2. Each lot of polycrystalline silicon is evaluated by float zoning a core taken from the lot. The core is taken perpendicular to the rod axis to assure that when zone refined in an argon atmosphere, the entire growth area is evaluated. Resistivity measurements are then made on the single crystal rod to determine exact donor or boron impurities. Further zoning in vacuum will remove all impurities except boron. By solving the equation $C_D - C_B = C_{NET}$ our Quality Assurance group can determine total acceptor and donor concentrations in parts per billion atomic (ppba) where:

C_D = Concentration of donor impurities

C_B = Concentration of boron impurities

C_{NET} = Net impurity concentration calculated after the one argon pass.

3. To measure minute non-doping impurities in the polycrystalline silicon, mass spectrometric analyses, as well as infrared spectrographic analyses, are carried out periodically as a final audit of quality.

In order to further assure the customer that all impurities are within specification limits, standard audit procedures are periodically conducted on all phases of the evaluation procedure. Each shipment is certified to the customer's specification.

PRODUCT CAPABILITIES

One-Piece Crucible Charge		
Diameter Range, mm to specification	76-210	
Diameter Midpoint,	*Tolerance, max*	
76-108mm	±6 mm	
108-159mm	±12 mm	
>159mm	±15 mm	
Weight Tolerance,		
no chips	Within 2.5%	
with chips	Within 1.0%	<140 mm diameter
with chips	Within 1.5%	≥140 mm diameter
Purity,		
boron content, ppba	≤0.3	
donor content, ppba	≤1.5	
Poly Rod		
Diameter Range, mm to specification	32-76	
Diameter Tolerance,		
as deposited, mm	±3.0	
centerless ground, mm	±.13	
Length,		
maximum for centerless ground, mm	533	
maximum as deposited, mm	864	
Bow, mm	≤3	
Purity,		
boron content, ppba	≤0.1	
donor content, ppba	≤0.3	
Nuggets*		
Dimensions, mm	6-50	
Weight, polyethylene bags	5 kg ± 1.0%	
Purity,		
boron content, ppba	≤0.3	
donor content, ppba	≤1.5	

* Uniform, random size pieces

In addition to its rigorous manufacturing and quality control procedures, Dow Corning, the world's largest seller of polycrystalline silicon, carries on a vigorous research and development effort aimed at improving both product quality and production efficiency.

CLEANING AND PACKAGING

All polycrystalline silicon products are cleaned using a degreasing and acid etching procedure. Polycrystalline rods and charges are individually packaged under clean room conditions to prevent surface contamination.

NOTE:
Dow Corning does not maintain semiconductor product specialists at all sales offices. For additional information please contact us at:

Midland—517-496-5072
Brussels—20/673.80.60
Los Angeles—213-570-8221
Milan—2/60.70.351
Munich—89/14861
New York—201-567-4960
Paris—1/977.0040
San Francisco—415-964-7744
Toronto—416-635-5115
Windsor, U.K.—734/57.251

Si USED FOR U-Si ALLOYS FOR RERTR & ANS PROGRAMS. NO FURTHER ANALYTICAL WORK DONE

RFD

DOW CORNING CORPORATION, MIDLAND, MICHIGAN 48640

Atlanta Boston Brussels Chicago Cleveland Dallas Detroit Greensboro Los Angeles New York San Francisco Sydney Tokyo Toronto

DOW CORNING

DOW CORNING

National Spectrographic Laboratories

DIVISION OF REXHAM CORPORATION #13-2694421
7650 HUB PARKWAY, CLEVELAND, OHIO 44125 • P.O. BOX 31480, CLEVELAND, OHIO 44131
TELEPHONE: 216-447-1550

XC
HRT
TCW
DRS (2)
CFK
SECTION FIL

TO Argonne National Laboratory
9700 South Cass Avenue
Argonne, IL 60439

Attn: Robert F. Domagala
MCT-Bldg. 212

DATE	CUSTOMER DESCRIPTION	YOUR ORDER NO.	REPORT NO.
8-2-88	Al	ANL P.O.# 82160050 REQ. # A 57462	08018-26

ELEMENTS DETERMINED in %	SAMPLE NO. 1100 Al 1" sheet (a)	SAMPLE NO. AESAR 1mm wire (b)	SAMPLE NO.	SAMPLE NO.	SAMPLE NO.	SAMPLE NO.	SAMPLE NO.
Cu	0.13	< 0.05					
Fe	0.70	0.18					
Si	0.082	0.063					
Mn	< 0.05	< 0.05					
Zn	< 0.05	< 0.05					
Others Each	< 0.05	< 0.05					
Others Total	< 0.10	< 0.10					
Al	Rem	Rem					

RERTR A.N.S

Lab No. 16156-16157

(a) 1100 Al SHEET PURCHASED BY TCW ON C.S. P.R.# A40049. RECVD AT ANL BLDG 212 SHOP 7-25-88. P.O.# 05

FOR ANS WORK → [(b) 1mm pure Al wire purchased from Johnson Matthey AESAR Product # Uncertain. Purchased by TCW Spring '83. [In ANS Cabinet] RFD

We certify the above analysis to be the true results on the designated samples.

8-8-88: ABOVE Al SHEET & "PURE" AL WIRE FOR WORK ON RERTR & ANS. MAT'L IN H-137. BOTH MEET SPECS FOR THEIR GRADE OF AL. RFD

NATIONAL SPECTROGRAPHIC LABORATORIES

Steven M. Gorski Reporting Officer

Sworn to and subscribed before me a Notary Public in and for the County of Cuyahoga, State of Ohio, this

DAY OF , 19

ORIGINAL REPORT OF ANALYSIS

ALCAN POWDERS AND PIGMENTS
DIVISION OF ALCAN ALUMINUM CORPORATION

ALCAN

LOCATION Joliet, Illinois

CERTIFICATE OF COMPLIANCE AND ANALYSIS

Product ALCAN 101 ALUMINUM POWDER

Purchase Order No. 63350043

To:
ARGONNE NATIONAL LABS
9700 SO CASS AVE
ARGONNE, IL 60439

Lot No. C0713 Weight 100 LBS

Date Shipped 12-09-86 Via SCHIEK

It is further certified that the following is an analysis of the above material, covering detailed requirement of applicable specification number ALCAN SPECIFICATIONS
dated _____ and _____
List applicable authorized waivers and changes

TEST PRESCRIBED	Specification Limit %		ANALYTICAL RESULT
	MINIMUM	MAXIMUM	
FREE ALUMINUM	99.0	----	99.4
COPPER	----	0.10	0.005
IRON	----	0.20	0.08
SILICON	----	0.12	0.014
MAGNESIUM	----	0.10	0.002
ZINC	----	0.10	0.005
VOLATILE CONTENTS	----	0.10	0.02
EASILY EXTRACTED FATTY & OILY MATTER	----	0.05	0.01
APPARENT DENSITY GM/CC	0.90	1.20	1.10
SCREEN ANALYSIS:			
+ 100 MESH	----	0.2	0
+ 200 MESH	----	----	5.2
+ 325 MESH	----	----	17.8
- 325 MESH	75.0	85.0	77.0

Name and Title of Official
Signed A. S. Rehal
A. S. Rehal, Quality Assurance Mgr.
Date DECEMBER 9, 1986

FORM-082C

National Spectrographic Laboratories

DIVISION OF REXHAM CORPORATION #13-2694421
7650 HUB PARKWAY, CLEVELAND, OHIO 44125 • P.O. BOX 31480, CLEVELAND, OHIO 44131
TELEPHONE: 216-447-1550

XC
HET
TCW
DRS (3)
CFK
KES
GLH
JLS

TO

Argonne National Laboratory
9700 South Cass Avenue
Argonne, IL 60439

Attn: Robert Domagala

ANS

DATE	CUSTOMER DESCRIPTION				YOUR ORDER NO.		REPORT NO.
7-22-88	Al Alloys			ANL P.O. #	81830024 DATED 7-1-88		07018-34

ELEMENTS DETERMINED ~~in%~~	SAMPLE NO. 3/4" 6061 Rod	SAMPLE NO. 101 Al Powder	SAMPLE NO.	SAMPLE NO.	SAMPLE NO. 3/4" 6061 Rod	SAMPLE NO. 101 Al Powder	SAMPLE NO.
Cu	0.21	0.003		Cd	0.0018	0.0028	
Fe	0.26	0.076		Co	<0.001	<0.001	
Si	0.55	0.076		Ga	0.009	0.004	
Mn	0.10	0.002		Li	0.0001	0.0001	
Mg	0.83	<0.001		V	X	0.013	
Zn	0.060	0.010					
Cr	0.15	<0.001					
Ti	<0.01	0.004					
Others Each	<0.05	<0.01					
Others Total	<0.10	<0.05					
B	<0.001	<0.001		X = No Analysis performed.			

Lab No. 14030-14031

NOTE (RFD, 7-26-88): THIS IS A FINAL EDITION OF NSL'S REPORT ON THESE TWO MATERIALS. SEE MY NOTES ON NSL'S REPORT OF 7-14-88. ALL INFO APPLIES.

We certify the above analysis to be the true results on the designated samples.

NATIONAL SPECTROGRAPHIC LABORATORIES

Reporting Officer

Sworn and subscribed before me a Notary Public in and for the County of Cuyahoga, State of Ohio, this

DAY OF , 19

ORIGINAL REPORT OF ANALYSIS

SPEC. No. 55736

SPECTROCHEMICAL ANALYSIS REPORT

	Our No.	Your No.	Material	Ag	Al	As	B	Ba	Be	Bi	Ca	Co	Cr	Cu	Fe	Hg	K	Li	Cd	Ga	
87-	0163-01	ALCAN 101	Al Powder	<.001	VS	<.05	<.001	<.05	<.001	<.005	<.01	<.005	(0.001)	0.005	0.2		<.05	<.001	<.01	0.005	

	Our No.	Your No.	Material	Mg	Mn	Mo	Na	Ni	P	Pb	Sb	Si	Sn	Sr	Ti	V	Zn	Zr			
87-	0163-01	ALCAN 101	Al Powder	0.001	0.003	<.005	<.01	0.01	<.1	0.005	<.01	(0.05)	<.01	<.1	0.005	0.01	<.05	<.05			

RESULTS REPORTED IN FOLLOWING UNITS

- ☐ parts per million
- ☑ per cent
- ☐ micrograms per ml.
- ☐ micrograms in total sample
- ☐

ESTIMATED ACCURACY OF RESULTS

- ☑ order of magnitude
- ☐ factor of two
- ☐ ___% of amount present

SYMBOL	MEANING
L	less than
G	greater than
.	element not investigated
—	element not detected
•	interference
( )	accuracy uncertain
?	presence uncertain

SYMBOL	MEANING	APPROX. CONC.
VS	very strong	100% to 10%
S	strong	10% to 1%
M	moderate	1% to 0.1%
W	weak	0.1% to 0.01%
T	trace	0.01% to 0.001%
FT	faint trace	0.001% to 0.0001%

REMARKS:

ALCAN 101 Al POWDER PURCHASED ON ANL P.O.# 6335004B (RECVD 12-86)
AS-RECVD, SIEVED -100 MESH
(NOT VACUUM ANNEALED)
THIS IS A NEW SUPPLY OF 101 Al POWDER
RFD

Plate No. 01848

By: R.A. Huff

Date: 2-11-87

Submitted By: R.F. Domagala Location: 212 Date Received: 1-19-87

Reports To: ~, T.C. Wiencek, D.R. Schmitt, ACL Office

CHM-61 (7-78)

XC: TCW, DRS, H-137C FILE HRT

ANALYTICAL CHEMISTRY LABORATORY
Argonne National Laboratory
Argonne, IL 60439

REPORT OF ANALYTICAL RESULTS

Sample Material: Alcan 101 Al Powder — Date Received: 1/19/87

Submitted by: R. Domagala — Date Reported: 4/9/87

Your Number	Our Number	Aliquot Wt., g	ppm H	ppm O
ALCAN 101 As-Rec'd. Al Powder	87-4027	0.0939	--	2185
		0.1006	--	2050
		Aver. ± s.d.		2118 ± 95
		0.0584	60.6	
		0.1318	57.5	
		0.0568	46.8	
			55.0 ± 7.2	
		ALCAN 101 Al POWDER PURCHASED ON ANL P.O. 63350043 (RECVD 12-86) AS-RECVD, SIEVED -100 MESH BUT NOT VACUUM DEGASSED. THIS IS A NEW SUPPLY OF 101 Al POWDER STORED IN ORIGINAL CONTAINER IN RED-LOCK CABINET IN H-137 RFD (NITROGEN NOT RUN)		

NOTE: Samples will be discarded one (1) month after date of report unless otherwise arranged. When making future inquiries regarding this work, you must reference *OUR* number(s) above. For further information about the results reported here, please call E. Streets at 2-4291.

Copies To: ~~R.~~ Domagala
T. Wiencek
D. Schmitt
D. Green
/vaa R. Heinrich (2)
CMT-84 (10-84) E. Streets
File (2)

Analyst(s): E. Streets

XC: HRT, TCW, DRS, H-137 FILE (2 COPIES)
RFD CHRON FILE

SPEC, No. 56005

ICP - SPECTROCHEMIC - ANALYSIS REPORT

	Our No.	Your No.	Material	Ag	Al	As	B	Ba	Be	Bi	Ca	Co	Cr	Cu	Fe	Hg	K	Li			
88-	0472-01	5-40	ANS S.S. SET SCREWS									0.39	17.42	0.31	71.1						

ANS

	Our No.	Your No.	Material	Mg	Mn	Mo	Na	Ni	P	Pb	Sb	Si	Sn	Sr	Ti	V	Zn	Zr			
89-	0472-01	6-40	ANS S.S. SET SCREWS		1.66	0.55		8.64													

XC
HRT
TCW
DRS (2)
& CEK
KES
JLS

RESULTS REPORTED IN FOLLOWING UNITS

- ☐ parts per million
- ☑ per cent
- ☐ micrograms per ml.
- ☐ micrograms in total sample
- ☐

ESTIMATED ACCURACY OF RESULTS

- ☐ order of magnitude
- ☐ factor of two
- ☑ 3-10 % of amount present

SYMBOL	MEANING
L	less than
G	greater than
	element not investigated
—	element not detected
•	interference
( )	accuracy uncertain
?	presence uncertain

SYMBOL	MEANING	APPROX. CONC.
VS	very strong	100% to 10%
S	strong	10% to 1%
M	moderate	1% to 0.1%
W	weak	0.1% to 0.01%
T	trace	0.01% to 0.001%
FT	faint trace	0.001% to 0.0001%

REMARKS: 7-22-88 (RFD) SCREWS ULTRASONICALLY CLEANED & DRIED

THIS ANALYSIS WAS CONDUCTED ON 7 (SEVEN) 5-40 SET SCREWS FROM THE "BATCH" OF SET SCREWS WHICH WILL BE USED FOR THE ANS "FUEL HOLDERS". THE SET SCREWS WERE STOCK ISSUE & DESCRIBED AS "304 STAINLESS STEEL." ANALYTICAL DATA FROM ALIQUOT OF SOLUTION OF ALL SEVEN SCREWS CONFIRMS GEN'L CATEGORY OF 304SS. Cr is slightly low but accuracy is 3 to 10% of AM'T. PRESENT. I SEE NO REASON TO CONDUCT ANY FURTHER ANALYSES ON THESE SCREWS. SCREWS ARE IN ANS CABINET IN H-137

AVERAGE WT.* = 0.087 ± 0.005 mg ; AVERAGE LENGTH** : 0.133 ± 0.003 in.

Plate No.

By: R.A. Huff (X3633)

Date: 7-19-88

Submitted By: R.F. Domagala Location: 212 Date Received: 7-11-88

Reports To: T.C. Wiencek, H.R. Thresh, DCL Office

* WT. AVERAGE BASED ON 50 UNITS] LENGTH & WT. PER SCREW
** LENGTH " " " 9 UNITS] RFD (7-89)

CHM-61 (7-78)

ARGONNE NATIONAL LABORATORY
9700 South Cass Avenue
Argonne, Illinois 60439

REPORT ON CHEMICAL ANALYSIS

Date Received: 9/16/83

Sample: Uranium Silicides

Source: R. Domagala

YOUR NUMBER	OUR NUMBER	Sample Weight (mgrs)	H (ppm)	O (ppm)	N (ppm)
E-172/173 LEU U_3Si	83-0619-01	62.3	33	0.53 w/o	240
E-178 HEU U_3Si_2	-02	69.7	9	560	66
E-180 HEU U_3Si_2	-03	79.8	6	410	100
E-177 HEU U_3Si	83-0635-01	62.4	18	0.43 w/o	330
E-179 HEU U_3Si	-02	70.4	14	0.34 w/o	290

VALUES FOR H-O-N DETERMINED ON SAMPLES -100 [redacted] +3YS MESH (85%)
— 3YS MESH (15%)
FOR [redacted] ALL SAMPLES
RFD

Reported by: M. Homa Date: 10/3/83

Copies to: ~~R.~~ Domagala, T. Wiencek, H. Thresh, K. Jensen, D. Graczyk, D. Green, R. Heinrich, File

Analyst: M. Homa

CHM-17A (7-67)
/vaa

Xtra

ARGONNE NATIONAL LABORATORY
9700 South Cass Avenue
Argonne, Illinois 60439

REPORT ON CHEMICAL ANALYSIS

Date Received: 9/1/83

Sample: U_3Si and U_3Si_2

Source: R. Domagala

YOUR NUMBER	OUR NUMBER	C (ppm)	U Isotopic, Wt. %	Total U, %	Si, Wt. %
E-172/173 U_3Si LEU	83-0619-01	220 = .022%	234 - 0.1120 ± .0005 235 - 19.833 ± .010 236 - 0.1382 ± .0005 238 - 79.917 ± .011	A - 95.435 B - 95.427 95.431 ±0.050	3.87_5 }3.88$_3$ 3.89_0 ±0.008
E-178 U_3Si_2 HEU	-02	NA	234 - 1.0590 ± .001 235 - 92.951 ± .005 236 - 0.2420 ± .0005 238 - 5.748 ± .003	A - 92.347 B - 92.288 92.317 ±0.050	7.48_6 }7.43$_9$ 7.39_2 ±0.05
E-180 U_3Si_2 MEU	-03	NA	234 - 0.3168 ± .0005 235 - 40.109 ± .010 236 - 0.4140 ± .0005 238 - 59.160 ± .011	A - 92.291 B - 92.300 92.295 ±0.050	7.469 }7.48$_2$ 7.495 ±0.013
		Analyses above conducted on powder Samples submitted to ACL. Powders were 85% −100+325 Mesh & 15% − 325 Mesh See also spectrographic analysis & H-O-N analyses			RFD

Reported by: E. Callis

Date: 9/26/83

Xc— HET
TCW
H-WING FILE
JLS

Copies to: ~~R.~~ Domagala, T. Wiencek, H. Thresh, K. Jensen, R. Heinrich, A. Essling, E. Callis, D. Green, E. Rauh, I. Fox, File

Analyst: I. Fox, E. Callis, E. Rauh, K. Jensen

CHM-17A (7-67)
/vaa

ARGONNE NATIONAL LABORATORY
9700 South Cass Avenue
Argonne, Illinois 60439

REPORT ON CHEMICAL ANALYSIS

Date Received: 8/30/83

Sample: U_3Si

Source: R. Domagala

YOUR NUMBER	OUR NUMBER	U Isotopic, Wt. %	Total U, %	Si, Wt. %
~~E-177~~ U_3Si HEU	83-0635-01	234 - 1.0540 ± 0.001 235 - 92.625 ± 0.005 236 - 0.2420 ± 0.0005 238 - 6.079 ± 0.003	A - 95.50 B - 95.32 95.41	3.89_4 } 3.91_4 ±.02 3.93_4
E-179 U_3Si HEU	-02	234 - 0.3161 ± 0.0005 235 - 40.060 ± 0.010 236 - 0.4133 ± 0.0005 238 - 59.210 ± 0.011	A - 95.44 B - 95.41 95.43	3.899 } 3.915 ±.016 3.930
		Analyses above conducted on powder Samples submitted to ACL Powders were 85% -100+325 Mesh & 15% -325 Mesh See also Spectrographic analysis & H-O-N analyses RFD		

Reported by: E. Callis

Date: 9/26/83

Copies to: ~~R.~~ Domagala
T. Wiencek
H. Thresh
D. Green
R. Heinrich
K. Jensen
A. Essling
File

Analyst: A. Essling
E. Callis
K. Jensen

XC — HRT
TCW
H-WING FILE
JLS

CHM-17A (7-67)
/vaa

SPECTROCHEMICAL ANALYSIS REPORT

83-0635-01,-02

Our No.	Your No.	Material	Ag *	Al	As	B	Ba	Be	Bi	Ca	Co	Cr	Cu	Fe	Mg	K	Li	W *	Ga *	Cd
54949	E177	U-Si	<1	.43			1.4	<.3		<10	33	5	132	94		<30	<.5	380	<1	<1
50	E179	"	"	.25			<1	"		10	20	20	10	158		"	"	110	"	"

Our No.	Your No.	Material	Mg	Mn	Mo	Na	Ni	P	Pb	Sb	Si	Sn	Sr	Ti	V	Zn	Zr
54949	E177	U-Si	3	.8	11	14	320		<10			<10	<.3	<1	<1	3	<1
50	E179	"	1.5	.6	<5	9	19		"			"	"	"	"	2	"

RESULTS REPORTED IN FOLLOWING UNITS

- [x] parts per million
- [ ] per cent
- [ ] micrograms per ml.
- [ ] micrograms in total sample
- [ ]

ESTIMATED ACCURACY OF RESULTS

- [ ] order of magnitude
- [x] factor of two for Mg, W, Ga
- [x] 10-20% of amount present, else

SYMBOL	MEANING
L	less than
G	greater than
	element not investigated
—	element not detected
*	interference
( )	accuracy uncertain
?	presence uncertain

SYMBOL	MEANING	APPROX. CONC.
VS	very strong	100% to 10%
S	strong	10% to 1%
M	moderate	1% to 0.1%
W	weak	0.1% to 0.01%
T	trace	0.01% to 0.001%
FT	faint trace	0.001% to 0.0001%

REMARKS:

E177 = HEU U_3Si

E179 = HEU U_3Si

SAMPLES SUBMITTED WERE

85% -100 +325 MESH

15% -325 MESH

RFD

Plate No. 1835

By: E. N. Huff

Date: 9-22-83

Submitted By: B.E. Donaghe Location: 212 Date Received: 8-30-83

Reports To: " T.C. Wiencek, M.R. Thiele

XC: HRT, TCW

H-WING FILE

SPECTROCHEMICAL ANALYSIS REPORT

83-0619-01→04

Our No.	Your No.	Material	Ag	Al	As	B	Ba	Be	Bi	Ca	Co	Cr	Cu	Fe	Hg	K	Li	W*	Ga*	Cd
54945	E172+E173	U-Si	<1	128			<1	<.3		11	22	15	55	179		<20	<.5	180	<1	<1
46	E178	"	"	20			"	0.8		<10	2	4	93	58		"	"		"	"
47	E180	"	"	19			"	<.3		"	<1	19	9	131		"	"		"	"
48	D181	U-Al		VS			"	"		"	"	1	10	43		"	"		"	"

Our No.	Your No.	Material	Mg	Mn	Mo	Na	Ni	P	Pb	Sb	Si	Sn	Sr	Ti	V	Zn	Zr
54945	E172+E173	U-Si	6	.9	<5	10	199		<10			<10	<.3	<1	<1	5	<1
46	E178	"	0.5	.4	"	9	.218		"			"	"	"	"	2	"
47	E180	"	0.5	.5	"	9	20		"			"	"	"	"	<1	"
48	D181	U-Al	<.5	1	<20	4	5		<100			"	"	1.6	3	1	"

RESULTS REPORTED IN FOLLOWING UNITS

- [x] parts per million
- [ ] per cent
- [ ] micrograms per ml.
- [ ] micrograms in total sample
- [ ]

ESTIMATED ACCURACY OF RESULTS

- [ ] order of magnitude
- [x] factor of two (as Mg, W, Ga)
- [x] 10-20% of amount present (Na)

SYMBOL	MEANING
L	less than
G	greater than
---	element not investigated
—	element not detected
•	interference
( )	accuracy uncertain
?	presence uncertain

SYMBOL	MEANING	APPROX. CONC.
VS	very strong	100% to 10%
S	strong	10% to 1%
M	moderate	1% to 0.1%
W	weak	0.1% to 0.01%
T	trace	0.01% to 0.001%
FT	faint trace	0.001% to 0.0001%

REMARKS:

E172 + E173 = LEU U_3Si

E178 = HEU U_3Si_2

E180 = MEU U_3Si_2

D181 = Du UAl_2

ALL SAMPLES WERE 85% -100 +325 MESH
15% -325 MESH

EXCEPT UAl_2 (D181) WHICH WAS SUBMITTED AS 'CHUNKS'

RFD

Plate No. 1435

By: E. N. Huff

Date: 9-22-83

Submitted By: R.F. Domagala Location: 212 Date Received: 8-25-83

Reports To: " , T.C. Wiancko, H.R. Thresh XC: HRT, TCW

H-WING COPY

CHM 61 (7 70)

FOR ANS
FANS (= HANS)

ANALYTICAL CHEMISTRY LABORATORY
Argonne National Laboratory
Argonne, IL 60439

REPORT OF ANALYTICAL RESULTS

Sample Material: UAl_2 Date Received: 7/17/89

Submitted by: R. Domagala Date Reported: 7/28/89

Your Number	Our Number	
E-270	89-0562-01	Isotopic Analysis:

	At. %	Wt. %
U234:	0.5589 ± 0.0005	0.5561 ± 0.0005
U235:	93.118 ± 0.002	93.048 ± 0.002
U236:	0.4241 ± 0.0005	0.4256 ± 0.0005
U238:	5.900 ± 0.001	5.971 ± 0.001

Mol. Wt. = 235.22

Mass Spec. Isotope Dilution Assay:

Wt. % U = 80.86
80.88
Avg. 80.87 ± 0.01

Aluminum Assay Data:

		Found	
E-270(A)	89-0562-01A	188.6 mg Al/g	Uranium separated from Al by anion exchange prior to gravimetric determination of aluminum using 8-hydroxyquinoline.
E-270(B)	-01B	189.3 mg Al/g	
ANALAR Al Metal Standard	ACL Standard Al		Carried 23.49 mg Al through the separation and determination steps along with the duplicate samples. Found 23.44_5 mg Al = 99.80% Recovery.

ANALYSIS OF $HEUAl_2$ POWDER FROM OUR INGOT (ARC-MELTED) E-270. POWDER -120+200 MESH. TO CONVERT Al VALUES TO Wt.% MOVE DECIMAL ONE PLACE TO LEFT. Al: 18.86 Wt.% & 18.93 Wt.% AVG = 18.90 Wt.%.
Σ(U+Al) = 80.87 + 18.90 = 99.77 Wt.%, BALANCE H-O-N + IMPURITIES. ANALYSES TO COME LFD 8-2-89

NOTE: Samples will be discarded one (1) month after date of report unless otherwise arranged. When making future inquiries regarding this work, you must reference *OUR* number(s) above. For further information about the results reported here, please call E. Rauh at 2-7399.

Copies To: R. Domagala, T. Wiencek, H. Thresh, D. Green, D. Graczyk, A. Essling, E. Rauh, K. Jensen, File

Analyst(s): A. Essling, E. Rauh, K. Jensen

XC: HBT, TCW, CFK, JRS, DRS, JLS

/amb

CMT-84 (10-84)

ANALYTICAL CHEMISTRY LABORATORY
Argonne National Laboratory
Argonne, IL 60439

REPORT OF ANALYTICAL RESULTS

ANS

Sample Material: UAl_2 Date Received: 7/18/89

Submitted by: R. Domagala Date Reported: 10/7/89

Your Number	Our Number	Oxygen, ppm	Nitrogen, ppm
E-270, UAl_2	89-0562-01	988 ± 77	45 ± 39

Oxygen and Nitrogen determined by inert-gas fusion. Hydrogen (also requested) was not determined because of mechanical difficulties with the hydrogen-analysis portion of the H-O-N Line. Arrangements for H determination are not planned unless dictated by Submitter's needs.

O & N Analyses on −120+200 mesh powder produced in N_2 glovebox from our ao-arc-cast ingot E-270. This is HEU "UAl_2". Previously, Isotopic U, Al & Spectrographic for impurities have been reported by our ACL. I am not requesting H analysis so this concludes the analysis of this mat'l which has been used in FANS batch No.2. XS mat'l is in H-137A

RFD
10-12-89

→ ANS FUEL ←

NOTE: Samples will be discarded one (1) month after date of report unless otherwise arranged. When making future inquiries regarding this work, you must reference *OUR* number(s) above. For further information about the results reported here, please call D. Graczyk at 2-3489.

D. Graczyk 10-10-89

Copies To: R. Domagala, T. Wiencek, H. Thresh, D. Green, D. Graczyk, R. Heinrich, H. Goodspeed, File

Analyst(s): H. Goodspeed

Don

XC: HRT DRS TCW FJK CFK JLS JRS ANS FILE

/amb

CMT-84 (10-84)

ICP-SPECTROCHEMICAL ANALYSIS REPORT UAl_2

SPEC NO. 56268

	Our No.	Your No.	Material	Ag	Al	As	B	Ba	Be	Bi	Ca	Co	Cr	Cu	Fe	Hg	K	Li	Cd		
89-	0562-01	E-270	U-Al		VS		(<10)	<2	21		11	<5	11	13	88		<20	<1	<2		

	Our No.	Your No.	Material	Mg	Mn	Mo	Na	Ni	P	Pb	Sb	Si	Sn	Sr	Ti	V	Zn	Zr			
89-	0562-01	E-270	U-Al	7	6	<10	38	16		<10				<.5		<2	3				

RESULTS REPORTED IN FOLLOWING UNITS

- [x] parts per million ($\mu g/g$)
- [ ] per cent
- [ ] micrograms per ml.
- [ ] micrograms in total sample
- [ ]

ESTIMATED ACCURACY OF RESULTS

- [ ] order of magnitude
- [ ] factor of two
- [x] 10 % of amount present

SYMBOL	MEANING
L	less than
G	greater than
	element not investigated
—	element not detected
•	interference
( )	accuracy uncertain
?	presence uncertain

SYMBOL	MEANING	APPROX. CONC.
VS	very strong	100% to 10%
S	strong	10% to 1%
M	moderate	1% to 0.1%
W	weak	0.1% to 0.01%
T	trace	0.01% to 0.001%
FT	faint trace	0.001% to 0.0001%

REMARKS:

ANS FUEL

SPEC. ANALYSIS OF −120+200 MESH POWDER. POWDER PRODUCED IN N_2 GLOVEBOX FROM OUR [redacted] AS-CAST ARC-MELT E-270 INTENDED COMPOSITION UAl_2 (HEU USED)

U & Al previously reported H-O-N still to come

RFD 8-21-89

XC: HRT JRS JLS TCW DRS CFK FJK

Plate No.

By: G. A. Huff

Date: 8-18-89

Submitted By: R.F. Domagala Location: 212 Date Received: 7-17-89

Reports To: -, T.C. Wiencek, N.R. Thresh, ACL Offic

CHM-61 (7-78)

Babcock & Wilcox
Naval Nuclear Fuel Division
Lynchburg, Virginia

NEW PRODUCTS

RAW MATERIAL & STRUCTURAL RELEASE

NPN-QC-9
2-17-83

FOR ANS
HEUAlx
7-21-89
INFO RECVD
9 PAGES

Distribution
Q.C. Audit & Release (1)
Q.C. Foreman (1)
Mfg. Foremen (1)
Prod. Control (2)
John & Louie (1) Fuel Plate Only
Accountability (1)

Contract/Job No. C29000113

B&W certifies that the supplies listed hereon conform to all contract requirements, including all applicable statistical requirements, and that substantiating data are on file.

Release No.	Component		Spec. & Rev. No.
	Name	Identification	
718-012	HEU Uranium Aluminide UAlx Powder	Lot 568	IN-F-5 TRA, Rev. 8 9-8-87
P.O. Number			TRTR-12 5-20-87
NA			

Sub-Contractor	Drawing		Last Oper.	Release For	Qty. & Weight
G.F.M	NA	GR/PC NA Rev. NA	Uranium Powder Prod	Production	17,716.74gm

Remarks:

Waivers: NONE

Signed Q.C. Brenda Triplett Date 7-14-89

B&W-NNFD
RTRFE-QC

POWDER PHYSICAL TEST ANALYSIS
06/01/89

NPN-QC-635
REVISION 0

LOT NUMBER 568 NPN 718 MATERIAL TYPE UALX-HEU

APPARENT DENSITY RUN No. 1
FULL CUP 149.43
EMPTY CUP-081.45
POWDER WT= 67.98 X .04 = 2.72 GM/CC

FLOW RATE RUN No. 1
27.70 SEC X 1.005 = 27.84 SEC

SIEVE TEST RUN No. 1 START WT = 100.00 0.00 / 100.00 = 0.00 % LOSS

SIEVE	TOTAL WT	POWDER WT		WT.%
45	0.00	00.00	=	0.00
100	0.03	00.03	=	0.03
170	41.72	41.69	=	41.69
200	54.95	13.23	=	13.23
270	75.92	20.97	=	20.97
325	88.83	12.91	=	12.91
PAN	98.78	09.95		
START-PAN = LOSS	1.22	PAN+LOSS = 11.17	=	11.17

INSPECTOR:M.HICKS DATE:06-01-89
Press RETURN to continue

B & H - N N F D
Lot No. 568 FUEL CERTIFICATION - UALX
STATUS (ACC/REJ = A/R) A EG&G/ORNL (E/O) E FUEL TYPE HEU RTRFE-OC
CORE TYPE ATR

I. PHYSICAL PROPERTIES

A. Crystalline Constituents (wt%) *(50 min)
UA12 7 *UA13 84 UA14 9 Unalloy U 0

B. Bulk Density (g/cc) 2.72

C. Particle Density 6.35

D. Seive Analysis (%)
1. -100 (99.5 min wt%) 99.97
2. +325 (70 min wt.%) 88.83
3. -325 (30 max wt.%) 12.91

E. Flow Rate (g/sec) 27.84

II. IMPURITY CONTENT - Nonmetalic (wt%)

1. Oxygen (.60 max) .330 2. Carbon (.18 max) .091
3. Nitrogen (.045 max) .009 4. Fat/Oil (.2 max) .01
5. Nonvolate(99.0 min) 100.0 6. Hydrogen(.020 max) .002

III. CHEMICAL COMPOSITION

Uranium Content (Wt%) (66 - 72 Wt%) 70.570
Aluminum Content (wt%) Balance 28.998

C. Isotopic Content

U-234 (1.2 (Univ .5) max wt% U) 1.019 U-235 (92-94 (Univ 19.55-19.95)wt% U) 93.057
U-236 (.7 (Univ 1.) max wt% U) 0.402 U-238 (5.05-7.05 (Univ Bal.) wt% U) 5.522

IMPURITY CONTENT - Metallic (ppm)

	ELEMENT	SYM	PPM's	EBC		ELEMENT	SYM	PPM's	EBC
1.	Barium	Ba	3.0	0.000366	14.	Nickel	Ni	20.0	0.022440
2.	Beryllium	Be	1.0	0.000015	15.	Phosphorus	P	20.0	0.001740
3.	Boron	B	2.0	1.999998	16.	Silicon	Si	30.0	0.001980
4.	Calcium	Ca	20.0	0.003160	17.	Silver	Ag	1.0	0.008236
5.	Cadmium	Cd	.5	0.162549	18.	Tin	Sn	5.0	0.000360
6.	Chromium	Cr	10.0	0.007990	19.	Tungsten	W	30.0	0.044880
7.	Cobalt	Co	5.0	0.046195	20.	Vanadium	V	20.0	0.028120
8.	Copper	Cu	20.0	0.017360	21.	Zinc	Zn	20.0	0.004820
9.	Iron	Fe	914.0	0.614208	22.	Zirconium	Zr	20.0	0.000580
10.	Lead	Pb	1.0	0.000011	23.	Samarium	Sm	.2	0.104915
11.	Magnesium	Mg	10.0	0.000400	24.	Europium	Eu	.2	0.086795
12.	Manganese	Mn	10.0	0.034430	25.	Gadolinium	Gd	.2	0.838916
13.	Molybdenum	Mo	30.0	0.012090	26.	Dysrosium	Dy	.2	0.019413

Total EBC Content (max 30 ppm) 4.061967

Press RETURN to continue

Ledoux & Company
EST 1880

CABLE ADDRESS "LEDOUX TEANECK"
TELEX 134340
FAX 201-837-1235

359 Alfred Avenue, Teaneck, New Jersey 07666 ○ Telephones: 201 837-7160
212 947-0953

INDEPENDENT CONTROL AND RESEARCH CHEMISTRY, INSTRUMENTAL AND CHEMICAL ANALYSIS • SAMPLING
WEIGHING, SHIPPERS' REPRESENTATION, BENEFICATION, AND STORAGE OF ORES AND METALS

June 13, 1989

Ledoux & Company Analysis # : 1092857

Material identified by client as: UAlx Lot# 568

Purchase Order #: DMP-00381

Sample Marked : NP-7461

Submitted to us for analysis : Babcock & Wilcox .

	NP-7461	NBS-U-930
Uranium-234	1.019 %	1.076 %
Uranium-235	93.057 %	93.275 %
Uranium-236	0.402 %	0.205 %
Uranium-238	5.522 %	5.444 %
Uranium-235 95%CF=	+/- 0.02	+/- 0.02

* * * * * * *

Invoice & 2 to : Babcock & Wilcox Company

LEDOUX & COMPANY

Ledoux & Company
EST 1882

CABLE ADDRESS "LEDOUX TEANECK"
TELEX 134340
FAX 201-837-1235

359 Alfred Avenue, Teaneck, New Jersey 07666 ○ Telephones: 201 837-7160
212 947-0953

INDEPENDENT CONTROL AND RESEARCH CHEMISTRY, INSTRUMENTAL AND CHEMICAL ANALYSIS • SAMPLING WEIGHING, SHIPPERS' REPRESENTATION, BENEFICATION, AND STORAGE OF ORES AND METALS

June 13, 1989

Ledoux & Company Analysis #: 1092857

Material identified by client as: UAlx LOT #568

Purchase Order : DMP-00381

Sample marked : NP-7461

Submitted to us for analysis by : Babcock & Wilcox Co.

Barium	3	ppm
Beryllium ...	<1	ppm
Boron	2	ppm
Cadmium	<0.5	ppm
Calcium	<20	ppm
Carbon	912	ppm
Chromium	10	ppm
Cobalt	<5	ppm
Copper	20	ppm
Dysprosium ..	<0.2	ppm
Europium	<0.2	ppm
Gadolinium ..	<0.2	ppm
Iron	914	ppm
Lead	1	ppm
Magnesium ...	<10	ppm
Manganese ...	10	ppm
Molybdenum ..	30	ppm
Nickel	20	ppm
Nitrogen	87	ppm
Phosphorous .	<20	ppm
Samarium	<0.2	ppm
Silicon	30	ppm
Silver	<1	ppm
Tin	5	ppm
Tungsten	30	ppm
Vanadium	20	ppm
Zinc	<20	ppm
Zirconium ...	20	ppm

* * * * * *

Invoice & 2 to: Babcock & Wilcox Company

LEDOUX & COMPANY

LRC-124

RADIOANALYTICAL
CHEMISTRY LABORATORY
ANALYSIS REQUEST

Babcock & Wilcox®
a McDermott company
LYNCHBURG RESEARCH CENTER

REQUESTER	CHARGE NUMBER	DATE	DUE DATE
A. B. Cohen	NPN 718	06/02/89	06/02/89

PRIORITY (SEE REVERSE OF LAST COPY)

A	B	C	D
NUMBER OF SAMPLES 1	RADIOACTIVE X NON-RADIOACTIVE	TEST NUMBER	

SAMPLE NUMBERS

893 = Lot #568

SPECIAL HANDLING AND DISPOSAL PROCEDURES

RETURN ALL MATERIAL

DESCRIPTION OF SAMPLES AND DESIRED ANALYSIS (INCLUDE MAXIMUM DESIRED ERROR LIMITS)

UALX for Phase Analysis

RESULTS

UAL2	7%	6%
UAL3	84%	85%
UAL4	9%	9%

Unalloyed U not detected

ANALYZED BY	DATE	APPROVED BY	DATE
EM	06/02/89		
REQUEST NUMBER 01535	**LABORATORY BOOK NUMBER** 1134		**PAGE** 38

This form consists of:
Original — Laboratory copy
Canary — Results copy
Pink — Inter-Laboratory copy
Goldenrod — Requester copy

Babcock & Wilcox
Naval Nuclear Fuel Division
Lynchburg, Virginia

QUALITY CONTROL

CHEMISTRY LABORATORY

PAGE 1 OF 1
DATE 2-23-87

CHEMISTRY ANALYSIS

Q2-103 Rev. 2

To: B. Triplett #61

Sample No.	Log No.	Material Type	Date
Listed Below	Listed below	UALX	07-13-89

NPN-718

UALX

Lab No.	Sample No.		W/O H	Oxygen
C-65382	S-2-0567	NP-7452	0.004	0.37%
		NP-7453	0.003	0.31
C-65383	S-2-0568	NP-7464	0.002	0.33
		NP-7465	0.002	0.29
C-65307	S-2-0569	NP-7476	0.004	0.30
		NP-7477	0.004	0.30

Knowingly and willfully falsifying or concealing a material fact on this form, or making false, fictitious or fraudulent statements or representations herein could constitute a felony punishable under Federal statutes.

Audited By [signature] Date 7-13-89 Q2-103

Special Products	Quailty Control	Chemistry Lab

BRENDA TRIPLETT

Contract_PAC-718___

Sample No.	Listed Below	Log No.	SP-342	Material Type	Listed Below	Date	7-3-89

UALX
S-2-00568

Sample No.	U%
NP-7464	* 70.35
	* 70.23
NP-7465	* 70.83
	* 70.86
NP-7467	66.34
	66.34
NP-7468	67.80
	67.67
NP-7458	
NP-7462	
NP-7459	

%-NON-VOLATILE
100.01%

DENSITY
6.35g/cc

FATTY & OILY
.005%

OXYGEN

CC DANNY CARWILE

* avg. - 70.57%

Knowingly and wilfully falsifying or concealing a material fact on this form or making false, fictious or fraudulent statements or representations therein could constitute a felony punishable under federal statues.

Audited By	R.W. Richardson	Date	7-3-89

Special Products	Quailty Control	Chemistry Lab

T DANNY CARWILE Contract PAC-718

Sample No.	Listed Below	Log No.	SP-342	Material Type	Listed Below	Date	6-8-89

S-2-00568

UALX

Sample No.	U%	
NP-7464	70.35%	
7464	70.23%	
NP-7465	70.83	
7465	70.86%	E70.5T PRODUCT
NP-7467	66.34%	
7467	66.34%	
NP-7468	67.80%	
7468	67.67%	E67.0T SCRAP

Knowingly and wilfully falsifying or concealing a material fact on this orm or making false, fictious or fraudulent statements or representations ierein could constitute a felony punishable under federal statues.

Audited By	R.W. Richardson	Date	6-8-89

Babcock & Wilcox Naval Nuclear Fuel Division Lynchburg, Virginia	NEW PRODUCTS	RAW MATERIAL & STRUCTURAL RELEASE

NPN-QC-9
2-17-83

FOR ANS
RECVD INFO
7-21-89
HEU_3O_8
6 PAGES

Distribution

Q.C. Audit & Release	(1)
Q.C. Foreman	(1)
Mfg. Foremen	(1)
Prod. Control	(2)
John & Louie	(1) Fuel Plate Only
Accountability	(1)

Contract/Job No. 82X-99775C

B&W certifies that the supplies listed hereon conform to all contract requirements, including all applicable statistical requirements, and that substantiating data are on file.

Release No.	Component		Spec. & Rev. No.
555-2806	Name	Identification	
P.O. Number N/A	Enriched U308 Uranium	Lot No. 512212	RRFE-UO-P, Revision 0 dated 7/19/82

Sub-Contractor	Drawing		Last Oper.	Release For	Qty. & Weight
GFM	N/A	GR/PC N/A Rev. N/A	Incoming Inspection	Production	126,856.85 gms.

Remarks:

Waivers: NONE

Signed Q.C. S Almond Date 1/24/89

Special Products	QUALITY CONTROL	CHEMISTRY LABORATORY	Page 1 of 1 Date 10-14-87
	CHEMISTRY ANALYSIS		Q2-159 Rev. 0

Tr D. Carwile #31

Sample No.	Log No.	Material Type	Date
Listed Below	C-63370	Listed Below	5-31-88

NPN-555

FZF- FCW- 48

Lot # 512212 PAC -504

Sample No.	U
NP-2951	84.68%
NP-2952	84.68
NP-2954	84.67
NP-2955	84.66
NP-2956	84.65
NP-2957	84.68
NP-2958	84.68
NP-2959	84.64

$\bar{X}$ 84.67

LEDOUX SAMPLE

LOT # 512212 NP-2960 93.164 ✓

now ... and willfully falsifying or concealing a material fact on this form, or making false, fictitious or ... udul... statements or representations herein could constitute a felony punishable under Federal statutes.

udited ...

y ...

ate 6-1-88

Q2-159

Ledoux & Company
EST 1880

CABLE ADDRESS "LEDOUX TEANECK"
TELEX 134340
FAX 201-837-1235

359 Alfred Avenue, Teaneck, New Jersey 07666 ○ Telephones: 201 837-7160
212 947-0953

INDEPENDENT CONTROL AND RESEARCH CHEMISTRY, INSTRUMENTAL AND CHEMICAL ANALYSIS • SAMPLING
WEIGHING, SHIPPERS' REPRESENTATION, BENEFICATION AND STORAGE OF ORES AND METALS

June 3, 1988

Ledoux & Company Analysis #: 1085002

Material identified by client as: U3O8 Powder LOT # 5H221L
Purchase Order : DMP-00381
Samples Marked : NP-2960 FZF-FCW-48
PAC 5C4
Submitted to us for analysis by : Babcock & Wilcox

	NP-2960	NBS-U-930
Uranium-234.....	1.010 %	1.080 %
Uranium-235.....	93.164 %	93.277 %
Uranium-236.....	0.389 %	0.205 %
Uranium-238.....	5.437 %	5.438 %

* * * * * * *

Invoice and 2 to: Babcock & Wilcox Company

LEDOUX & COMPANY

E W Hall

Chemical and Spectographic Data
Work Request 1988, RFSW 6935
Sample Lot 521212

Component	Specification	Y-12 Analysis
Uranium (wt %)	> 84.5	.8460 ✓
Assay (wt %)	> 93.0	93.18 ✓
Density (g/cc)	> 8.0	8.2 ✓
Surface Area (M^2/gm)	.07 + .003	.072 ✓
% UO_2	< 1.0%	< 1.0% ✓

Impurities (ppm Metal Basis)

Element	Specificaion	Analysis
Al	100	6 ✓
B	2	< .1 ✓
Ba	10	< 2 ✓
Be	0.2	< .1 ✓
Ca	50	< 10 ✓
Cd	0.5	< .1 ✓
Co	3	< 1 ✓
Cr	*	< 2 ✓
Cu	20	1 ✓
Fe	*	< 10 ✓
K	20	< 10 ✓
Li	5	< .2 ✓
Mg	< 100	30 ✓
Mn	5	< 1 ✓
Na	20	7.5 ✓
Ni	*	1 ✓
P	100	< 100 ✓
Si	50	< 10 ✓
V	2	< 1 ✓
F	20	< .200 ✓
Cr, Ni, Fe*	150	< 13 ✓

Screen
Analysis by Syntron Sieve

Mesh		%
	+170	0 ✓
-170	+200	24
-200	+230	29
-230	+270	17
-270	+325	18
-325		12 ✓

Nuclear Materials Control
September 28, 1987

Babcock & Wilcox NNFD

RECEIPT OF NUCLEAR MATERIAL-RTRFE

E4-11
Rev. 0

Date Received 5-12-88 Document No. _____ Carrier SST

Type Material HFIR U308 Containers: No. 16 Type 6M Condition Good

Remarks _____ Marking Good

Date & Time Rec. 5-12-88 1030 Date & Time Ck. Complete 5-13-88 1029

Outer Cont. I.D.	Seal	Inner I.D. Lot.Can.NP#.or Item ID		Label Gross	Actual Gross	Diff.	Label Net.	Actual Net.	Diff.	
2009	4862	512212	Can 1	4362	4362	0	4000 kg	3999.61	-.39	
↓	↓		Can 2	4362	4363	1	4.000 kg	4000.03	+.03	
2014	4863		Can 3	4364	4365	1	4.000 kg	3999.80	-.20	
↓	↓		Can 4	4359	4359	0	4.000 kg	4000.39	+.39	
2016	4864		Can 5	4364	4364	0	4.000 kg	3999.98	-.02	
↓	↓		Can 6	4367	4367	0	4.000 kg	4001.12	+1.12	
2010	4865		Can 7	4364	4364	0	4.000 kg	3999.77	-.23	
↓	↓		Can 8	4361	4362	1	4.000 kg	4001.18	+1.18	
2024	4866		Can 9	4361	4361	0	4.000 kg	4000.49	+.49	
↓	↓		Can 10	4366	4366	0	4.000 kg	4000.50	+.50	
2037	4867		Can 11	4361	4362	1	4.000 kg	4000.16	+.16	
↓	↓		Can 12	4364	4364	0	4.000 kg	4000.40	+.40	
2047	4868		Can 13	4361	4361	0	4.000 kg	4000.60	+.60	
↓	↓		Can 14	4359	4361	2	4.000 kg	3999.04	-.96	
2052	4869		Can 15	4363	4364	1	4.000 kg	4000.74	+.74	
↓	↓		Can 16	4362	4363	1	4.000 kg	4000.59	+.59	
2057	4870		Can 17	4360	4361	1	4.000 kg	3998.87	-1.13	
↓	↓		Can 18	4360	4360	0	4.000 kg	4000.33	+.33	
2062	4871		Can 19	4359	4359	0	4.000 kg	4000.25	+.25	
↓	↓		Can 20	4362	4363	1	4.000 kg	3999.72	-.28	
2063	4872		Can 21	4360	4360	0	4.000 kg	4000.92	+.92	
↓	↓		Can 22	4360	4360	0	4.000 kg	4000.32	+.32	
2093	4873		Can 23	~~4362~~ 4392	~~4363~~ 4363	0	4.000 kg	3999.62	-.38	
↓	↓		Can 24	4364	4364	0	4.000 kg	3998.41	-1.59	
F-036	4874		Can 25	4365	4365	0	4.000 kg	4000.21	+.21	
↓	↓		Can 26	4361	4361	0	4.000 kg	3999.19	-.81	
F-064	4875	512212	Can 27	4360	4360	0	4.000 kg	3999.30	-.70	

Continued on pg 2 of 2

*MPakeri 5/13/88
N.N.Foust 5-13-88

Received by N.N.Foust/MPakeri Date 5-13-88

Nuclear Materials Control
September 28, 1987

Babcock & Wilcox N

RECEIPT OF NUCLEAR MATERIAL-RTRFE

E4-1A
Rev. 0

Date Received 5-12-88 Document No. _____ Carrier SST

Type Material HFIR U308 Containers: No. 16 Type 6M Condition Good

Remarks _____ Marking Good

Date & Time Rec. 5-12-88 1030 Date & Time Ck. Complete 5-13-8

Outer Cont. I.D.	Seal	Inner I.D. Lot.Can.NP#.or Item ID		Label Gross	Actual Gross	Diff.	Label Net.	Actual Net.	Diff.
F-064	4875	512212 Can 28		4360	4360	0	4.000 kg	3999.58	-.42
F-125	4876	Can 29		4361	4361	0	4.000 Kg	4000.44	+.44
↓	↓	Can 30		4362	4363	1	4.000 Kg	3999.92	-.08
F-140	4877	Can 31		3791	3791	0	3.428 Kg	3428.43	+.43
↓	↓	512212 Can 32		3788	3789	1	3.427 Kg	3426.94	-.06
						12	126,855	126856.85	+1.85

Page 2

Received by MPAkers / H. N. Forist Date 5-13-88

Knowingly and willfully falsifying or concealing a material fact on this form, or making false, fictitious or ... could constitute a felony punishable under Federal statutes.

A-33

Appendix B. SUPPLEMENTARY OPTICAL AND SCANNING ELECTRON MICROGRAPHS OF HANS-1 AND HANS-2 FUEL SAMPLE

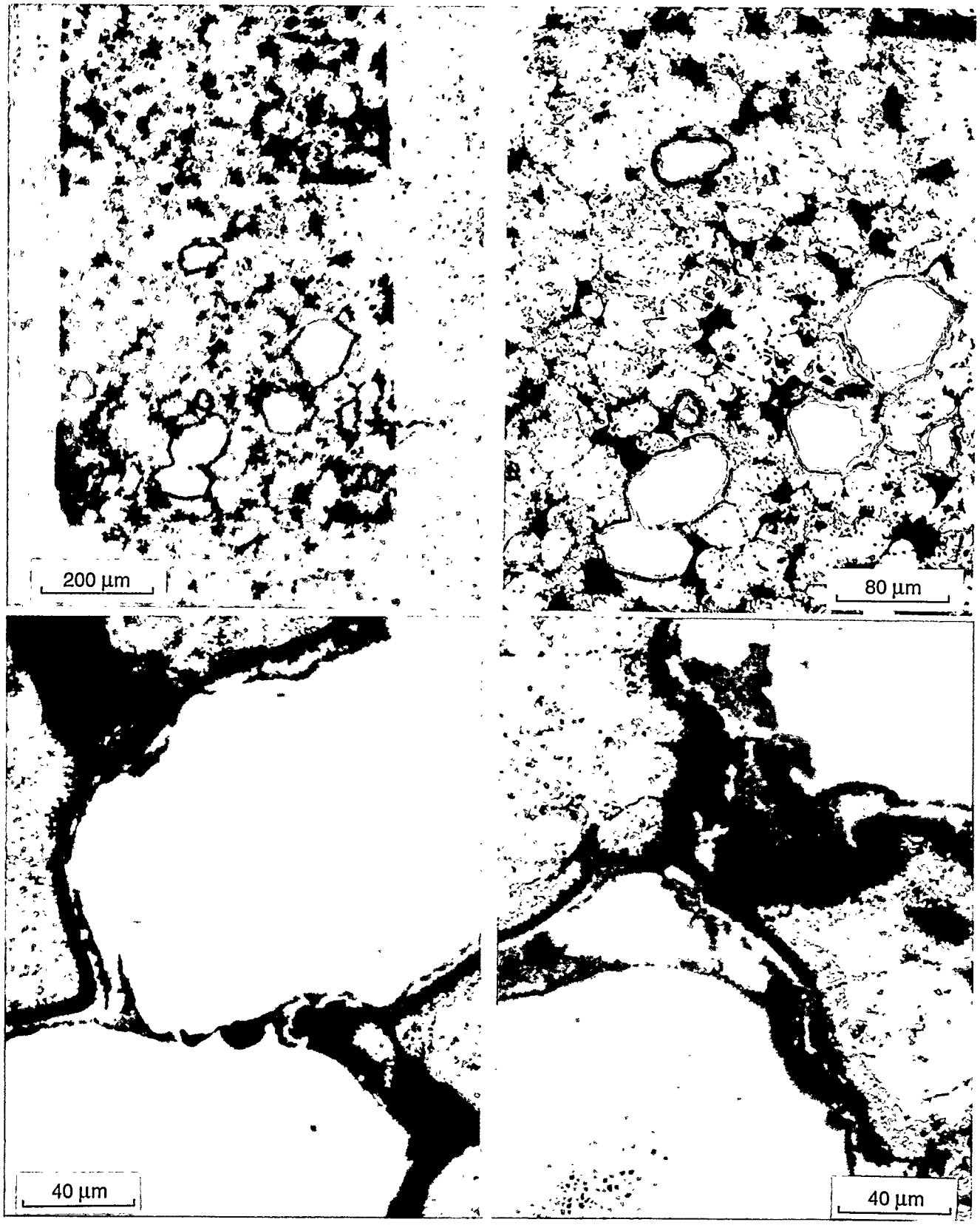

HANS-1, Sample #9, U_3Si_2, 425°C, Optical

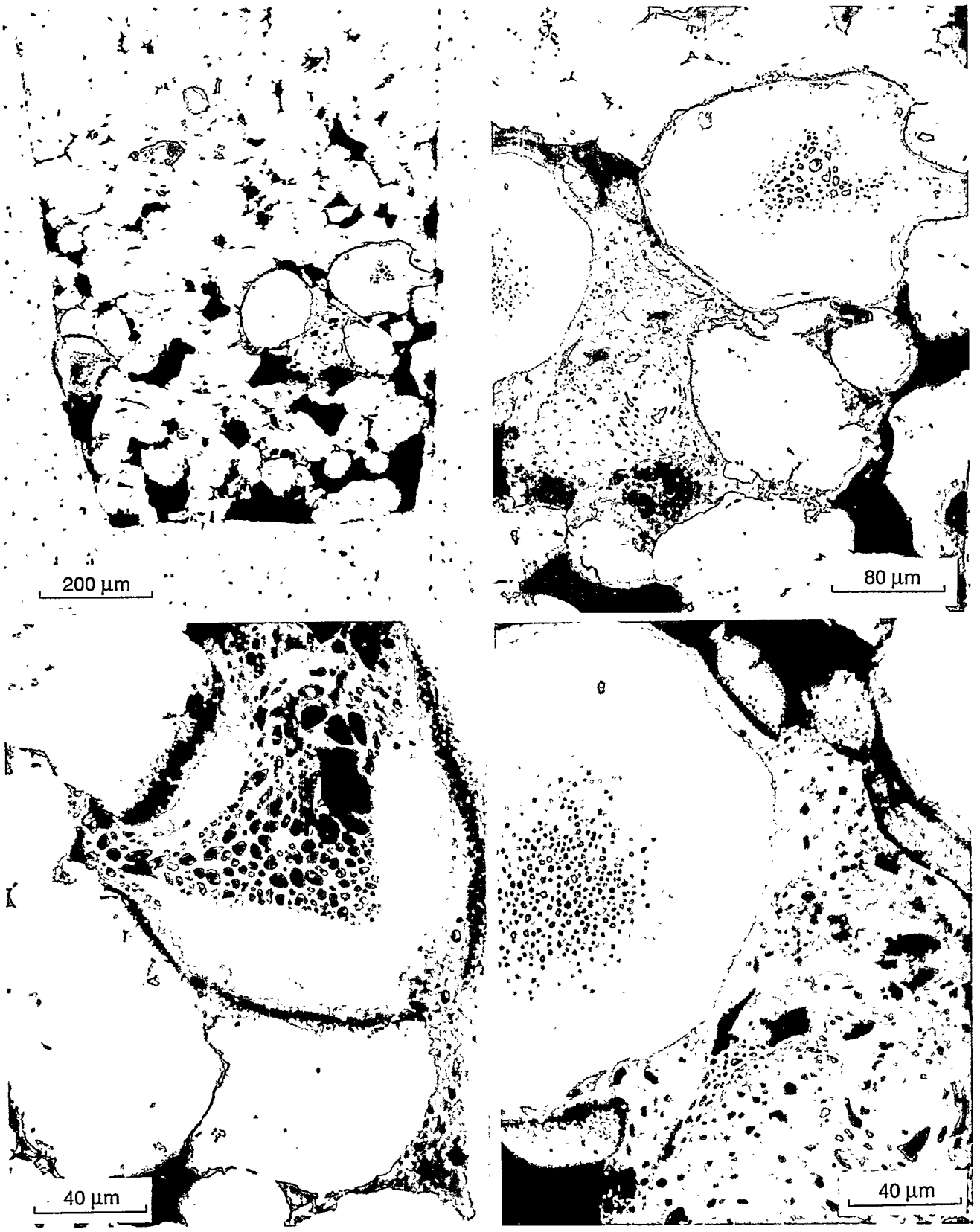

HANS-1, Sample #15, U_3Si_2, 425°C, Optical

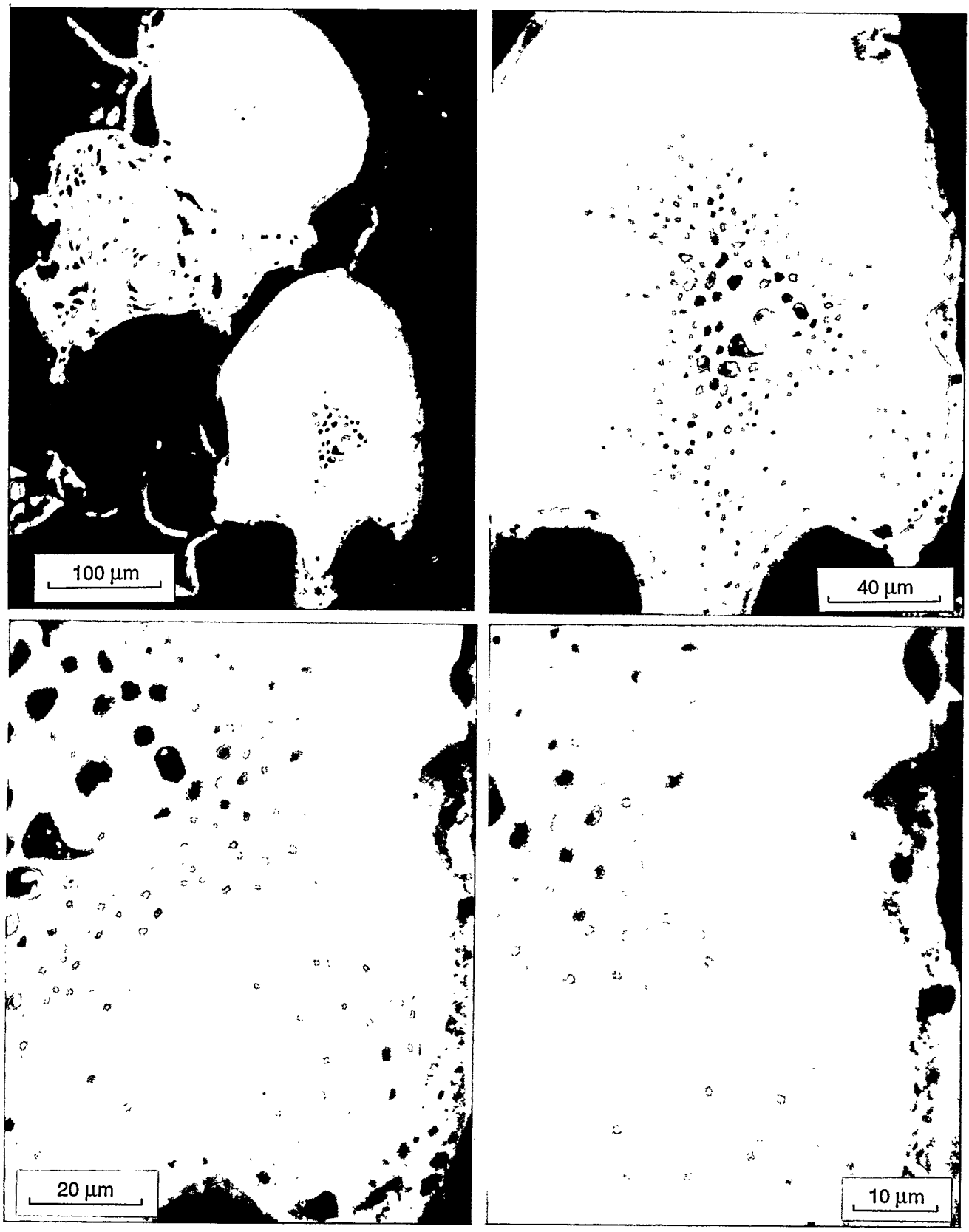

HANS-1, Sample #15, U_3Si_2, 425°C, SEM

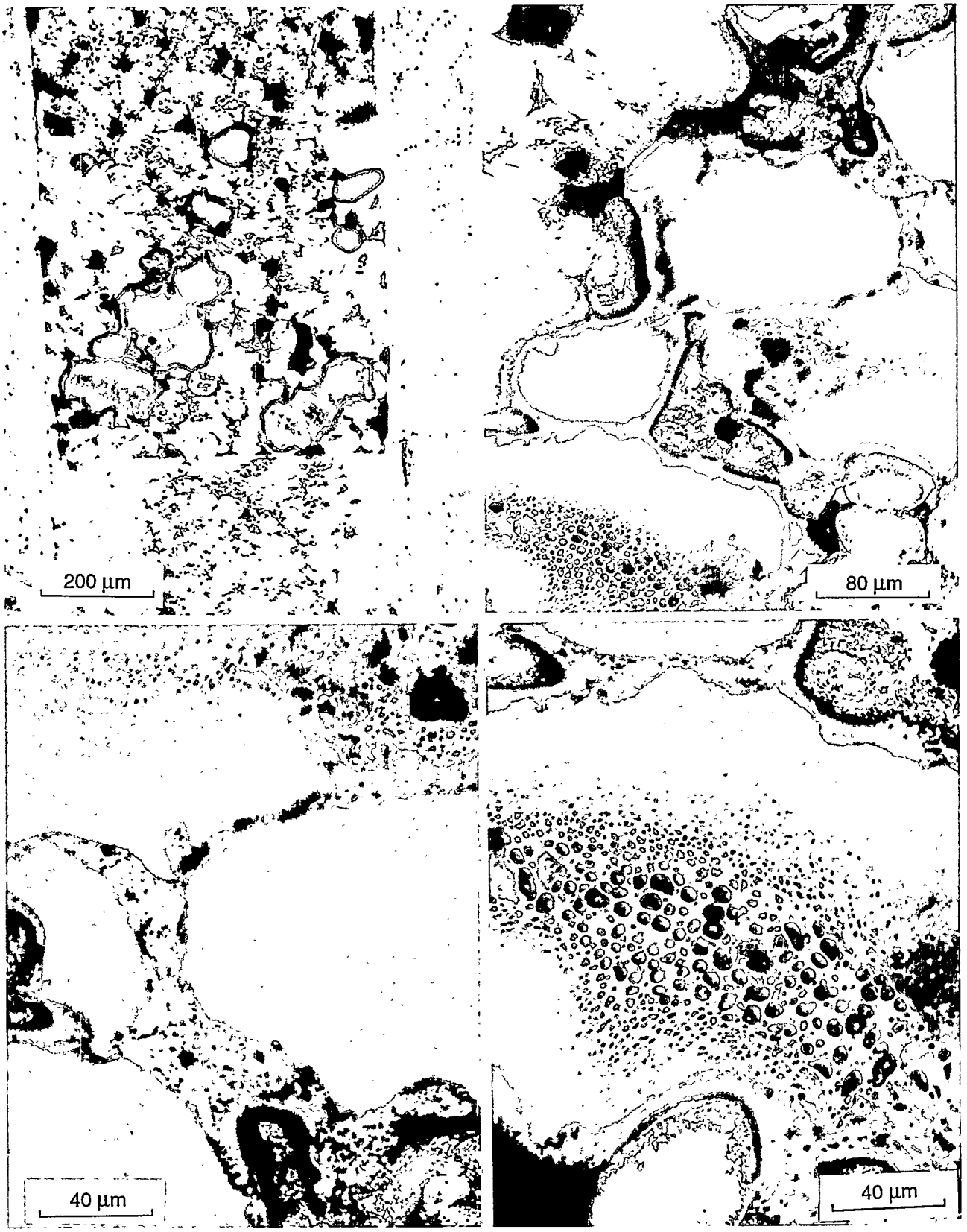

HANS-1, Sample #10, U_3Si_2, 425°C, Optical

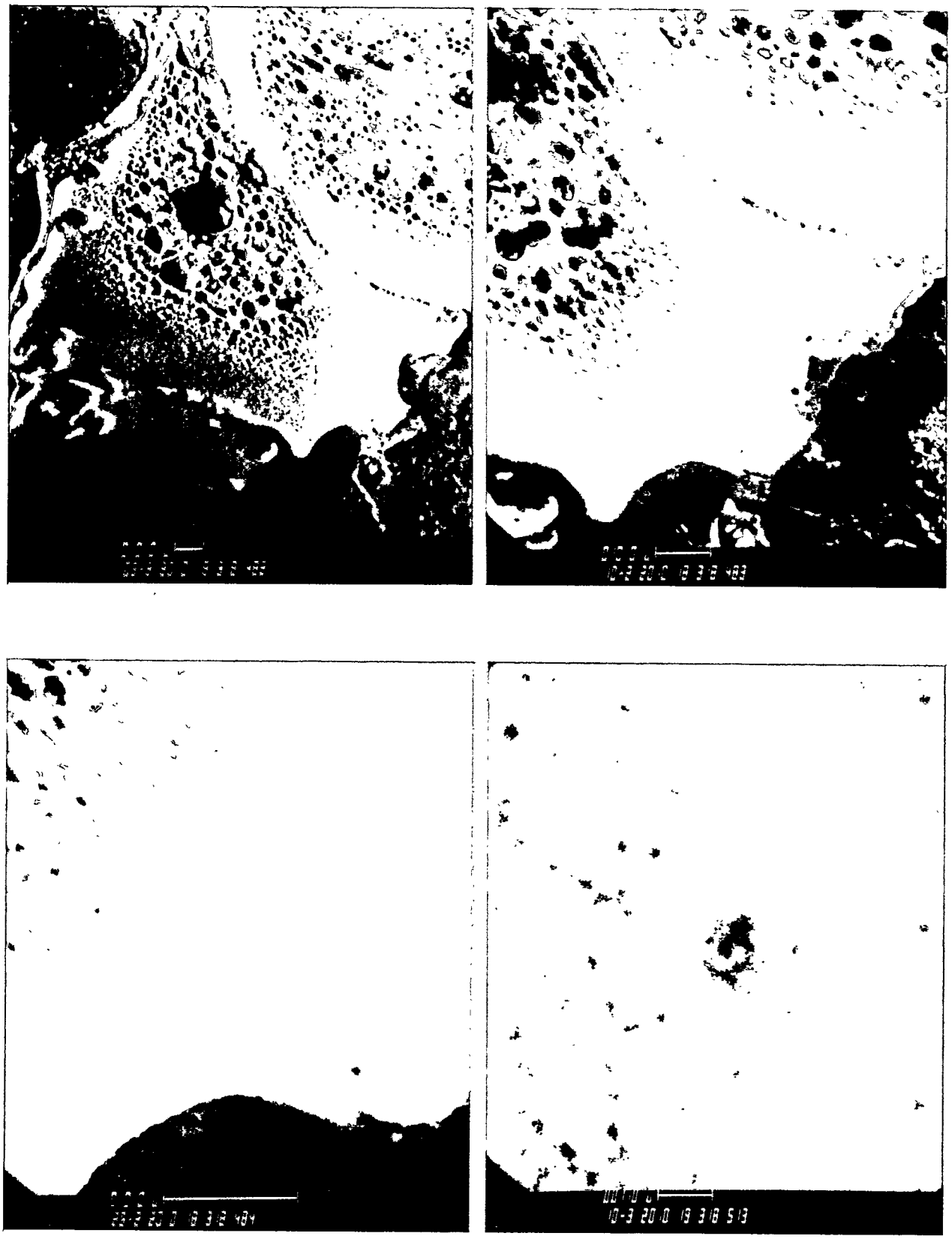

HANS-1, Sample #10, U_3Si_2, 425°C, SEM

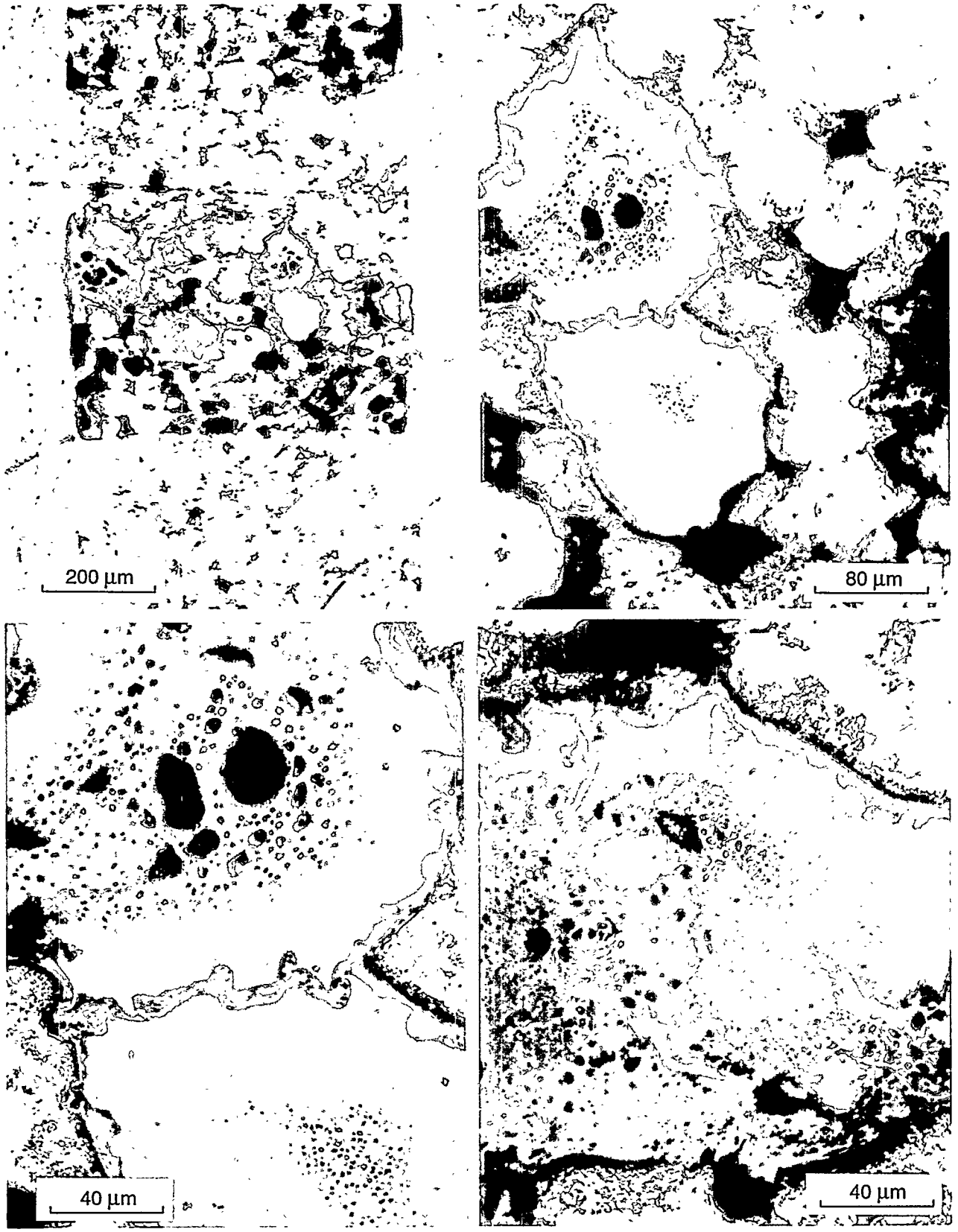

HANS-1, Sample #8, U_3Si_2, 375°C, Optical

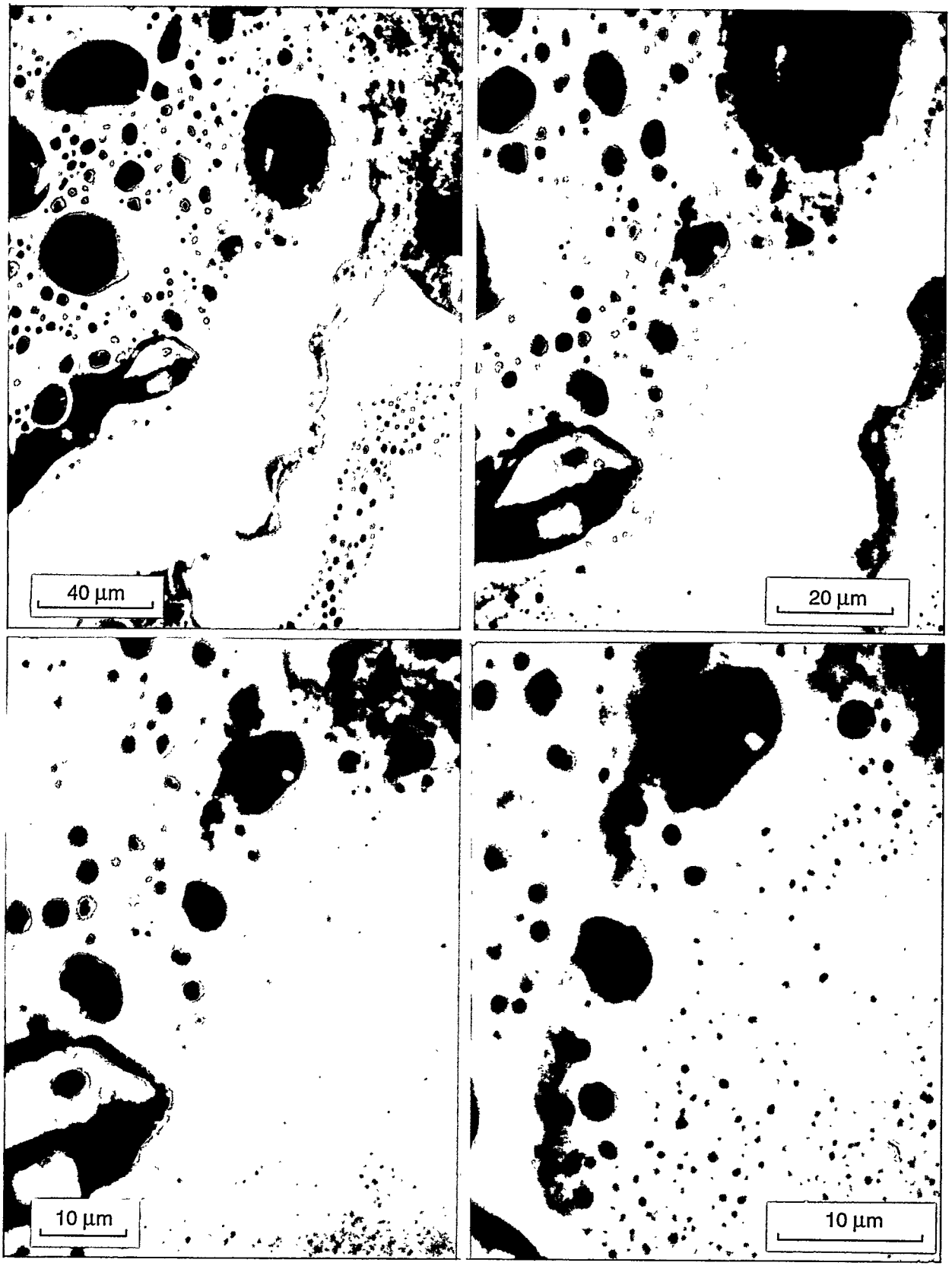

HANS-1, Sample #8, U_3Si_2, 375°C, SEM

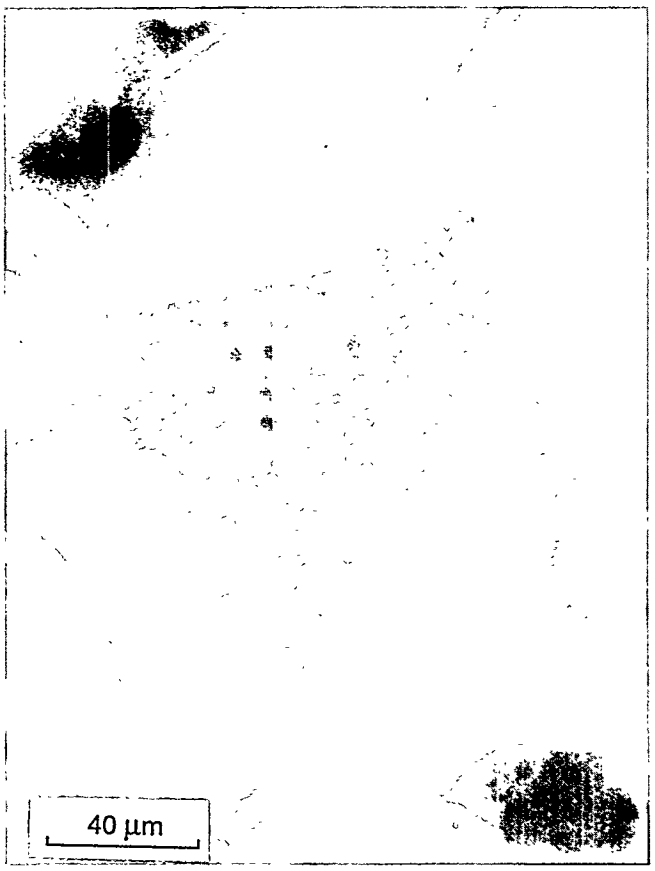

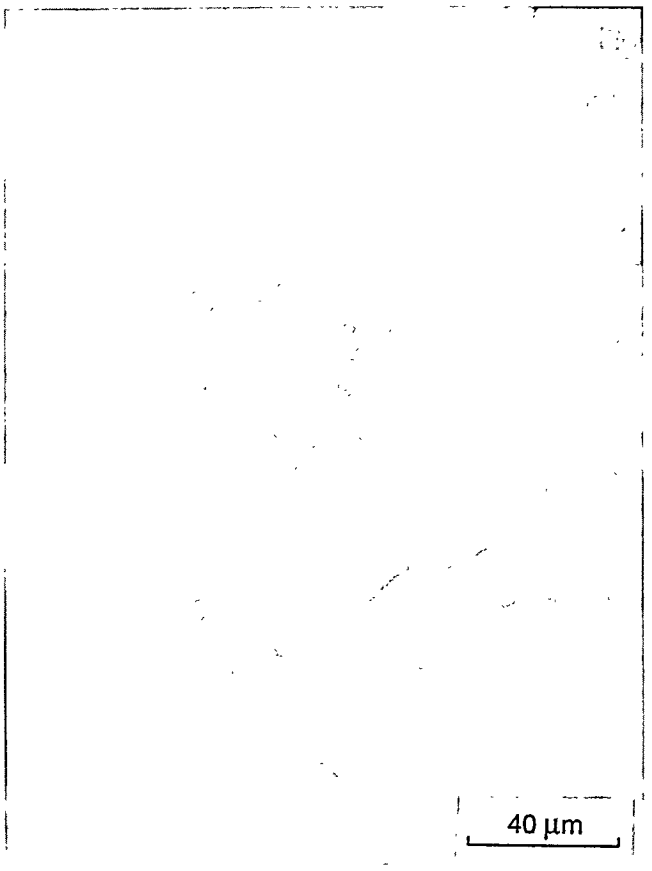

HANS-1, Sample #16, U_3Si_2, 375°C, Optical

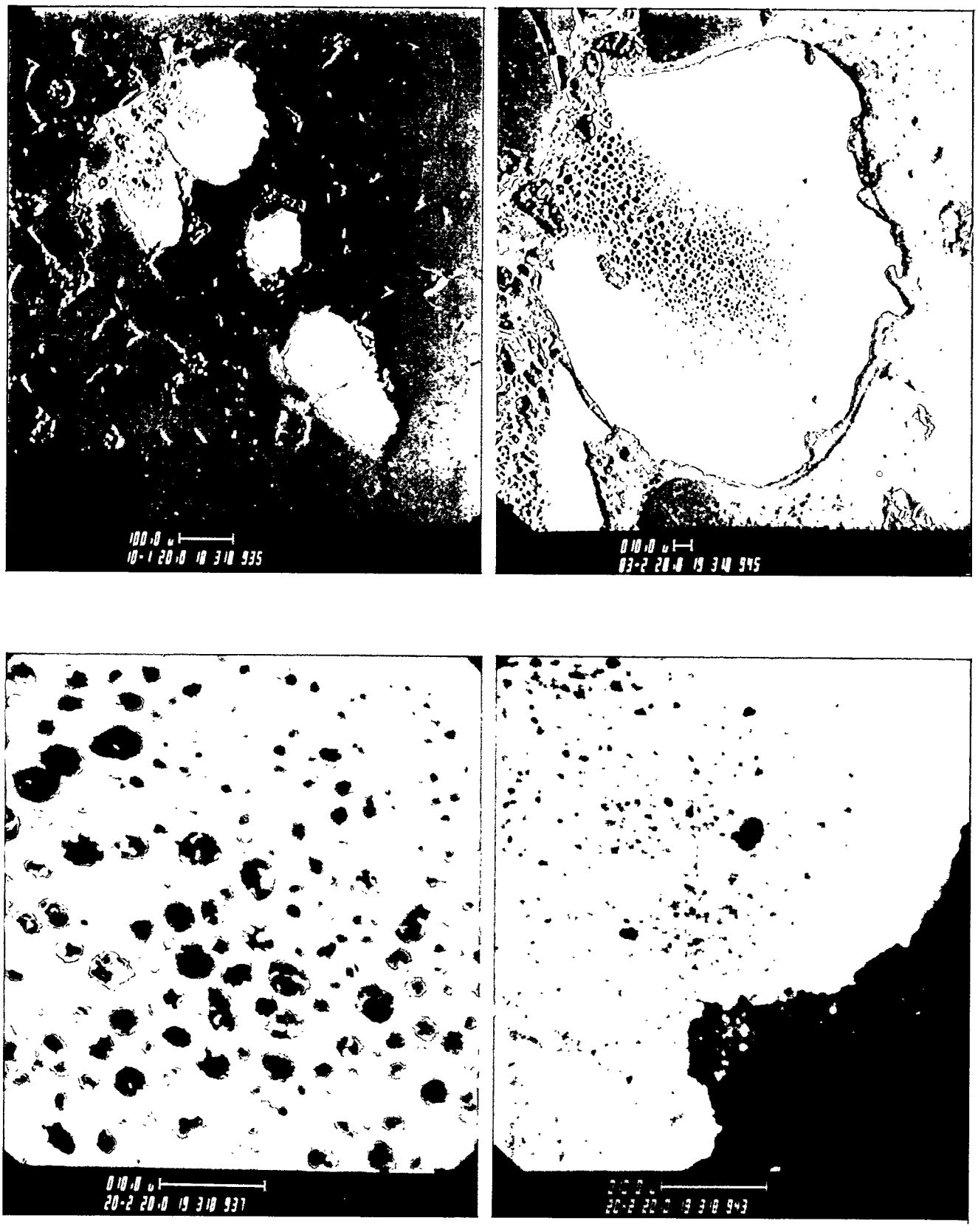

HANS-1, Sample #16, U_3Si_2, 375°C, SEM

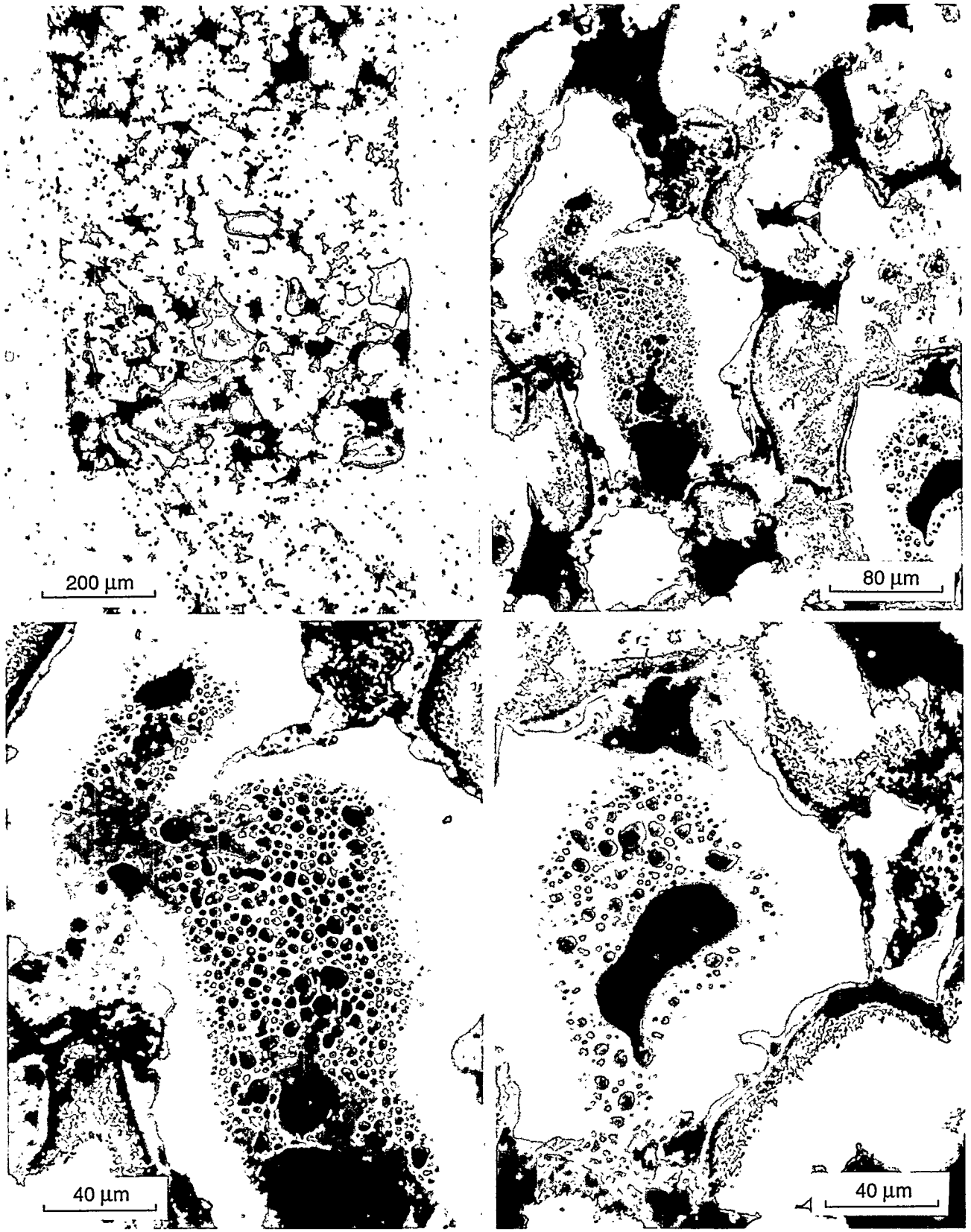

HANS-1, Sample #17, U_3Si_2, 325°C, Optical

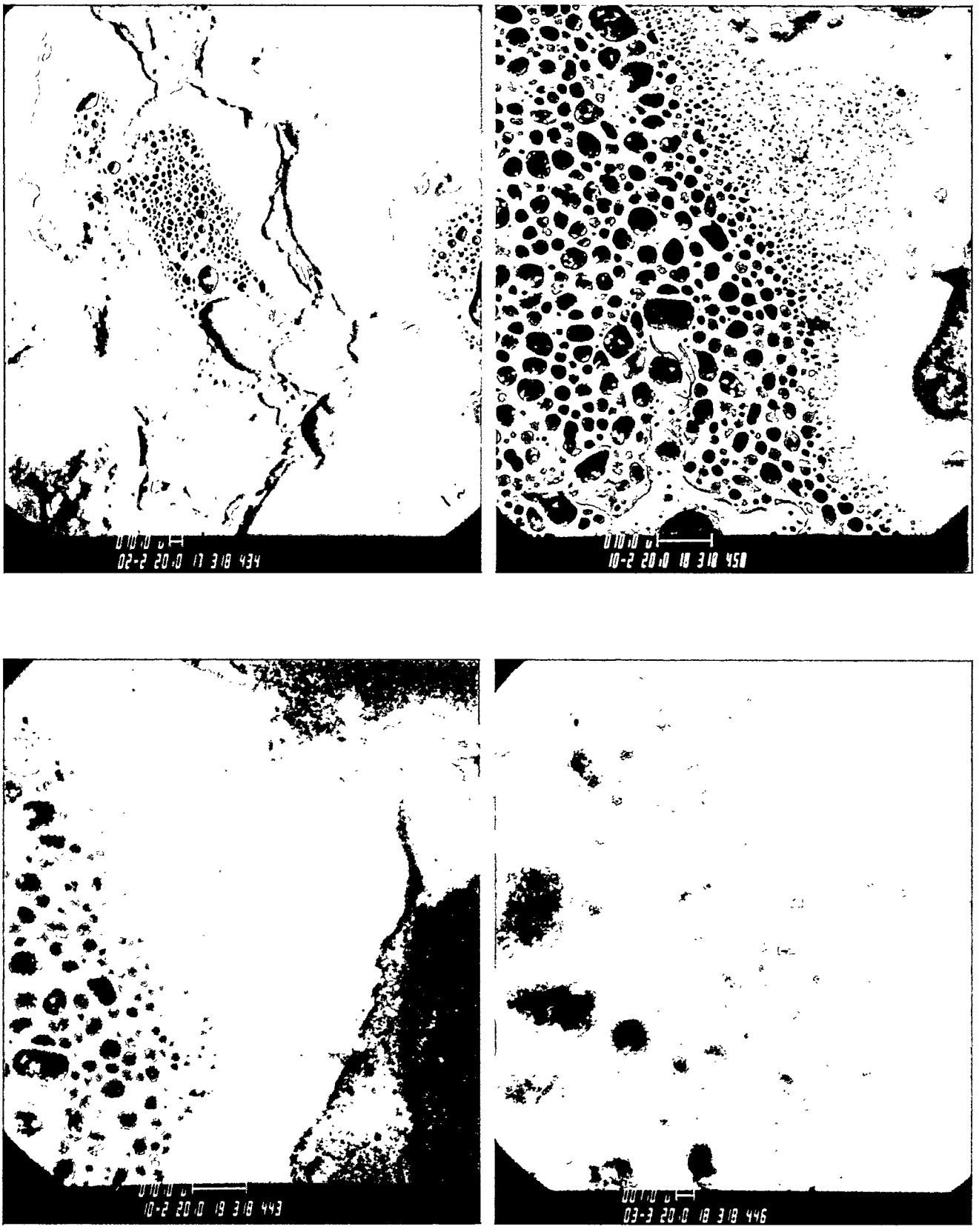

HANS-1, Sample #17, U_3Si_2, 325°C, SEM

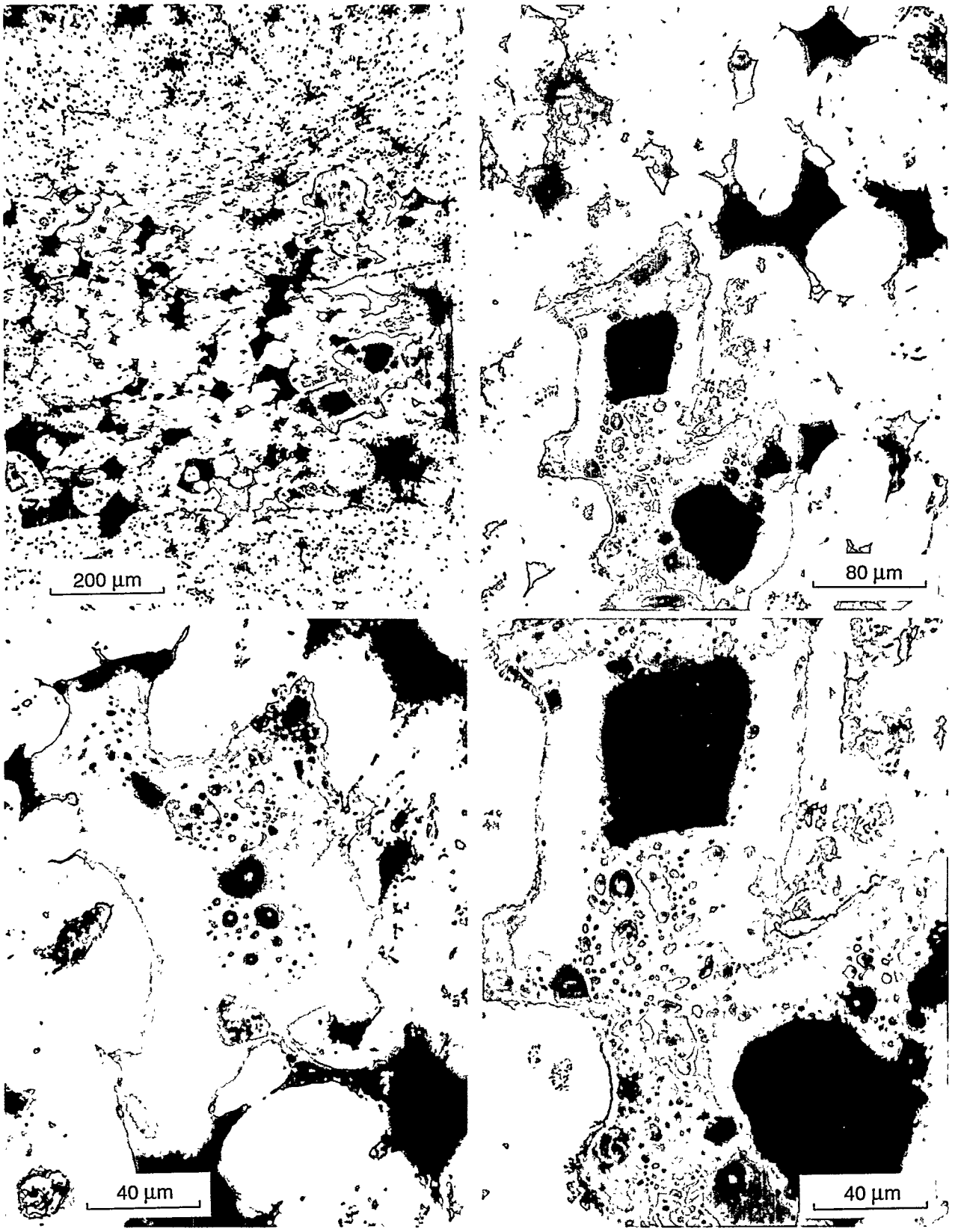

HANS-1, Sample #7, U_3Si_2, 325°C, Optical

HANS-1, Sample #4, U_3Si_2, 250°C, Optical

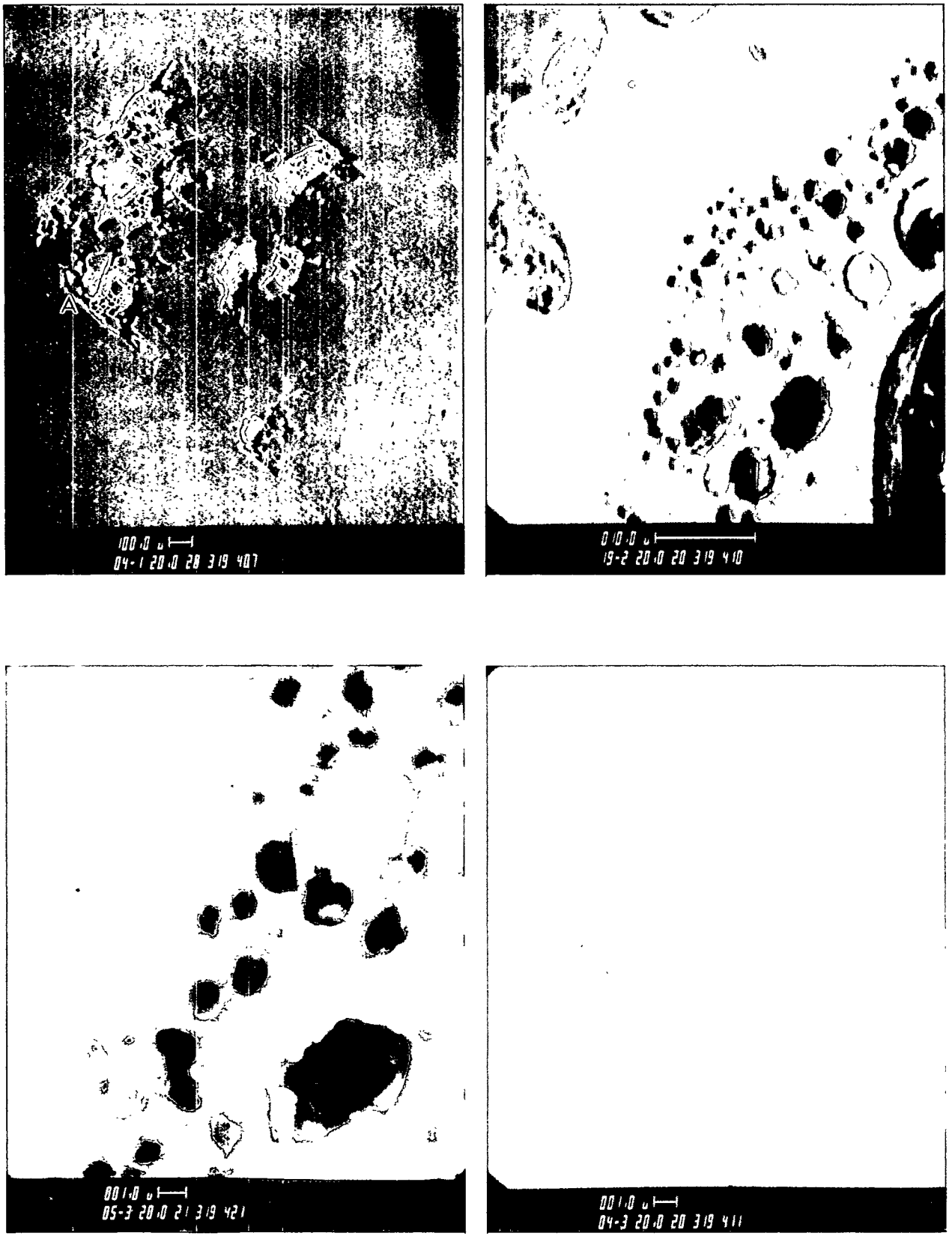

HANS-1, Sample #18, U_3Si_2, 250°C, SEM

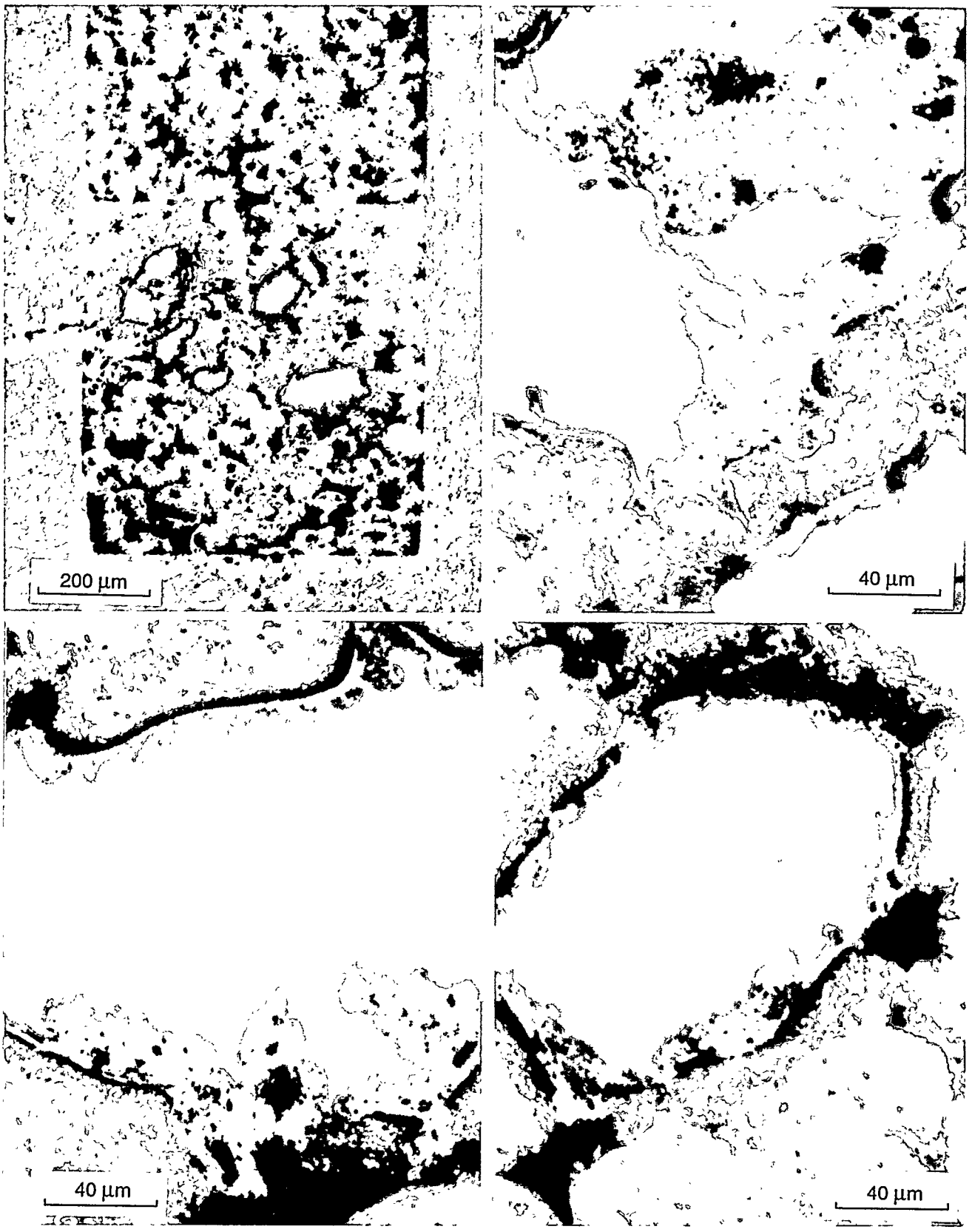

HANS-1, Sample #14, U_3Si, 375°C, Optical

HANS-2, Sample #11, U_3Si_2, 425°C, Optical

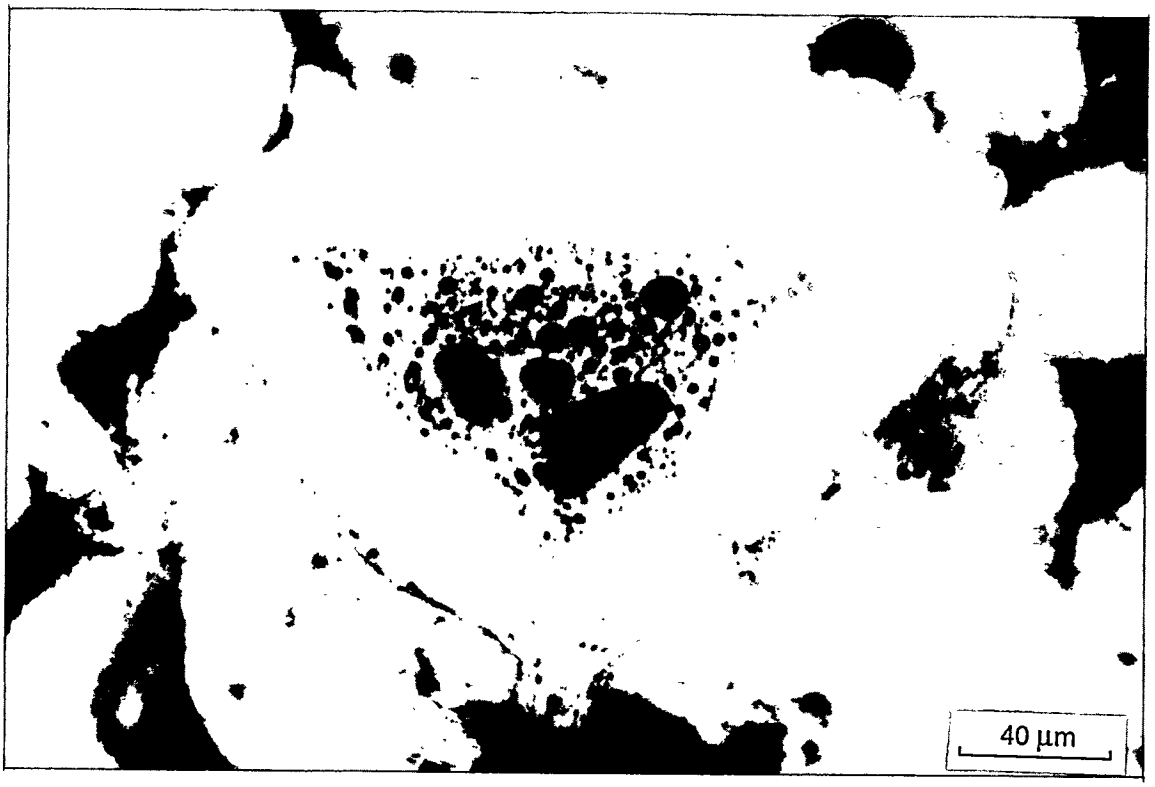

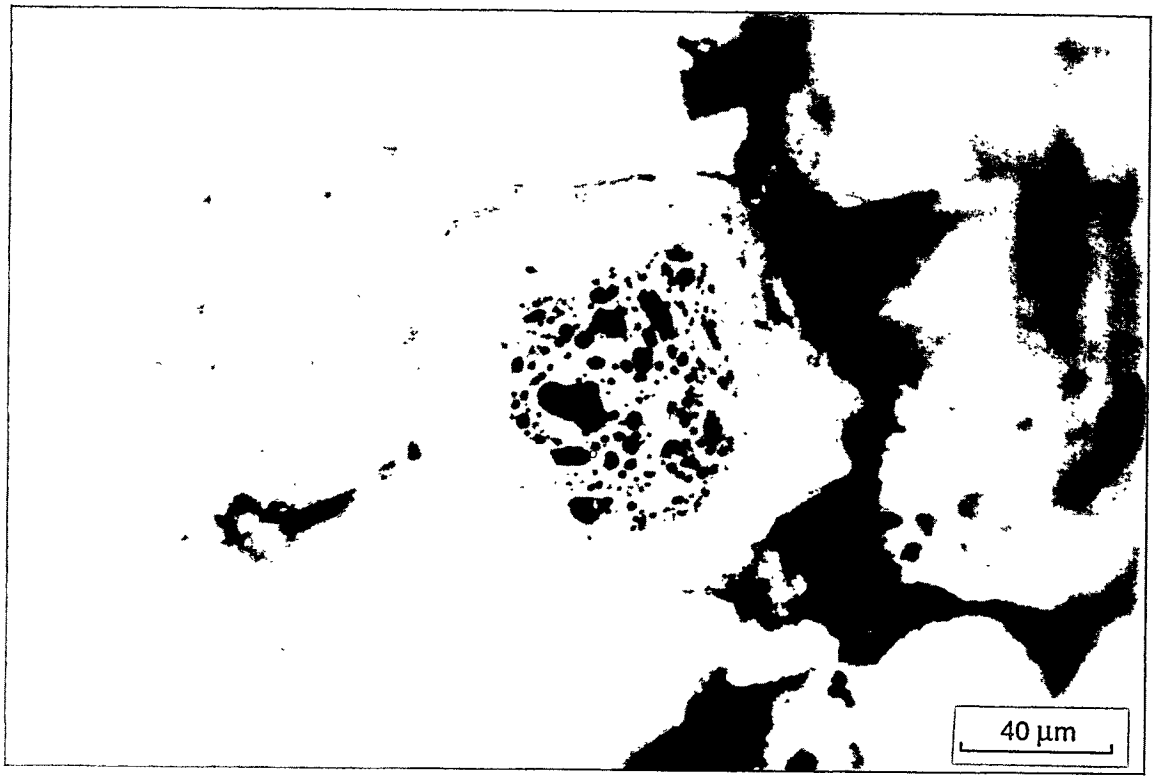

HANS-2, Sample #14, U_3Si_2, 325°C, Optical

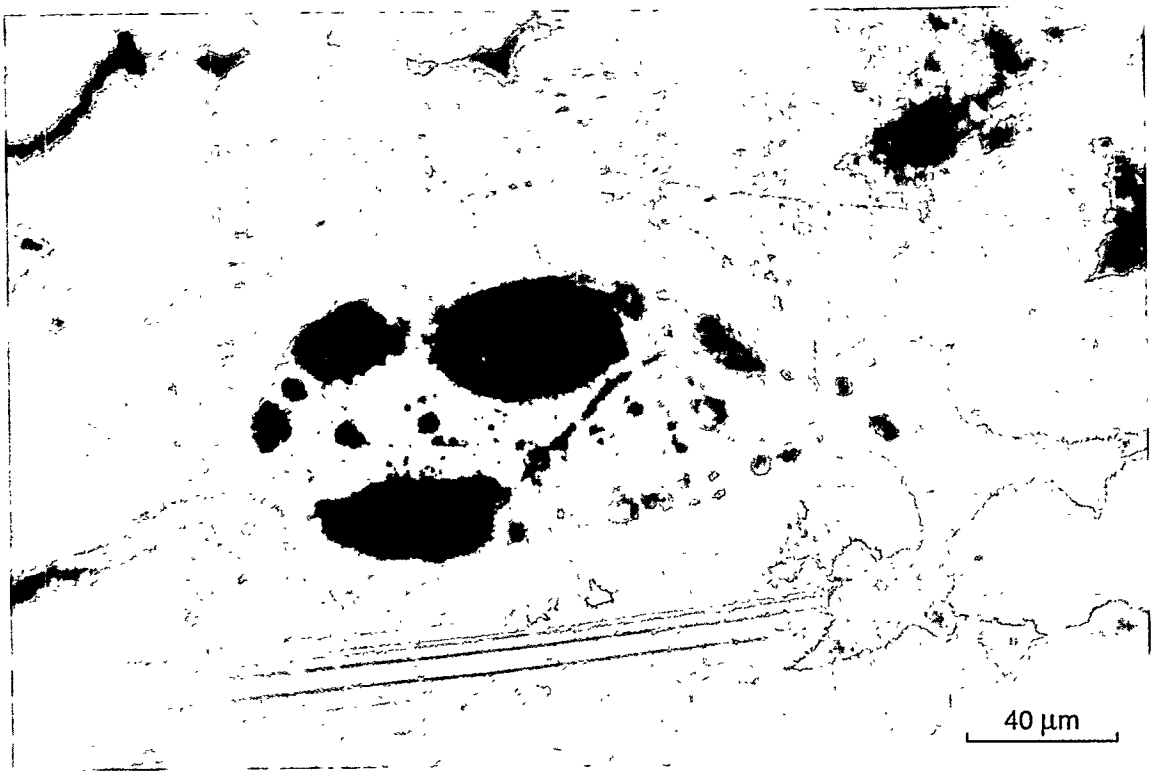

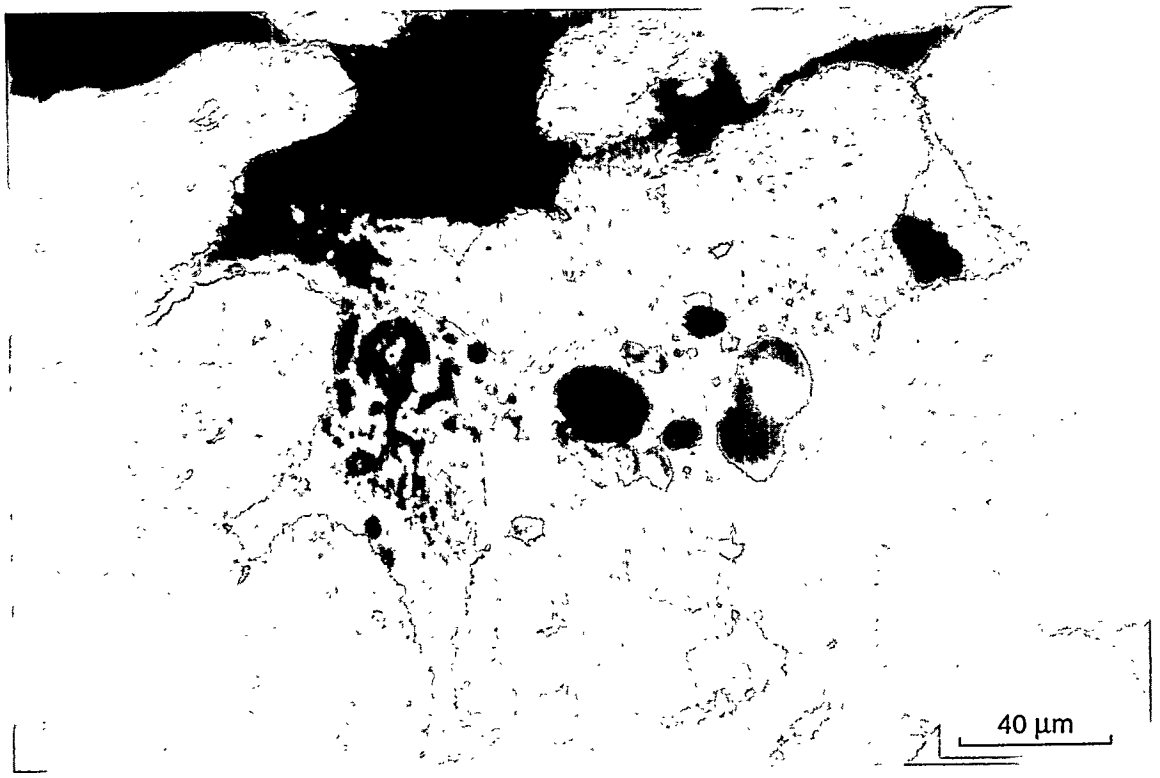

HANS-2, Sample #16, U_3Si_2, 250°C, Optical

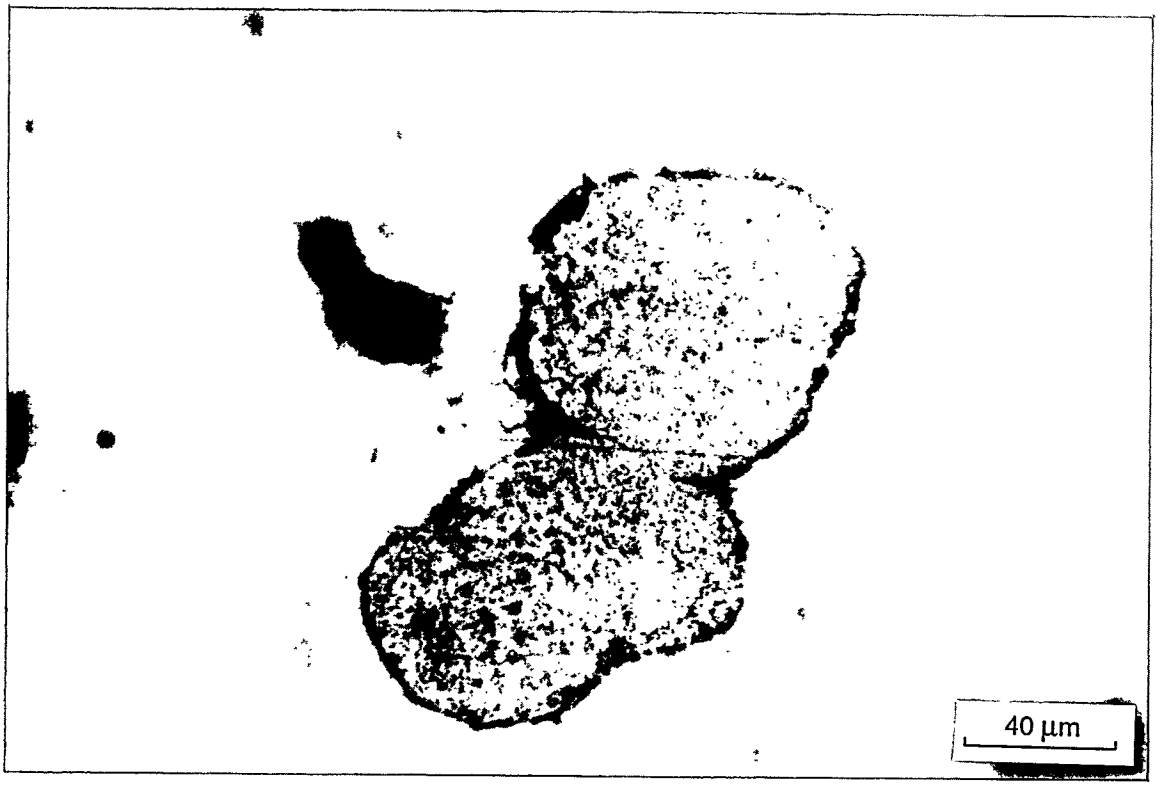

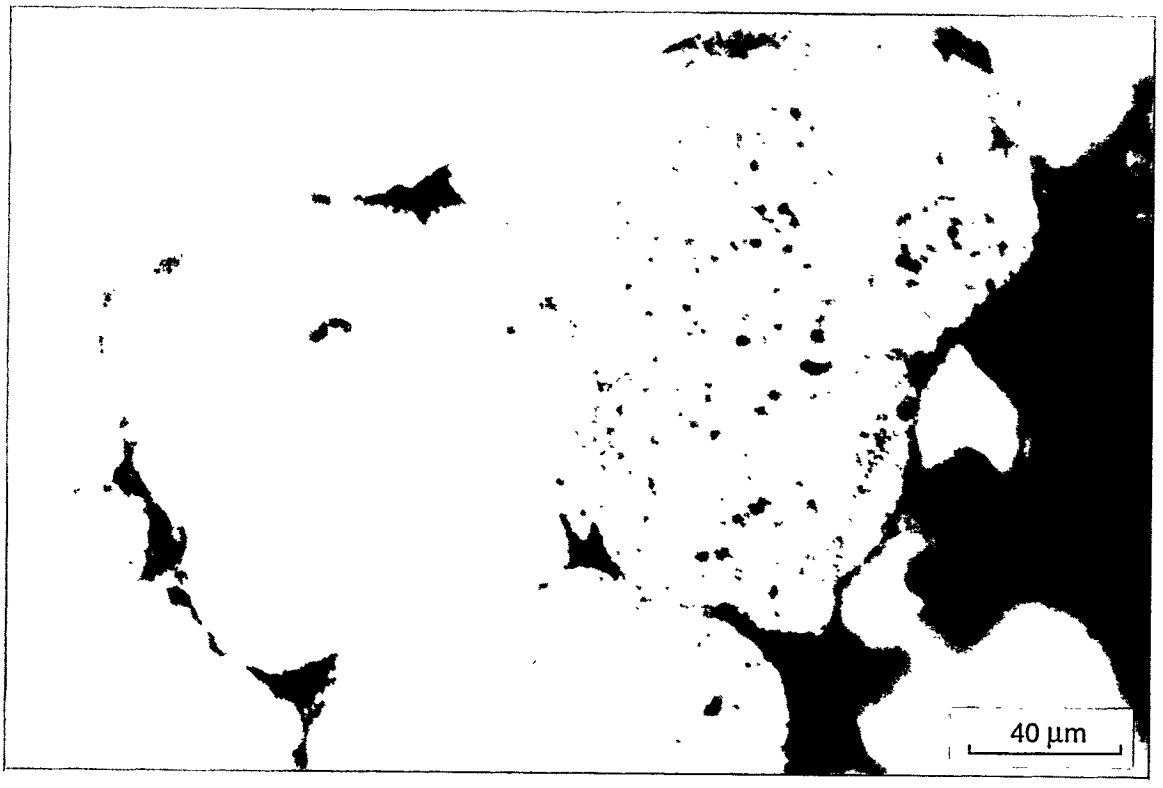

HANS-2, Sample #1, U_3O_8, 425°C, Optical

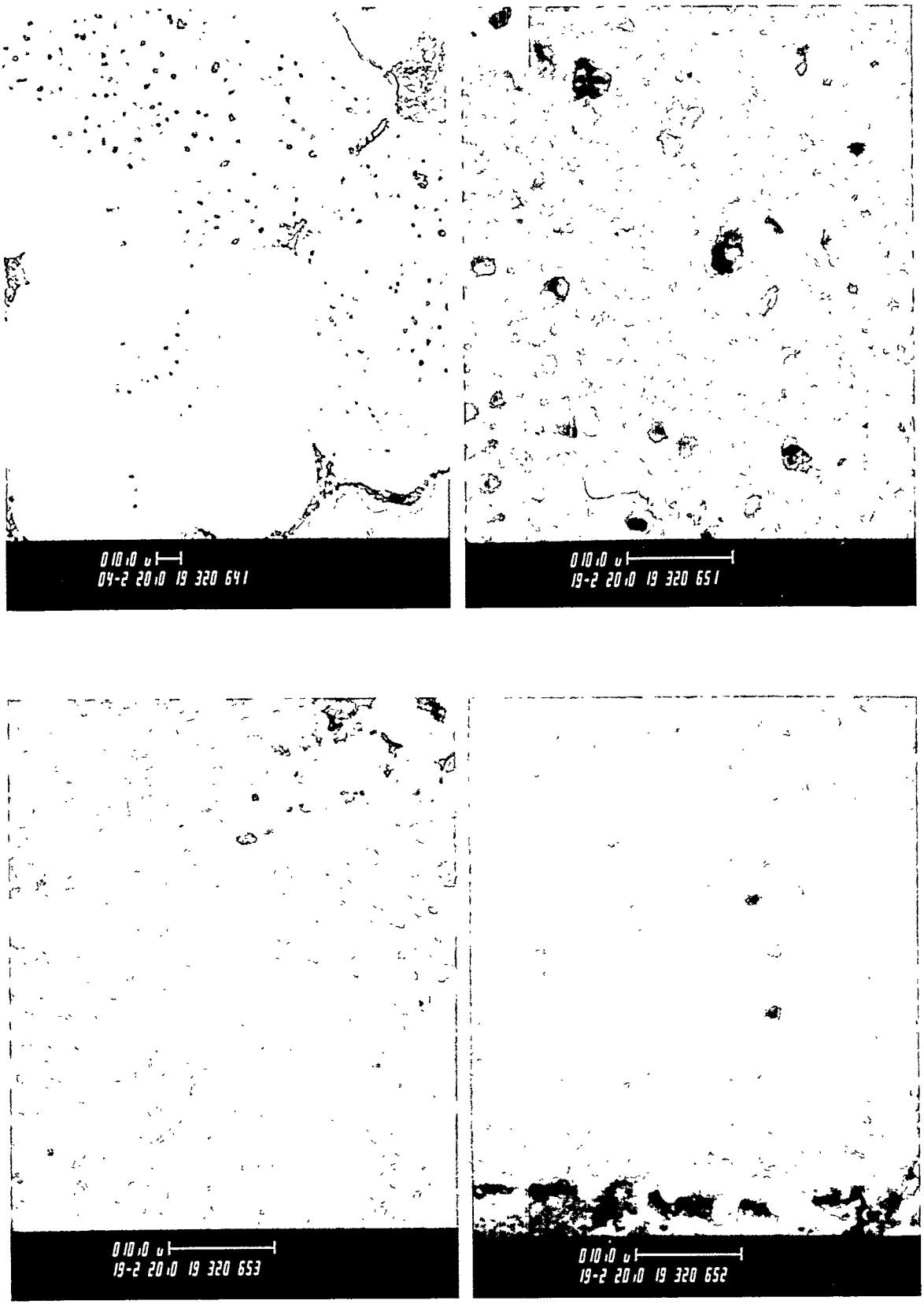

HANS-2, Sample #1, U_3O_8, 425°C, SEM

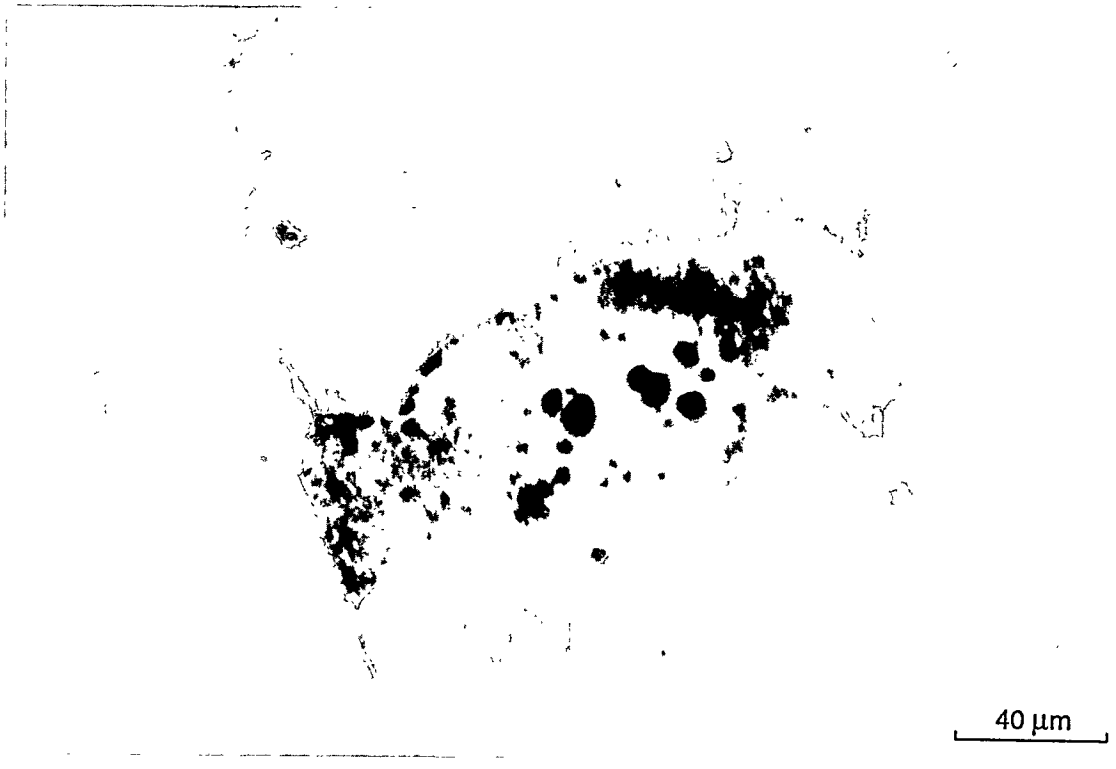

HANS-2, Sample #3, U_3O_8, 250°C, Optical

HANS-2, Sample #8, UAl_2, 425°C, Optical

HANS-2, Sample #6, UAl_2, 375°C, Optical

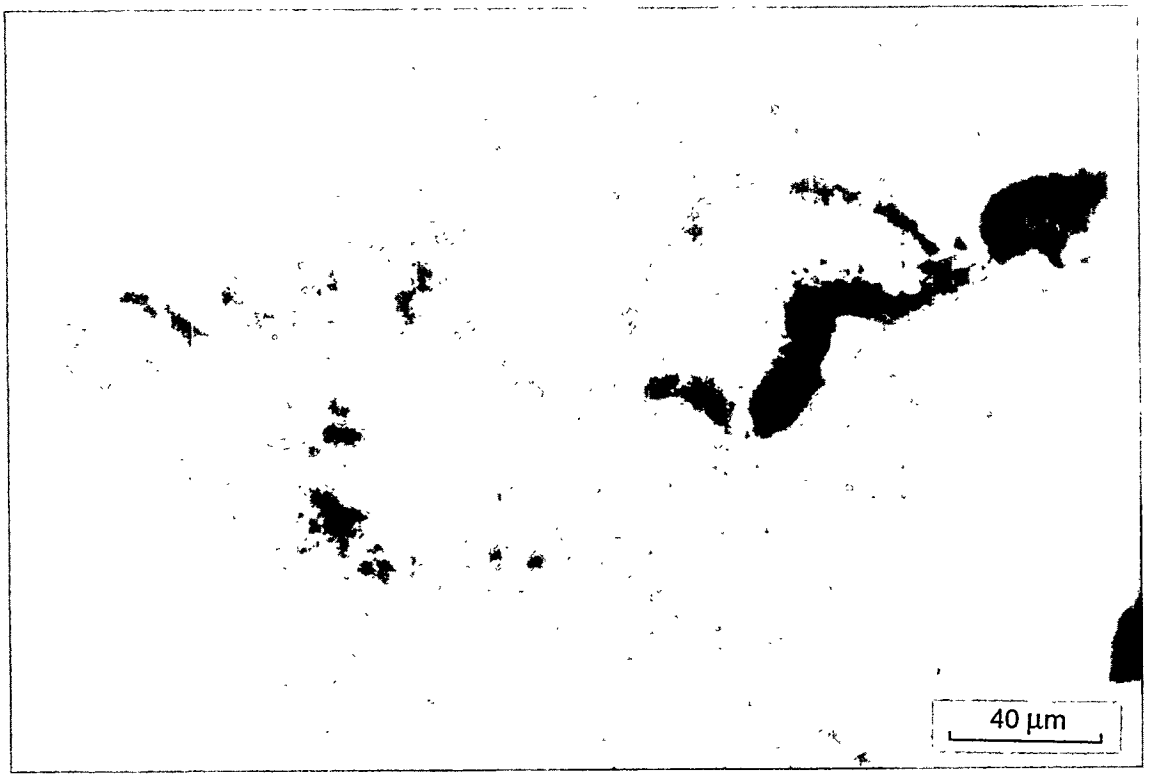

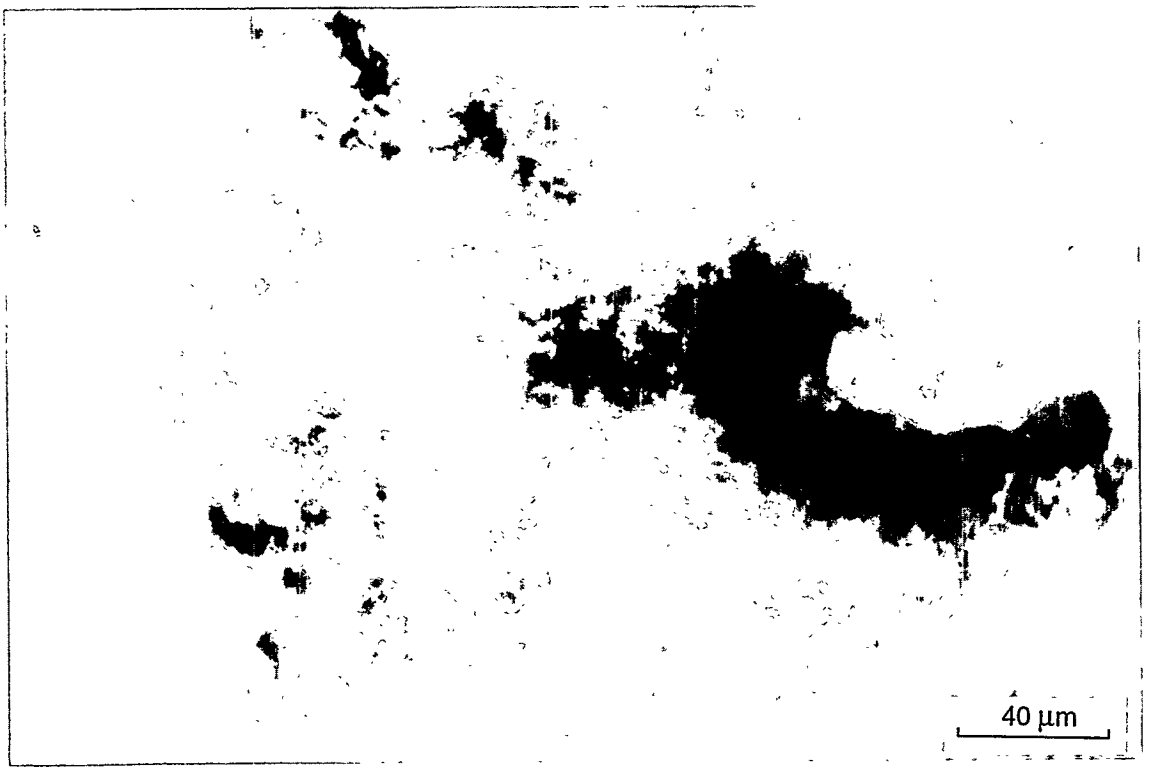

HANS-2, Sample #17, UAl_x, 425°C, Optical

HANS-2, Sample #12, UAl_x, 375°C, Optical

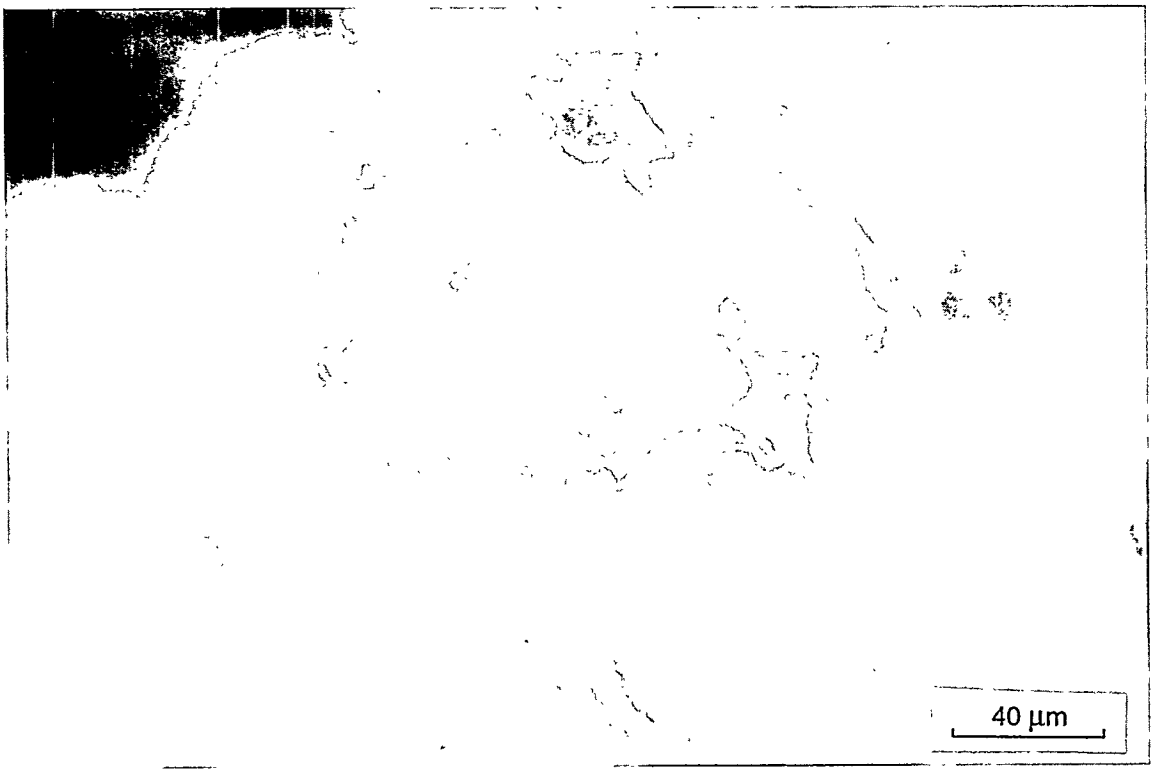

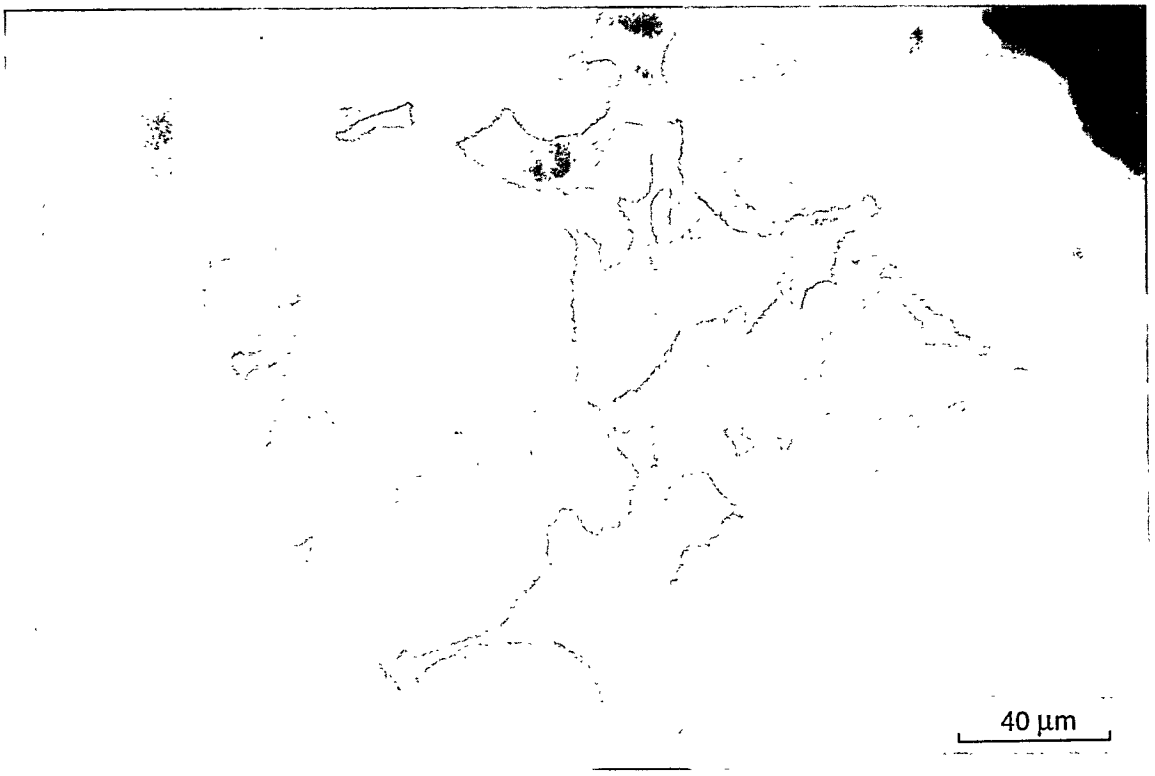

HANS-2, Sample #15, UAl_x, 250°C, Optical

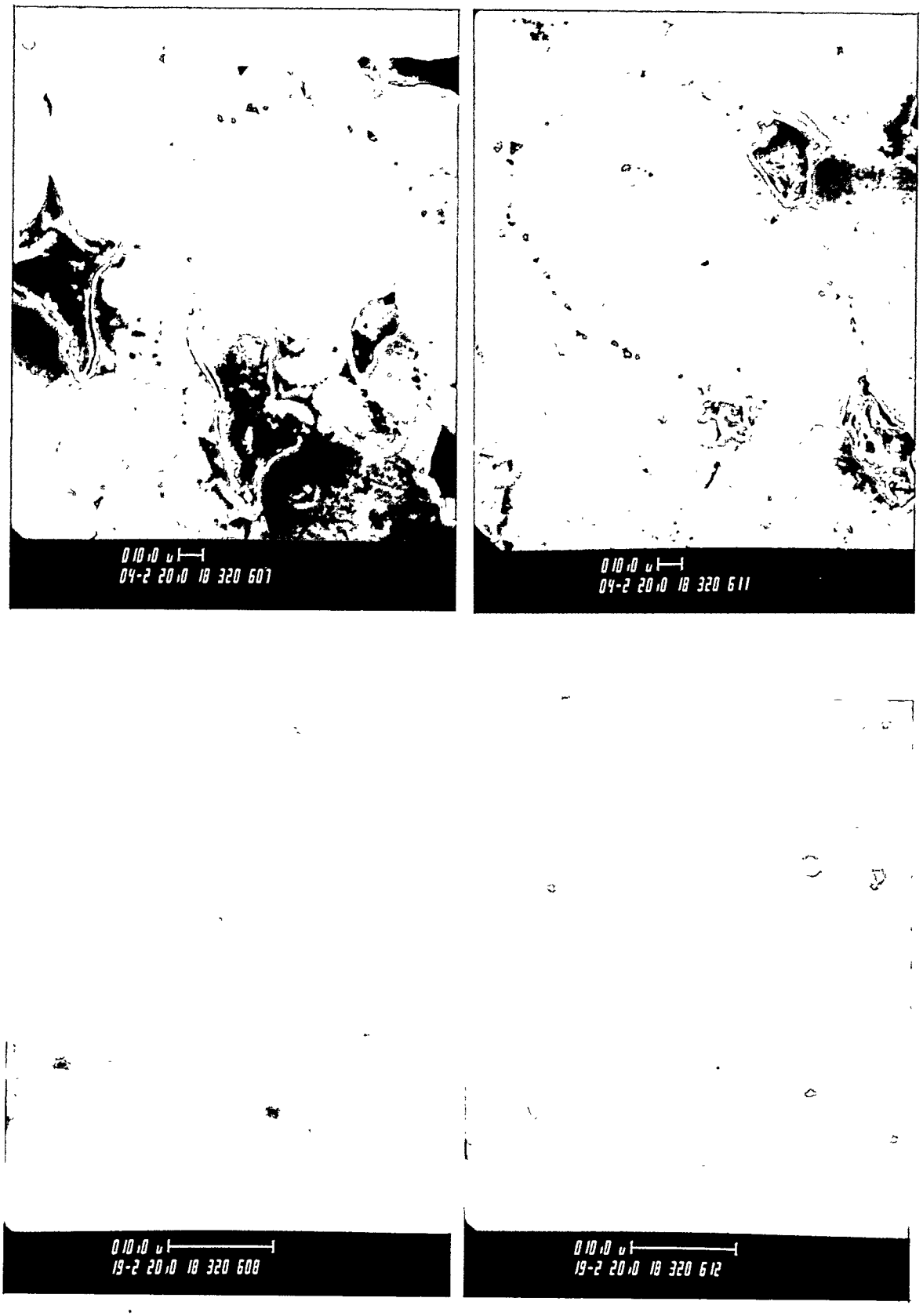

HANS-2, Sample #15, UAl_x, 250°C, SEM

INTERNAL DISTRIBUTION

1. D. J. Alexander
2. B. R. Appleton
3. R. L. Beatty
4–8. J. H. Campbell
9. J. E. Cleaves
10–19. G. L. Copeland
20. K. Farrell
21. D. K. Felde
22. G. F. Flanagan
23. R. M. Harrington
24. J. B. Hayter
25. R. W. Knight
26. D. G. Morris
27. S. J. Pawel
28. C. C. Queen
29. P. L. Rittenhouse
30. R. B. Rothrock
31. J. D. Sease
32. D. L. Selby
33. R. P. Taleyarkhan
34. M. R. Upton
35. C. D. West
36. B. A. Worley
37. G. T. Yahr
38. G. L. Yoder
39. ORNL Patent Office
40. Central Research Library Document Reference Section
41. Y-12 Technical Library
42–43. Laboratory Records Dept.
44. Laboratory Records, RC

EXTERNAL DISTRIBUTION

45–49. G. L. Hofman, Argonne National Laboratory, 9700 Cass Avenue, Argonne, IL 60439

50–54. J. E. Mays, Research and Test Reactor Fuel Elements, Babcock and Wilcox Co., P.O. Box 785, Lynchburg, VA 24505

55–59. B. W. Pace, Babcock and Wilcox Co., P.O. Box 785, Lynchburg, VA 24505

60–89. J. L. Snelgrove, Coordinator, Engineering Applications, RERTR Program, Argonne National Laboratory, 9700 Cass Avenue, Argonne, IL 60439

90. U. S. Department of Energy, ANS Project Office, Oak Ridge Operations Office, FEDC, MS-8218, P. O. Box 2009, Oak Ridge, TN 37831-8218

91–92. Office of Scientific and Technical Information, P.O. Box 63, Oak Ridge, TN 37831